December 2015

Iodine-131: Measurement and Application of a Novel Tracer in Lake Michigan

Michael Patrick Montenero
University of Wisconsin-Milwaukee

IODINE-131: MEASUREMENT AND APPLICATION OF A NOVEL TRACER IN LAKE MICHIGAN

by

Michael Patrick Montenero

A Thesis Submitted in

Partial Fulfillment of the

Requirements for the Degree of

Master of Science

in Freshwater Sciences and Technology

at

The University of Wisconsin-Milwaukee

December 2015

ABSTRACT

IODINE-131: MEASUREMENT AND APPLICATION OF A NOVEL TRACER IN LAKE MICHIGAN

by

Michael Patrick Montenero

The University of Wisconsin-Milwaukee, 2015
Under the Supervision of Professor James T. Waples

Iodine-131 is a short-lived (half-life=8.0233 days), gamma emitting, radiopharmaceutical that, when excreted by patients, enters aquatic systems via sewage effluent discharged from water reclamation facilities (WRFs). Here, I report on ^{131}I activities in the nearshore of southwest Lake Michigan in the vicinity of Milwaukee, Wisconsin. This is the first report on ^{131}I activity in any of the Great Lakes of North America.

The flux of ^{131}I from Milwaukee's two WRFs was monitored from July 2013 to December 2014. Mean discharge of ^{131}I from the Jones Island WRF was $(0.664 \pm 0.012)\times10^{8}$ Bq d^{-1} (mean effluent ^{131}I activity: ~0.25 Bq L^{-1}; n = 29). Mean discharge of ^{131}I from the South Shore WRF was $(2.07 \pm 0.68)\times10^{8}$ Bq d^{-1} (mean effluent ^{131}I activity: ~0.74 Bq L^{-1}; n = 29). The mean combined flux of ^{131}I from both WRFs into Lake Michigan was $(2.78 \pm 0.72)\times10^{8}$ Bq d^{-1}.

Measureable activities of ^{131}I were found in samples of *Cladophora* algae that were collected along a ~40 km section of Lake Michigan shoreline, from Atwater Park (8 km north of the Jones Island WRF) to Wind Point (13 km south of the South Shore WRF). ^{131}I activity in all *Cladophora* algae samples (n = 30) ranged from below detection to ~39 Bq g^{-1} dry weight.

Cladophora samples containing ^{131}I were found at the shoreline of most public beaches in the area including Atwater Park, Bradford Beach, South Shore Beach, Bay View Park, Grant Park, and Bender Park. Detection of ^{131}I in algae still attached to bottom substrate is an unequivocal metric of recent (days to weeks) exposure to treated sewage effluent. ^{131}I activity in dreissenid mussels (n = 17) ranged from below detection to ~0.7 Bq g^{-1} dry weight, and its mean was approximately one order of magnitude less than activity found in *Cladophora* algae.

Bottom trawls of lakebed material were made at 1, 5, and 8 km from shore in the vicinities of both WRFs. Analysis of collected materials revealed most ^{131}I activity in sloughed *Cladophora* algae, with overall ^{131}I activity decreasing with distance from shore but still measureable at 8 km out. Under steady state conditions, estimates of sloughed *Cladophora* transport along the lake bottom ranged from 200 to 500 m d^{-1} in both the south and east (offshore) directions.

Estimates of sediment deposition in the Milwaukee outer harbor were made with measurements of ^{131}I and the naturally occurring cosmogenic radionuclide ^{7}Be (half-life = 53.44 days) in bottom sediment (n = 67) and the outer harbor water column (dissolved + particle-bound fractions; n = 21). Concordance between both radionuclide derived particle flux estimates could only be achieved if it was assumed that bottom scavenging of both particle-bound and dissolved nuclide fractions was occurring, with particle transport dominated by vertical convection rather than gravitational settling. Mean non-steady state estimates of sediment deposition in the outer harbor from 29 July to 8 October, 2014 were 5.48 ± 0.93 tonne d^{-1} as derived by ^{131}I, and 7.6 ± 1.3 tonne d^{-1} as derived by ^{7}Be. Estimates of sediment loading from the Milwaukee River to the outer harbor, which were derived from USGS gauged discharge and turbidity measurements, had a mean of 9.1 tonne d^{-1} over the same time interval. I conclude from these results that as much as

60 to 80% of riverine particulate material delivered to the outer harbor is retained within the harbor and not discharged to the lake during periods of relatively low river flow.

TABLE OF CONTENTS

LIST OF FIGURES

LIST OF TABLES

ACKNOWLEDGEMENTS

First and foremost, I would like to thank my major advisor, Jim Waples, for supporting me, challenging me, and teaching me more than I could have ever imagined. He found me as a wandering biochemistry graduate who liked ecology, water and field work, and somehow got me to do a project in ecological radiochemistry (if there is such a thing). The financial support, guidance, education and freedom he gave me helped me to grow in ways I didn't always want to, but were immeasurably valuable. His friendship and willingness to go the extra mile for me will not be forgotten. I apologize to his family, from whom I have stolen him for far too many hours.

I thank my committee of mentors: Harvey Bootsma, Kirk Cochran and Rebecca Klaper, who have instructed and guided me through this project. I thank their patience with the many forms this work has evolved through on the way to its completion, and their dedication in perfecting it. I am also grateful for these professors and others who have taught me many skills through their courses, which have been a key part of this program. Others around the School of Freshwater Sciences were also extremely helpful in lending equipment, expertise, and samples they had collected to help me along during the development of this work.

I am especially grateful for those who have assisted me in the field, through many hours of hard and often uncomfortable work. As much as I like cranking up batches of smelly mud from below a sewage outfall in the sun and the rain, I recognize that the novelty may wear off after a few hours. The Milwaukee Metropolitan Sewerage District was very helpful in providing me with expertly prepared sewage effluent samples over a year and a half. The staff of the several smaller wastewater treatment plants we sampled were also very cooperative. I heartily thank our 2014 summer undergraduate assistant, Elizabeth Dilbone. Her hard work contributed

greatly to this project, and helped to give it the direction and momentum it needed. I am confident that she has what it takes to find great success in her own graduate career and beyond.

This work made use of the entire range of the University's diverse fleet: the incredibly versatile and reliable R/V *Neeskay*, the very capable R/V *Osprey*, and the glorified pontoon boat, the unsung hero, the R/V "*Party Barge*". The captain and crew of the R/V *Neeskay*, especially Capt. Greg Stamatelakys and Geoff Anderson, were incredibly helpful, patient and informative. Without them, untold hundreds of papers, theses and dissertations would surely never have seen the light of day. Chris Ney must also be thanked for providing essential training and maintenance for the University's smaller vessels.

I also thank Val Klump for his generous support of this work. He made the discovery that motivated this project, and has provided excellent guidance for Jim and myself as we struggled to figure things out. Most of all, I am grateful for the loan of his two gamma detectors, which provided two-thirds of the sample throughput for this project. Without his help, this would be a far inferior project.

Most of all, I would like to thank my family for their support of me throughout this important, formative and difficult chapter of my life. My parents Pat and Barb have provided me with financial, moral and emotional support and never doubted my abilities. My sister Kelly has blazed the trail for both of us in the marine and aquatic sciences, encouraging me to dream bigger than I ever would on my own. Last but not least, I thank my wife Ellen for her immeasurable support. She has been incredibly patient and encouraging through it all, giving me the motivation I needed to bring this work to fruition. Without all those listed above, none of this would have been possible.

Financial support for this project was generously provided by the University of Wisconsin Sea Grant Institute, whose funding has produced much research that has changed the world for the better. Additional funding was provided by the University of Wisconsin-Milwaukee.

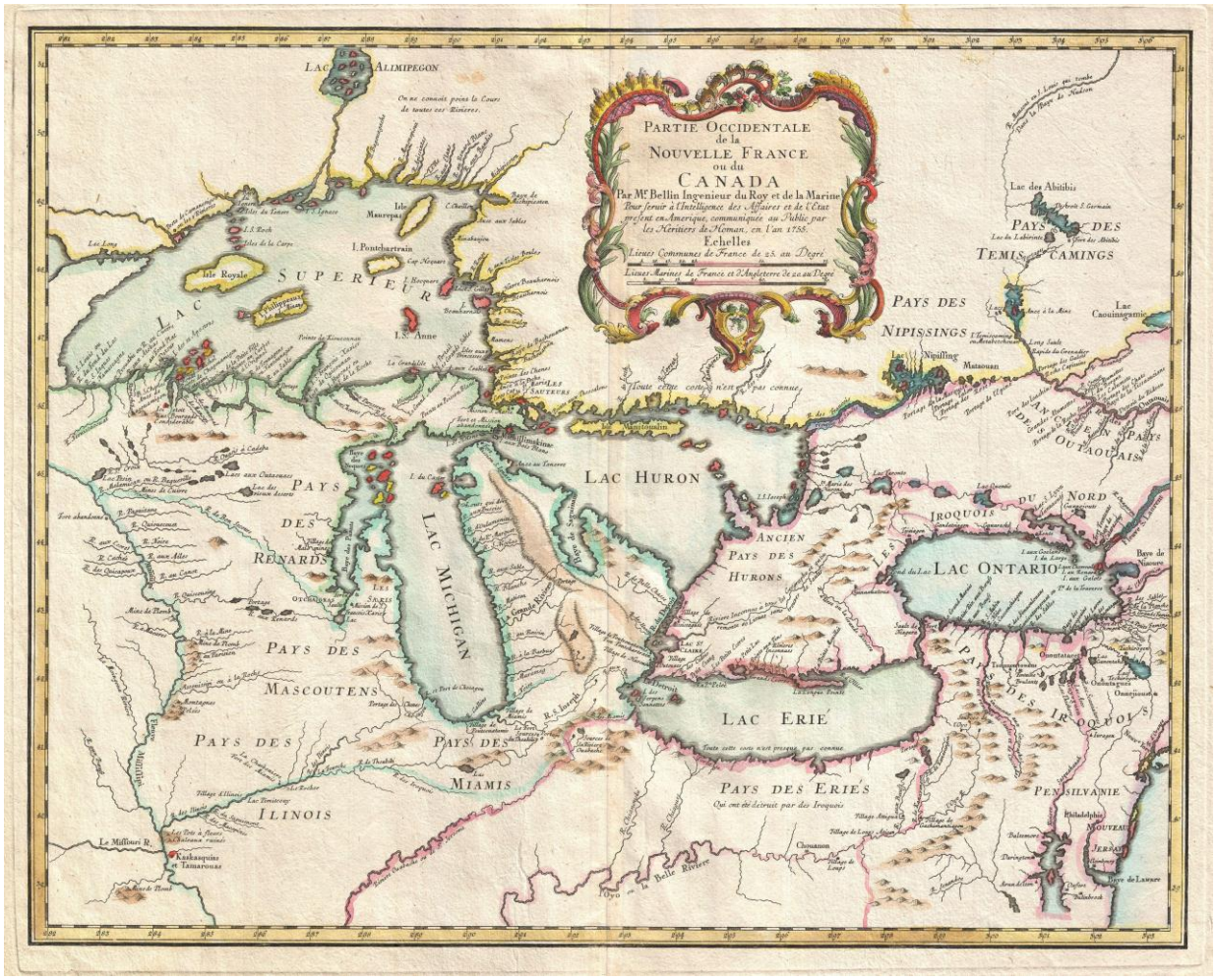
PARTIE OCCIDENTALE
de la
NOUVELLE FRANCE
ou du
CANADA
Par Mr Bellin Ingenieur du Roy et de la Marine
Pour servir à l'Intelligence des Affaires et de l'Etat
present en Amerique, communiquée au Public par
les Heritiers de Homan, en l'an 1755.
Echelles
Lieues Communes de France de 25. au Degré
Lieues Marines de France et d'Angleterre de 20 au Degré
LAC ALIMIPEGON
Isle Royale
LAC SUPERIEUR
I. Pontchartrain
I.S. Anne
LES SAUTEURS
LAC HURON
LAC MICHIGAN
PAYS DES RENARDS
PAYS DES MASCOUTENS
PAYS DES MIAMIS
PAYS DES ILINOIS
ANCIEN PAYS DES HURONS
LAC ONTARIO
LAC ERIE
PAYS DES ERIES
PAYS DES IROQUOIS
PAYS DES NIPISSINGS
PAYS DES TEMISCAMINGS
PAYS DES OUTAOUAIS
PENSILVANIE
Lac des Abitibis
Lac Caouingamic
Nipilling
Mataouan
Le Missouri R.

1. Introduction to iodine-131

1.1. ^{131}I background

Iodine-131 (^{131}I) is the most commonly used radiopharmaceutical in the United States and has been in use in nuclear medicine since the 1940s (Rose et al. 2012). ^{131}I is primarily used to treat hyperthyroidism and thyroid cancer, but is also used as a tracer for diagnostics and imaging (Chapman 1946, Rasmuson 2006). ^{131}I use for hyperthyroidism occurs at an average rate of 150 per million people per year. Its use for thyroid cancer is lower at 83 per million people per year (Rose et al. 2012). However, thyroid cancer patients typically receive a dose of 4000-8000 MBq (1MBq = 10^6 disintegrations per second of activity), while hyperthyroidism patients typically receive only 100-1000 MBq (Valentin 2004).

About 70% of the ^{131}I activity administered to patients passes through the body and directly into the waste stream (Smith et al. 2008), and upon treatment at water reclamation facilities (WRFs), as little as ~1% of ^{131}I is scavenged in sewage sludge, with the remaining activity discharged in treated sewage effluent to receiving water bodies (Martin and Fenner 1997, Rose et al. 2012).

^{131}I emissions to the environment from WRFs have been studied for decades (Moss 1973). Many studies have searched for ^{131}I in sewage sludge (e.g. Barci-Funel et al. 1993, Cosenza et al. 2015, Erlandsson and Mattsson 1978, Jiménez et al. 2011, Martin and Fenner 1997, Stetar et al. 1993, etc.) and in saltwater bodies that receive sewage effluent (e.g. Rose et al. 2012, Smith et al. 2008, Veliscek Carolan et al. 2011, Waller and Cole 1999, etc.). However, relatively few studies have studied ^{131}I in freshwater environments and directly in sewage effluent (e.g. Fischer et al. 2009, Rose et al. 2013, Rose et al. 2015, Sodd et al. 1975). Furthermore, ^{131}I has never been

systematically studied in the Great Lakes, despite their regional and global importance as a freshwater resource and the growing concern over treated sewage discharge of pharmaceuticals and personal care products (PPCPs) (e.g. Benotti and Brownawell 2009, Gomez et al. 2012, Jiang et al. 2010).

1.2. Suitability of ^{131}I for freshwater research

Radionuclides with known sources, half-lives and biogeochemistry have been used to trace complex environmental processes and fluxes (e.g. Cochran and Masque 2003, Waples et al. 2006). ^{131}I is only beginning to be used in this fashion (Rose et al. 2015), but is particularly well suited for use as a tracer in freshwater systems for a number of reasons:

1. ^{131}I is specifically sourced to sewage wastewater. Other than its use as a radiopharmaceutical, the only other significant sources of ^{131}I in the environment are releases from industrial uses, nuclear weapon testing and production, or accidental releases from nuclear power plants and nuclear fuel reprocessing, which have not occurred near Lake Michigan. Additionally, due to the short half-life of ^{131}I (half-life 8.0233 d; Nichols et al. 2008), atmospheric contamination from other regions is at worst short-lived and unlikely. Therefore, if the flux of ^{131}I in sewage effluent to a local aquatic system is known, the entire flux and inventory of ^{131}I in that system is known.

2. ^{131}I detection indicates exposure to a source of the radionuclide in the last several days to weeks. Because ^{131}I is primarily sourced from treated sewage, detection of ^{131}I is an unequivocal tracer of recent sewage effluent exposure. Other possible sewage tracers such as PPCPs degrade according to long, variable and understudied effective half-lives

and can accumulate over time (e.g. Benotti and Brownawell 2009, Gomez et al. 2012, Jiang et al. 2010).

3. ^{131}I is a gamma emitter (364.489 keV, 81.2% of emissions; Nichols et al. 2008). Therefore, it is easily measured via gamma spectroscopy at concentrations too dilute for most other methods. For example, a relatively high source ^{131}I activity of ~0.2 Bq/L in treated sewage wastewater has an equivalent concentration of ~0.3 attomoles/L (i.e., 0.3×10^{-18} mol/L). PPCPs, on the other hand, are ubiquitous in open waters near urban areas, but are often too dilute to be detected without elaborate pre-concentration procedures. Gamma spectroscopy is also nondestructive and unaffected by the chemical form of ^{131}I.

4. Iodine is bioconcentrated in many species as a micronutrient. ^{131}I behaves in the same way as stable I, which is enriched in aquatic organisms such as algae (Amachi 2008, Ishikawa et al. 2004, Karlander and Krauss 1972, Kleinschmidt 2009, Ullman and Aller 1985, Veliscek Carolan et al. 2011). Macroalgae, in particular, concentrate iodine in aquatic environments. Concentration factors for various species of macroalgae have been reported at 10^4 (Valentin 2004), 10^5 (Amachi 2008), and as high as 10^6 (Martinelango et al. 2006) times the concentration in seawater, with macroalgae accumulating up to 5% I by dry weight (Küpper et al. 1998). Although iodine concentrations in the Great Lakes are much lower than that of seawater (Ullman 1982), freshwater macroalgae still share the I-concentrating properties of their saltwater counterparts. *Cladophora spp.*, a common genus of freshwater macroalgae, accumulates I (Verdel et al. 2000) to levels of about 78-240 mg/kg in the Black Sea (Pimenova et al. 2004). *Cladophora glomerata* is ubiquitous in the nearshore zones of the Great Lakes (Bootsma et al. 2004, Greb et al. 2004), making

it a potentially useful tool in the study of ^{131}I in that region. Iodine is a micronutrient in many aquatic organisms besides algae, and is known to accumulate to some degree in shellfish, some plankton, mammals and fish (Amachi 2008, Ullman 1982). This trait simplifies the process of finding ^{131}I in the aquatic environment.

5. The biogeochemistry of iodine is also somewhat well known. Iodine has been widely found to be enriched in sediments relative to overlying water (Bojanowski and Paslawska 1970, Martin et al. 1993, Mohiuddin et al. 2010, Shishkina and Pavlova 1965, Ullman 1982, Ullman and Aller 1985). Iodine is especially enriched in surface sediments, and its concentration falls in deeper sediments (Mackin et al. 1988, Shishkina and Pavlova 1965, Ullman and Aller 1985). Iodine has been shown to associate with organic particles and metal oxides, which settle from the water column to the surface of the sediment bed (Mackin et al. 1988, Price and Calvert 1973, Price and Calvert 1977, Ullman 1982, Ullman and Aller 1985). This, along with its ability to be bioconcentrated, makes ^{131}I in the environment easily accessible to sampling equipment. Iodine is present in the water column as well, but at lower concentrations (1.1 µg/L in the upper Great Lakes; Tiffany et al. 1969). The particle reactivity of iodine and ^{131}I varies greatly by location, but the K_d (activity per kg sediment / activity per L water) has been shown to be to be 10^3-10^4 L/kg in freshwater systems (Rose 2011, IAEA 2010), a moderate value which should allow it to be detected in both the dissolved and particle-bound phases in the water column, further extending its potential applications as a tracer of both sewage-derived material and sediment.

1.3. Study site

Approximately 10 million people depend on Lake Michigan (58,000 km^2) as a primary source of drinking water. Roughly half of these people also use Lake Michigan as a repository for treated and untreated sewage wastewater. The population of greater Milwaukee is over 2 million, making it the largest city on Lake Michigan that discharges its wastewater into the lake (Chicago reversed the flow of the Chicago River in 1900, sending its waste to the Mississippi River). Milwaukee is also the fourth largest city (after Detroit, Toronto and Cleveland) in the Great Lakes region that discharges its wastewater into the Great Lakes.

Most of the greater Milwaukee area located within the Lake Michigan watershed is serviced by the Milwaukee Metropolitan Sewerage District (MMSD). MMSD serves about 1.1 million people and consists of the Jones Island WRF, which is located near the Milwaukee outer harbor and primarily serves the combined sewers in the more highly urbanized downtown area, and the South Shore WRF, which is located south of Milwaukee on Lake Michigan and primarily serves the separated sewer systems in smaller municipalities in the greater Milwaukee area (MMSD, pers. comm. 2015; **Figure 1**).

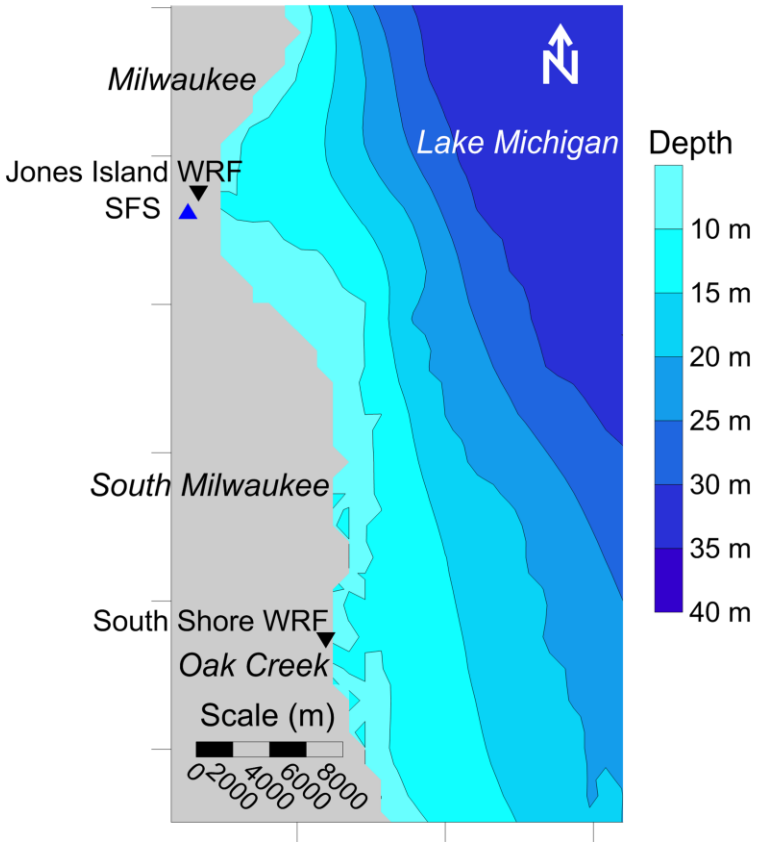

Figure 1 Shoreline of Lake Michigan in the Milwaukee area showing the two water reclamation facilities (WRFs) operated by the Milwaukee Metropolitan Sewerage District, and the University of Wisconsin-Milwaukee School of Freshwater Sciences (SFS).

Much of this study is focused on the Milwaukee outer harbor, which is part of the Milwaukee Estuary Area of Concern (International Joint Commission 1987; **Figure 2**). This urban freshwater harbor receives the combined Milwaukee, Menomonee, and Kinnickinnic Rivers, which carry runoff nutrients, sediments, and industrial contaminants from a 2590 km^2 mixed land use watershed (Zou and Christensen 2012). Moreover, the outer harbor receives treated sewage effluent directly from the Jones Island WRF (maximum capacity 1.25 billion L/d), which has been shown to contain pharmaceuticals and personal care products above levels of concern (Blair et al. 2013).

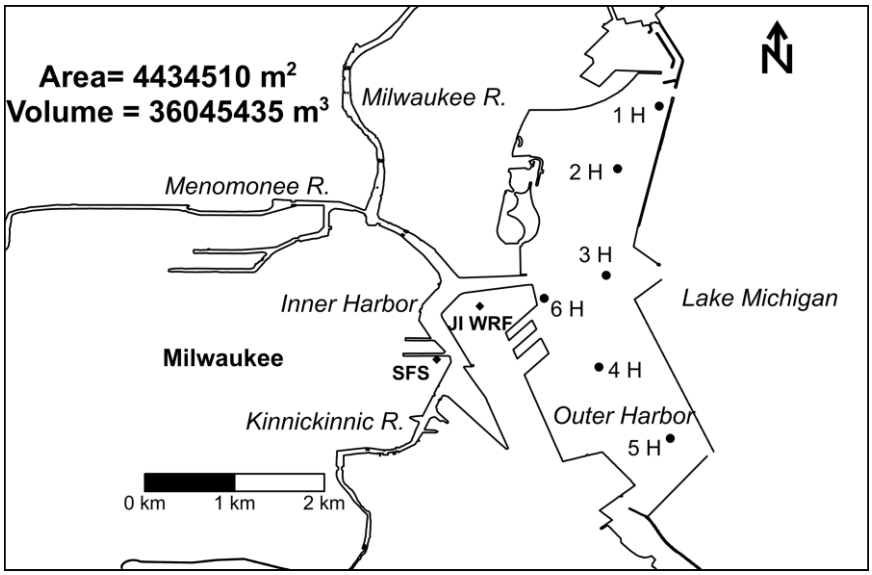

Figure 2 The Milwaukee harbor. Six sampling sites in the outer harbor (1-6 H) are shown as well as the University of Wisconsin-Milwaukee School of Freshwater Sciences (SFS) and the Jones Island Water Reclamation Facility (JI WRF), whose outfall is located near 6 H.

1.4. Thesis outline

The research presented here represents the first effort to systematically measure ^{131}I in sewage effluent, water, sediment, and biota in the Laurentian Great Lakes. An organizational outline of my work follows.

In chapter 2, I explain the method of gamma spectroscopy and outline the materials and equipment used to measure and calculate ^{131}I activity.

In chapter 3, I present measurements of ^{131}I activity in: (*i*) sewage effluent (chapter 3.1), (*ii*) *Cladophora* algae (chapter 3.2), (*iii*) dreissenid mussels (chapter 3.3), (*iv*) Lake Michigan benthic trawls (chapter 3.4), (*v*) Milwaukee outer harbor sediment (chapter 3.5), and (*vi*) Milwaukee outer harbor water (chapter 3.6)

In chapter 4, I provide ancillary measurements of beryllium-7 (^{7}Be), a short-lived (half-life: 53.2 d) cosmogenic radionuclide, that I use together with ^{131}I (in chapter 5) to investigate short-term sediment deposition.

In chapter 5, finally, I employ ^{131}I as a tracer of: (*i*) sewage effluent exposure (chapter 5.1), (*ii*) benthic material transport (chapter 5.2), and (*iii*) sediment deposition in the Milwaukee outer harbor (chapter 5.3).

Raw data and related parameters required to recalculate all sample activities are provided in 13 appendices (appendices A – M).

2. Gamma Spectroscopy

In this study, the radioactivity of all samples was measured by gamma spectroscopy. The section below outlines the materials, methods, and calculations used to determine sample activity.

2.1. Gamma detectors

Gamma spectroscopy analysis for ^{7}Be and ^{131}I were carried out on three high-purity germanium gamma detectors. Detector 1 is a Canberra well detector (model no. GCW4023), detectors 2 and 3 are Ortec planar detectors (model no. GMX-23210-P and LO-AX-70450/30-S, respectively).

2.2. Counting containers

Three different counting containers were used, depending on the amount of sample available (**Figure 3**). The largest amount of sample possible was generally used and balanced with the counting efficiency of each container to maximize radionuclide counts. The smallest container, referred to in this study as the "vial", is a 5 ml transport tube (Cat. No. UP2282) from United Laboratory Plastics (cap diameter 20mm, tube diameter 15mm, tube height 58mm). Samples in vials were only counted in the well detector (detector 1).

The mid-size container used is referred to in this study as a "jar". Jar containers are made by Parkway Plastics, Inc. (P/N: A0830600PPC, volume 230mL, diameter 83mm, height 55mm) and sit directly on top of the detector. The largest container used is referred to in this study as a "Marinelli beaker". It is a liquid and solid analysis container from GA-MA & Associates, Inc. (Model 538G-E, 127mm height, 140mm diameter, 84mm well height, 96mm well diameter, 947mL volume) and fits on top and around the sides of the detector.

Figure 3 Three types of counting containers (from left): Marinelli beaker, jar and vial.

2.3. Counting Efficiency

The counting efficiencies of each sampling container on each gamma detector were determined using a europium-152 (^{152}Eu) standard (see Appendix L). ^{152}Eu (half-life = 13.53y) is a commonly used radionuclide for detector efficiency calibration because it emits at several different energies and has a convenient half-life (peaks used: 121, 344, 779, 965 keV; Nichols et al. 2008). Therefore, a measurement of a known activity of ^{152}Eu provides the data needed to derive an equation to calculate a detector's efficiency at any energy for a given container geometry. This was done with each sampling container to obtain accurate counting efficiencies. The ^{152}Eu standard was in a dry sediment medium for the jar and vial geometries, and in aqueous solution for the Marinelli beaker geometry, as this came closest to the type of samples most often used in each container.

Calculated efficiencies varied from around ~2% for Marinelli beakers to ~3% for jars and ~20% for vials. Efficiency measurements and equations for each detector can be found in Appendix M.

2.4. Radionuclide activity calculations

Gamma spectroscopy is often a trade-off between the length of analysis and uncertainty in its results. Samples were centered on the detector surface and counted for at least two days, or until ^{131}I and ^{7}Be peak areas had reached sufficiently low (<20%) error. Gamma analysis reports an output of counts detected within a peak at the emission energy of interest. This value can be used to calculate the activity of a radionuclide in a sample when combined with detector efficiency, time, and characteristic information for the radionuclide of interest. This section walks through the calculations used to find activity from counts.

Gamma spectrum analysis was performed using Genie 2000 software (v. 3.2, Canberra Industries, Inc.) on detector 1, and Maestro software (v. 6.04, Advanced Measurement Technology, Inc.) on detector 2 and 3. Peak analyses reported net peak areas and net area uncertainty (± 1 standard deviation). Net peak areas are hereafter referred to as "raw counts".

First, the raw count (ct) was used to calculate counts per second (cps) using the live time of gamma analysis in seconds (t_L), or the amount of time the detector was able to receive emissions during gamma analysis. This differs slightly from the total analysis time because every time an emission hits the detector, there is a split second of dead time during which the detector is busy processing the previous emission. The detector cannot process any additional emissions during the dead time, so live time is used to calculate cps:

$$cps = \frac{ct}{t_L} \quad (1)$$

A number of factors are required to convert raw sample cps to sample activity (disintegrations per second, or Becquerels, abbreviated Bq). The first is decay of the sample during gamma analysis. This factor can be significant for short-lived radionuclides. There is a correction factor that can be used to account for this decay (CF). It is a function of t_L and the decay constant of the radionuclide (λ). The decay constant is a function of the radionuclide's half-life ($t_{1/2}$), and is in units of inverse time (e.g. d^{-1}):

$$\lambda = \frac{\ln(2)}{t_{\frac{1}{2}}} \tag{2}$$

CF, the correction factor for decay during sample counting, is:

$$CF = \frac{t_L \lambda}{1 - e^{-t_L \lambda}} \tag{3}$$

Another factor needed to convert cps to activity is the branching fraction of the radionuclide at the peak energy. Many radionuclides emit at several different energies through multiple modes of decay, and some happen more often than others. The peak energy measured here is the most common emission energy for the radionuclide, (i.e., ^{131}I: 364.18 keV; ^{7}Be: 477.82 keV), but is not the only one. The fraction of emissions at the measured energy is the branching fraction (BF). For ^{131}I, BF = 0.812, and for ^{7}Be, BF = 0.1044 (Nichols et al. 2008).

The last factor used to convert cps to activity is the counting efficiency (Eff). Counting efficiencies were calculated as described in chapter 2.3. above.

Using the three above factors, cps can be converted to activity at the time of analysis (A'), in units of Becquerels (Bq), or disintegrations per second:

$$A' = \frac{cps \times CF}{BF \times Eff} \tag{4}$$

A' must then be converted to activity at time of collection (A_0). This is accomplished by using an exponential decay equation incorporating λ and the time elapsed between sample collection and the start of gamma analysis (t_c):

$$A_0 = \frac{A'}{e^{-\lambda t_c}} \quad (5)$$

A_0, the activity of the sample at collection, is the activity referred to in this study. This activity can then be normalized by dividing by the volume, area or dry weight it represents. A walkthrough of these calculation steps for an example sewage effluent sample is shown below in Example 1.

Example 1 *Calculation of sample activity for an example effluent sample.*

Sample	South Shore Effluent Example
Time collected	12/9/14 17:00
Time of gamma analysis start	12/12/14 09:59
Time elapsed after collection (t_c)	2.71 d
Container	Marinelli beaker
^{131}I peak energy (E)	364.18 keV
^{131}I counts (ct)	1606
Live time (t_L)	257514 s
^{131}I half-life ($t_{1/2}$)	8.0233 d
^{131}I branching fraction (BF)	0.812
Detector	2
Sample volume (V)	0.800 L
WRF Discharge	2.69×10^8 L/d

Calculation of counts per second (cps):

$$cps = \frac{ct}{t_L}$$

$$cps = \frac{1606}{257514\ s} = 0.00624 s^{-1}$$

^{131}I decay constant (λ):

$$\lambda = \frac{ln\,2}{t_{\frac{1}{2}}}$$

$$\lambda = \frac{ln\,2}{8.0233\ d} = 0.0864\ d^{-1}$$

Correction factor for decay during counting (CF) after converting t_L from seconds to days:

$$CF = \frac{t_L\lambda}{1 - e^{-t_L\lambda}}$$

$$CF = \frac{2.98d \times 0.0864d^{-1}}{1 - e^{-2.98d \times 0.0864d^{-1}}} = 1.13$$

Sample counting efficiency (Eff) for a Marinelli beaker on Detector 2:

$$Eff = 0.0065 + 0.0540 \times e^{-0.0040E}$$

$$Eff = 0.0065 + 0.0540 \times e^{-0.0040 \times 364.18keV} = 0.0191$$

^{131}I activity at time of analysis (A'):

$$A' = \frac{cps \times CF}{BF \times Eff}$$

$$A' = \frac{0.00624s^{-1} \times 1.13}{0.812 \times 0.0191} = 0.453Bq$$

^{131}I activity at time of collection (A_0):

$$A_0 = \frac{A'}{e^{-\lambda t_c}}$$

$$A_0 = \frac{0.453Bq}{e^{-0.0864d^{-1} \times 2.71d}} = 0.573Bq$$

From this point, the sample volume can be used to calculate the ^{131}I activity per unit volume:

$$\frac{A_0}{V} = \frac{0.573Bq}{0.800L} = 0.716Bq/L$$

3. Milwaukee-sourced ^{131}I in southern Lake Michigan

In this chapter, I address the overarching question of whether or not ^{131}I is released from Milwaukee's WRFs to Lake Michigan, and if so, where in Lake Michigan can ^{131}I activity be found. Concentrations and fluxes of ^{131}I from the Jones Island and South Shore WRFs are first presented in section 3.1. Concentrations of ^{131}I in *Cladophora* algae and dreissenid mussels collected along ~40 km of Lake Michigan shoreline (in the vicinity of Milwaukee) are then presented in sections 3.2 and 3.3, respectively. In section 3.4, results are given showing ^{131}I activities in benthic trawls of bottom material collected in both nearshore (~1 km) and offshore (~8 km) Lake Michigan. In section 3.5, a time-series of ^{131}I activities in bottom sediment of the Milwaukee Outer Harbor is presented. Finally, in section 3.6, a time-series of ^{131}I activities in the water column of the Milwaukee Outer Harbor, with distinct measurements of both particle-bound and dissolved fractions, is presented.

3.1. Sewage effluent

3.1.1. Methods

To determine the presence of ^{131}I in Milwaukee sewage effluent, composite effluent samples were taken from the MMSD WRFs.

MMSD provided 24-hour (05:00-05:00) composite sewage effluent samples from both WRFs on a ~biweekly basis. This sample interval proved to be an optimal balance between the ~8 day half-life of ^{131}I (ensuring that activity from the previous sampling date would still be present in the environment) and effective sample throughput (~10 samples of any kind per week). 800mL of this composite sample was placed in a 947mL Marinelli beaker for gamma spectrometry. If less than 800mL of effluent sample was available, the entire sample was added

to the beaker and the volume was brought up to 800mL with deionized water for consistent counting geometry. Bleach was also added from 20 June 2013 to 30 June 2014 for sanitary reasons, but was later deemed unnecessary. We found the addition of bleach to have no effect on sample activity, however (see Appendix A). The sewage effluent samples were then analyzed for ^{131}I activity by gamma spectroscopy (see chapter 2.).

After ^{131}I activity in sewage effluent was quantified, the ^{131}I flux from the WRF was also calculated. MMSD reports effluent discharge data every 15 minutes. Mean discharge was calculated over the 24-hour period of each composite sample and multiplied by the effluent ^{131}I activity to determine the ^{131}I flux from each WRF. An example calculation of this is shown above in Example 1 (chapter 2.3.). Example 1 is continued below to show the calculation of ^{131}I flux from the WRF.

Example 1, continued

The ^{131}I activity per unit volume of the effluent sample, 0.716Bq/L, is multiplied by the mean WRF discharge during the sample collection period, which is 2.69×10^{8}L/d, to give the ^{131}I flux from the WRF ($J_{I131,WRF}$):

$$J_{I131,WRF} = \frac{A_0}{V} \times Discharge$$

$$J_{I131,WRF} = 0.716Bq/L \times (2.69 \times 10^{8} L/d)$$

$$J_{I131,WRF} = 1.93 \times 10^{8} Bq/d$$

3.1.2. Results and Discussion

^{131}I activity was consistently found in the sewage effluent from both Jones Island and South Shore WRFs. ^{131}I activities and fluxes were always nonzero, and generally fluctuated within an order of magnitude (**Figure 4**).

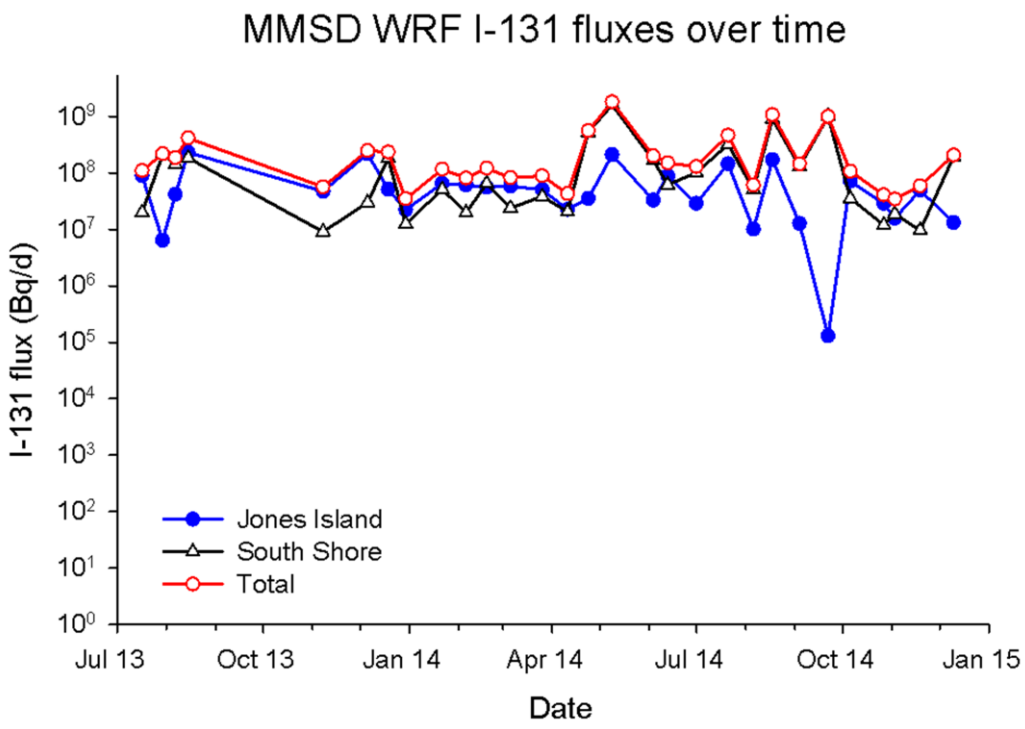

Figure 4 ^{131}I fluxes from the two Milwaukee Metropolitan Sewerage District (MMSD) water reclamation facilities (WRFs) over time. Standard deviations can be found in Appendix A.

The flux of ^{131}I from Jones Island WRF to the Milwaukee outer harbor varied from $(1\pm96)\times10^{5}$ to $(2.29\pm0.11)\times10^{8}$ Bq/d over the entire time it was monitored (July 2013-December 2014), and from $(1\pm96)\times10^{5}$ to $(1.71\pm0.11)\times10^{8}$ Bq/d over June-October 2014, when outer harbor sampling took place. The mean ^{131}I flux from Jones Island WRF was $(6.64\pm0.12)\times10^{7}$ Bq/d.

The activity of ^{131}I in sewage effluent from the Jones Island WRF varied from 0.0005±0.04 to 0.95±0.05 Bq/L (mean: 0.25±0.26 Bq/L; n=29). The discharge of treated sewage effluent varied from 2.1×10^{8} to 5.7×10^{8} L/d (mean: 2.9×10^{8} L/d; **Figure 5**).

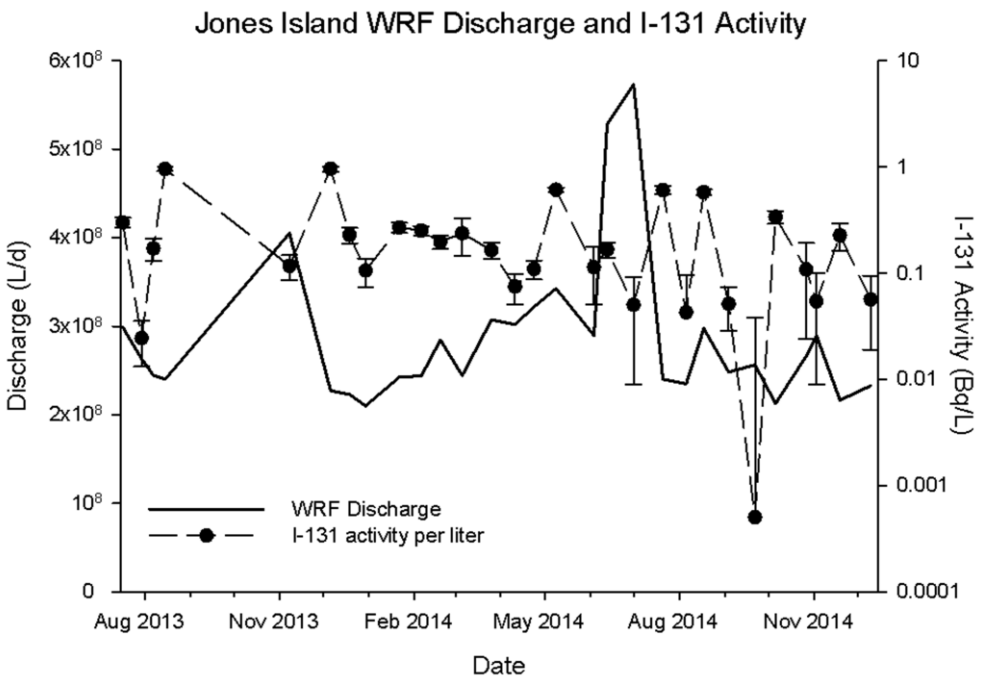

Figure 5 Sewage effluent discharge and ^{131}I activity from Jones Island Water Reclamation Facility (WRF) over time.

The flux of ^{131}I from South Shore WRF to Lake Michigan varied from $(9.1\pm6.3)\times10^{6}$ to $1.599\pm0.021\times10^{9}$ Bq/d over June 2013-December 2014. The mean ^{131}I flux from South Shore WRF was $(2.07\pm0.68)\times10^{8}$ Bq/d over the same time period.

The activity of ^{131}I in sewage effluent from the South Shore WRF varied from 0.03±0.02 to 4.52±0.06 Bq/L (mean: 0.74±1.21 Bq/L; n=29). The discharge of treated sewage effluent varied from 2.2×10^{8} to 4.3×10^{8} L/d (mean: 2.8×10^{8}) (**Figure 6**).

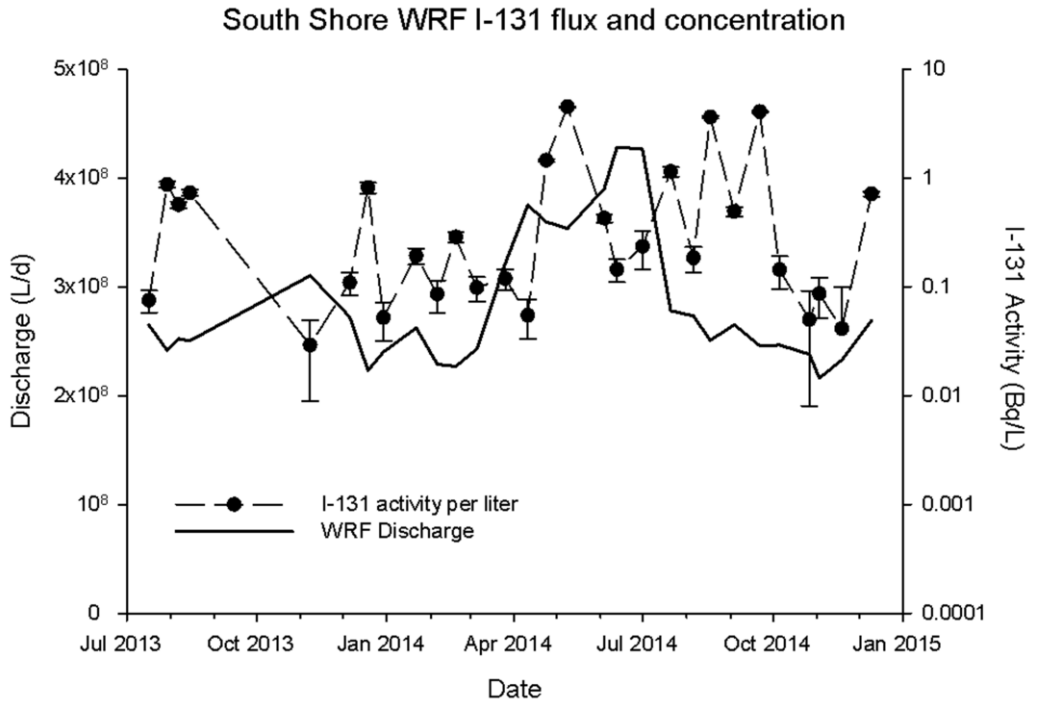

Figure 6 Sewage effluent discharge and ^{131}I activity from South Shore Water Reclamation Facility (WRF) over time.

The combined flux of Milwaukee-sourced ^{131}I into Lake Michigan was relatively consistent and predictable, where decreases in ^{131}I flux from one WRF were compensated by increased ^{131}I fluxes from the other WRF. The ^{131}I flux from the two combined WRFs varied from $(3.4\pm1.5)\times10^{7}$ Bq/d to $(1.807\pm0.024)\times10^{9}$ Bq/d. The mean combined ^{131}I flux was $(2.78\pm0.72)\times10^{8}$ Bq/d.

To test our assumption that all significant ^{131}I activity found in the Milwaukee area of Lake Michigan originates from the MMSD WRFs, we also tested the sewage effluent of the four largest WRFs in the Lake Michigan basin within 50km of the JI WRF at Cedarburg, West Bend, South Milwaukee and Racine. WRFs discharging to the Milwaukee River (i.e., Cedarburg and West Bend) showed no quantifiable ^{131}I activity (data shown in Appendix A). This is consistent with a report by Apfelbaum et al. (2007) stating that non-MMSD WRFs in the Milwaukee River

watershed account for less than 1% of the watershed's wastewater. The Racine WRF, situated 35km of the JI WRF on Lake Michigan, did show notable ^{131}I activity (data shown in Appendix A). Even so, the flux of ^{131}I from the Racine WRF was only $(7.22\pm0.23)\times10^{7}$ Bq/d, or 25% of the mean flux from the combined MMSD WRFs. Additionally, Racine WRF is well to the south of our study area in a part of the lake with a prevailing southerly current (Beletsky et al. 1999), and on the other side of Wind Point, a large geographical feature and likely barrier to interference from Racine ^{131}I (**Figure 7**). The hypothesis of Wind Point acting as a geographical barrier to Racine ^{131}I moving north is supported by our finding of ^{131}I activity in *Cladophora* algae on the northern and southern sides of the point, but not off the tip of the point itself (see chapter 2.2.2.).

Figure 7 Western coastline of Lake Michigan showing the cities of Milwaukee and Racine separated by Wind Point.

The mean total measured ^{131}I flux of ~3×10^{8} Bq/d from both (JI and SS) MMSD WRFs was close to the expected flux derived from simple demographics. Using Milwaukee County cancer incidence rates from the National Cancer Institute, average incidence rates for hyperthyroidism, and typical U.S. ^{131}I treatment dosages (Smith et al. 2008), roughly 3×10^{11} to 1×10^{13} Bq of ^{131}I are administered to Milwaukee patients per year. Taking into account that ~70% of administered ^{131}I is excreted from the body (Smith et al. 2008), ~1% of sewage ^{131}I activity is removed in sewage sludge (Martin and Fenner 1997, Rose et al. 2012), and roughly estimating the residence time in sewage infrastructure as one day (MMSD pers. comm.), gives an estimated flux of 5×10^{8} to 8×10^{9} Bq d^{-1} of ^{131}I leaving the combined MMSD WRFs. The low end of this estimate is within a factor of two of our finding. This demonstrates the ease with which metropolitan areas can calculate a rough estimate of ^{131}I flux in sewage effluent discharge. If a metropolitan area produces a predicted ^{131}I flux at least as large as that of Milwaukee, it is likely that ^{131}I could be found in the receiving water body, as we demonstrate in the results below.

3.2. *Cladophora*

3.2.1. Methods

In order to assess the spatial extent and magnitude of ^{131}I activity in nearshore Lake Michigan near Milwaukee, the green algae *Cladophora glomerata* (Linnaeus) Kuetzing (referred to as simply *Cladophora* in this study) was sampled. Sites along the shoreline and in the nearshore zone were periodically sampled between July 2013 and July 2014. Samples were taken by hand, and excess water was squeezed from the algae before placing it in a sealed container. The samples were then analyzed for ^{131}I activity by gamma spectroscopy (described in chapter 2.).

Certain samples were attached to rocks, while others had already sloughed and drifted in. Additionally, some samples were analyzed dry and ground, and others were wet and whole. The different counting methods gave similar results, as discussed below. These differences in sample processing are all recorded in Appendix H. All *Cladophora* samples were weighed wet, and then dried and weighed dry, regardless of whether they were analyzed wet or dry. The samples were dried by squeezing out any excess water, spreading them out and drying for 48 hours at 60ºC. If analyzed dry, the samples were ground in a coffee grinder for an even and well-packed geometry. ^{131}I activity per unit dry weight was then calculated by dividing the ^{131}I activity in the sample by its dry weight. Example 2 below walks through the calculation process.

Example 2 *Calculation of sample activity for an example* Cladophora *sample.*

Sample	Grant *Cladophora* Example
Time collected	9/30/13 13:45
Time of gamma analysis start	10/2/13 13:06
Time elapsed after collection (t_c)	1.97 d
Condition	Live, attached
Type	Dried, ground
Container	Vial
^{131}I peak energy (E)	364.27 keV
^{131}I counts (ct)	430
Live time (t_L)	163898 s
^{131}I half-life ($t_{1/2}$)	8.0233 d
^{131}I branching fraction (BF)	0.812
Detector	1
Sample Dry Weight (DW)	0.00233 kg

Calculation of counts per second (cps):

$$cps = \frac{ct}{t_L}$$

$$cps = \frac{430}{163898\ s} = 0.00262 s^{-1}$$

^{131}I decay constant (λ):

$$\lambda = \frac{ln\,2}{t_{\frac{1}{2}}}$$

$$\lambda = \frac{ln\,2}{8.0233\ d} = 0.0864\ d^{-1}$$

Correction factor for decay during counting (CF) after converting t_L from seconds to days:

$$CF = \frac{t_L\lambda}{1 - e^{-t_L\lambda}}$$

$$CF = \frac{1.90d \times 0.0864d^{-1}}{1 - e^{-1.90d \times 0.0864d^{-1}}} = 1.08$$

Sample counting efficiency (Eff) for a vial on Detector 1:

$$Eff = \frac{0.0251 + 0.168}{e^{-(E-756)/-17.9}}$$

$$Eff = \frac{0.0251 + 0.168}{e^{-(364.27\ -756)/-17.9}} = 0.194$$

^{131}I activity at time of analysis (A'):

$$A' = \frac{cps \times CF}{BF \times Eff}$$

$$A' = \frac{0.00262s^{-1} \times 1.08}{0.812 \times 0.194} = 0.00305Bq$$

^{131}I activity at time of collection (A_0):

$$A_0 = \frac{A'}{e^{-\lambda t_c}}$$

$$A_0 = \frac{0.00305Bq}{e^{-0.0864d^{-1} \times 1.97d}} = 0.00362Bq$$

^{131}I activity per unit dry weight:

$$\frac{A_0}{DW} = \frac{0.00362Bq}{0.00233kg} = 1.55Bq/kg\ DW$$

2.2.2. Results and Discussion

^{131}I activity was found in *Cladophora* across a wide stretch of Milwaukee area shoreline, as well as in the nearshore zone (**Figure 8**). This includes areas both north and south of both MMSD WRFs. For sites sampled at multiple time points, activities varied. The highest ^{131}I activities were usually seen at Grant and Bender parks, just north and south of South Shore WRF, respectively. ^{131}I activity was found to some degree in all *Cladophora* samples, except at the Wind Point Jetty, and at one time point at Atwater (data shown in Appendix H). The data in

Table 1 and **Figure 8** show mean ^{131}I activities for samples with measured dry weights.

Additional ^{131}I activity measurements in *Cladophora* are listed in Appendix H.

Table 1 Mean ^{131}I activities per gram dry weight (g DW) in *Cladophora* at various sites in the Milwaukee area of Lake Michigan, listed in geographical order from north to south.

Site	Mean ^{131}I Bq/g DW			*n*
Atwater	0.96	±	0. 93	3
Bradford	5.46	±	0.64	3
Lorier	20.1	±	1.5	1
S. Wall	1.47	±	0.23	2
Green Can	0.62	±	0.14	1
Grant	38.84	±	0.75	3
Bender	14.61	±	0.40	4
Reef 2	0.60	±	0.48	1
Wind Pt N	0.30	±	0.19	1
Wind Pt Jetty	0	±	0	1
Wind Pt S	0.132	±	0.048	1

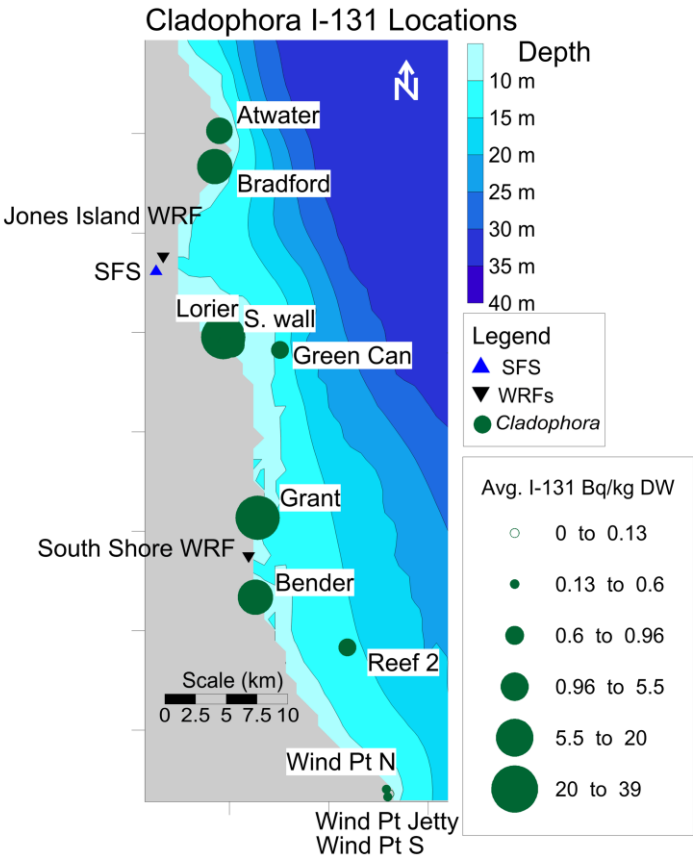

Figure 8 Locations and relative ^{131}I activities per kg dry weight in the Milwaukee nearshore area of Lake Michigan.

Comparing ^{131}I activities in samples that were analyzed both wet and dry didn't show any clear differences, though our data are not extensive enough for a thorough comparison. Any differences in ^{131}I activity between the wet and dry counts of the same sample were within one standard deviation (**Table 2**). However, for one sampling date at the S. wall station, attached and sloughed *Cladophora* samples were collected at the same time. The attached *Cladophora* sample contained a slightly higher (but just within one standard deviation) ^{131}I activity per unit dry weight. This difference, however, is expected to be very variable depending on the sample location, and from where the sloughed *Cladophora* has drifted in. For this reason we preferentially collected live, attached *Cladophora* whenever it was present. These results

informed us to focus on counting subsequent samples wet to use less time on processing before gamma analysis. Although there was no apparent ^{131}I loss in the drying and grinding process, counting precision was not improved. Additionally, the loss of a few days of time to sample processing was likely to offset any benefit of concentrating the ^{131}I signal through drying and grinding.

Table 2 Comparison of ^{131}I activities of *Cladophora* before and after drying. The bottom two rows compare ^{131}I activities per gram dry weight between samples collected at the same time and place, but in different condition, i.e. one live and attached sample and one sloughed sample.

Site	Date	Condition	^{131}I Activity
Atwater	7/8/13	Wet, squeezed	0.046 ± 0.020 Bq/sample
Atwater	7/8/13	Dry, ground	0.042 ± 0.071 Bq/sample
Bender	7/10/13	Wet, squeezed	0.354 ± 0.022 Bq/sample
Bender	7/10/13	Dry, ground	0.309 ± 0.032 Bq/sample
S. wall	9/10/13	Collected live, dried	0.354 ± 0.022 Bq/g
S. wall	9/10/13	Collected sloughed, dried	0.309 ± 0.032 Bq/g

Unsurprisingly, *Cladophora* collected from the sites closest to the WRF outfalls regularly had the highest ^{131}I activities. This was especially apparent at the sites nearest the SS WRF, Grant and Bender parks. The area surrounding the JI WRF outfall is the highly urbanized Milwaukee harbor, which due to high turbidity does not have any notable *Cladophora* growth. Even so, the closest site to JI WRF, Lorier, showed very strong ^{131}I activity.

One of the most notable results is the moderate ^{131}I activity at the Bradford site, and the low, but measurable activity found at the Atwater site. Because these sites are north of Milwaukee harbor and both MMSD WRFs, they are often thought to be less influenced by urban pollution. Atwater in particular, is often used as a more pristine reference site to contrast with more urban sites nearer the Milwaukee harbor (Olapade et al. 2006).

There are public beaches at the Atwater, Bradford, Grant and Bender sites, making the ^{131}I activities found there particularly notable. Since ^{131}I is sourced from recent treated sewage, its often-high activity in *Cladophora* found at beaches indicates that the area was recently bathed in treated (or, in the event of a sewer overflow or infrastructure failure, untreated) sewage. This fact suggests possible concerns from a public health perspective. This topic is further discussed in chapter 5.2.

3.3. Dreissenid mussels

Dreissenid mussels in Lake Michigan consist of two invasive Ponto-Caspian mussel species: *Dreissena polymorpha* (Pallas, 1771) and *Dreissena rostriformis bugensis* Andrusov, 1897. These mussels coat the lakebeds of the Great Lakes almost entirely (Nalepa et al. 2010). This leads to the question of if dreissenid mussels effectively concentrate ^{131}I. No studies to date have examined stable iodine or ^{131}I in relation to dreissenids, but if they were found to concentrate ^{131}I, their year-round ubiquity even in deep water would make them useful additions to *Cladophora* as bioconcentrators of ^{131}I and sentinels of recent sewage effluent exposure.

3.3.1. Methods

To assess the potential for dreissenid mussels to concentrate ^{131}I, mussels were sampled in the nearshore (depth < 15m) and offshore (depth >15m) zones. Sampling was carried out opportunistically from July 2013 to July 2014. Mussels were collected by PONAR grab or by hand. Mussel samples were processed differently in a variety of ways to determine the most efficient way to measure ^{131}I. Samples were counted either wet or dry (48 hours at 60ºC), but were weighed both wet and dry. Some samples were not weighed due to their large mass and the presence of rocks and sediment. These samples were simply analyzed qualitatively for the presence of ^{131}I. Some samples were also dissected using a small metal spatula, and were

separated into tissue and shells. Additionally, the larger dried samples were ground by coffee grinder to make a well packed and even counting geometry. The type of processing was recorded for each sample (data shown in Appendix G). Each sample was analyzed by gamma spectrometry (chapter 2.) and ^{131}I activities were calculated per unit dry weight. For samples collected by PONAR grab, the activity per unit area (calculated using the footprint area of the PONAR grab) was also calculated. An example calculation is shown in Example 3 below.

Example 3 *Calculation of sample activity for an example dreissenid mussel sample.*

Sample	S. wall mussels Example
Time collected	9/24/14 11:35
Time of gamma analysis start	9/28/14 15:38
Time elapsed after collection (t_c)	4.17 d
Part	Tissue
Type	Dried, ground
Container	Vial
^{131}I peak energy (E)	364.00 keV
^{131}I counts (ct)	23
Live time (t_L)	171616 s
^{131}I half-life ($t_{1/2}$)	8.0233 d
^{131}I branching fraction (BF)	0.812
Detector	1
Sample Dry Weight (DW)	0.00441 kg
Sampled Area	0.0350 m^2

Calculation of counts per second (cps):

$$cps = \frac{ct}{t_L}$$

$$cps = \frac{23}{171616\ s} = 0.000134 s^{-1}$$

^{131}I decay constant (λ):

$$\lambda = \frac{ln\,2}{t_{\frac{1}{2}}}$$

$$\lambda = \frac{ln\,2}{8.0233\ d} = 0.0864\ d^{-1}$$

Correction factor for decay during counting (CF) after converting t_L from seconds to days:

$$CF = \frac{t_L \lambda}{1 - e^{-t_L \lambda}}$$

$$CF = \frac{1.99d \times 0.0864d^{-1}}{1 - e^{-1.99d \times 0.0864d^{-1}}} = 1.09$$

Sample counting efficiency (Eff) for a vial on Detector 1:

$$Eff = \frac{0.0251 + 0.168}{e^{-(E-756)/-17.9}}$$

$$Eff = \frac{0.0251 + 0.168}{e^{-(364.00-756)/-17.9}} = 0.194$$

^{131}I activity at time of analysis (A'):

$$A' = \frac{cps \times CF}{BF \times Eff}$$

$$A' = \frac{0.000134s^{-1} \times 1.09}{0.812 \times 0.194} = 0.000922Bq$$

^{131}I activity at time of collection (A_0):

$$A_0 = \frac{A'}{e^{-\lambda t_c}}$$

$$A_0 = \frac{0.000922Bq}{e^{-0.0864d^{-1} \times 4.17d}} = 0.00132Bq$$

^{131}I activity per unit dry weight:

$$\frac{A_0}{DW} = \frac{0.00132Bq}{0.00441kg} = 0.299Bq/kg$$

^{131}I activity per unit area:

$$\frac{A_0}{Area} = \frac{0.00132Bq}{0.0350m^2} = 0.0378Bq/m^2$$

3.3.2. Results and Discussion

Dreissenid mussels were not sampled as widely as *Cladophora*, but some samples did show ^{131}I activity (**Table 3**, **Figure 9**). ^{131}I activities per unit dry weight ranged from zero to 3.7±1.3 Bq/kg, with the highest sample being found at the S. wall site just south of the Milwaukee outer harbor. By area, ^{131}I activities ranged from zero to 0.86±0.58 Bq/m^2, with the highest sample being found at site 5H, near the southern gap of the outer harbor. ^{131}I was found in mussels in and near the Milwaukee outer harbor, but not at sites north of the harbor.

Unfortunately, due to the opportunistic nature of our mussel sampling, no mussel samples were taken near South Shore WRF.

Table 3 Mean ^{131}I activity per square meter and per kilogram (dry weight) in whole dreissenid mussel samples at various sites in the Milwaukee area, shown in geographical order (north to south). N/A indicates that area or mass data were not available for the sample.

Site	^{131}I Mean Bq/m^2			*n*	^{131}I Mean Bq/kg DW			*n*
Atwater	0	±	0	2	0	±	0	2
Linwood	0	±	0	1	N/A	±	N/A	0
Bradford	N/A	±	N/A	0	0	±	0	1
Hoan Bridge	N/A	±	N/A	0	0.5	±	2.9	1
5 harbor	0.55	±	0.29	3	N/A	±	N/A	0
S. Wall	0.40	±	0.50	1	0.70	±	0.26	2

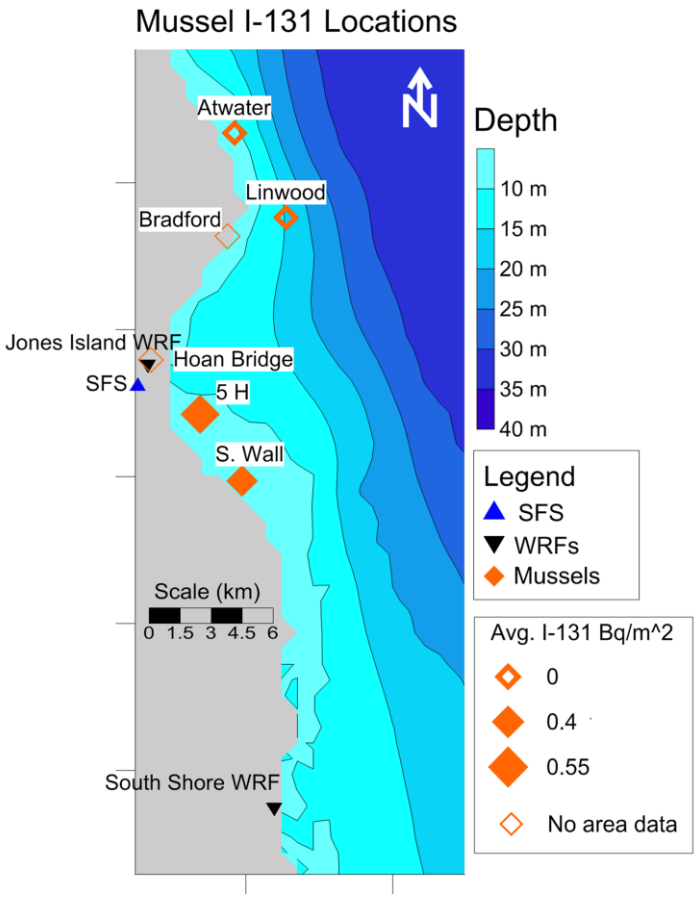

Figure 9 Locations and mean ^{131}I activity per square meter in dreissenid mussel samples in the Milwaukee area of Lake Michigan.

Attempts to determine whether ^{131}I was more concentrated in mussel shell versus mussel tissue were largely inconclusive. Results suggest significant ^{131}I activity can be found in both the mussel tissue and in (or on) the mussel shell. However, a number of mussel samples could not be processed and counted in time. Initial counts of ^{131}I activity in several whole mussel samples decayed past the limit of detection before both mussel parts could be analyzed. This is a limitation imposed by our number of detectors and slow sample throughput.

Mussel samples that could be separated and counted before complete ^{131}I decay are shown in **Table 4**. In the sample from 24 September 2014, the shells had higher ^{131}I activity (both in total for the same organisms, and per unit dry weight) than the tissue, but are within the one standard deviation. For 10 October 2013, mussel shells and tissue can't be compared per unit dry weight. However, when shells and tissue of the same organisms are compared, the shells show more ^{131}I activity than the tissue. Different whole mussels from the same date contained less ^{131}I per unit dry weight than the tissue sample, however, making the results even less clear. Because of this, and the large amount of time lost during the dissection process, mussel samples that were collected later were simply counted whole. Unfortunately, all samples that were analyzed both before and after drying contained no ^{131}I, so the effect of drying on ^{131}I activity could not be examined.

Table 4 Comparison of the different parts of selected mussel samples and their ^{131}I activity. The shells from 10/10/13 were not weighed, however the tissue and shells of the 10/10/13 sample came from the same organisms, but the whole mussels from the same date are different organisms.

Site	Date	Part	^{131}I Bq	^{131}I Bq/kg
S. wall	9/24/14	Shells	0.0269 ± 0.0346	0.66 ± 0.85
S. wall	9/24/14	Tissue	0.0013 ± 0.0027	0.30 ± 0.61
S. wall	10/10/13	Tissue	0.0693 ± 0.0229	3.7 ± 1.2
S. wall	10/10/13	Shells	0.1238 ± 0.0310	N/A ± N/A
S. wall	10/10/13	Whole	0.9107 ± 0.0685	1.144 ± 0.086

Dreissenid mussel samples contained much less ^{131}I per unit dry weight than *Cladophora* samples. The mean ^{131}I activity in all *Cladophora* samples was 10.4±4.7 Bq/kg, while for dreissenid mussels it was only 1.06±0.56 Bq/kg. However, dreissenid mussels were largely sampled at different sites than *Cladophora*. A comparison between *Cladophora* and dreissenid mussels at their common sites (though not always common dates) is shown below (**Table 5**). In this comparison as well, *Cladophora* usually shows higher ^{131}I activities per unit dry weight. These two organisms are also compared in 3.4.2. below.

Table 5 Comparison of ^{131}I activity per kg dry weight in *Cladophora* and dreissenid mussel samples taken at the same sites.

Type	Site	Date	Details	^{131}I Bq/kg
Cladophora	Atwater	8/9/13	Live, dried	1.55 ± 1.68
Mussels	Atwater	9/24/14	Whole, dried	0 ± 0
Cladophora	Bradford	9/4/13	Live, dried	2.92 ± 0.19
Mussels	Bradford	9/4/13	Whole, dried	0 ± 0
Cladophora	S. wall	9/10/13	Live, dried	2.53 ± 0.40
Cladophora	S. wall	9/10/13	Sloughed, dried	0.41 ± 0.23
Mussels	S. wall	10/10/13	Tissue, dried	3.7 ± 1.2
Mussels	S. wall	10/10/13	Whole, dried	1.144 ± 0.086

Dreissenid mussels contained ^{131}I activity near JI WRF and the Milwaukee outer harbor. However, outside of that area, they do not consistently show ^{131}I activity. When ^{131}I activity in mussels was found, it was lower than ^{131}I activity in *Cladophora* (chapter 3.2.). Dissecting the mussels and analyzing the tissue did not prove to be an effective way to concentrate the ^{131}I activity, and the time needed to dissect each mussel made dissection detrimental to efficient sample measurement. Despite the ubiquity of dreissenid mussels year-round in Lake Michigan, they do not appear to be especially effective concentrators of ^{131}I, unless they are near the radionuclide's source. However, in large enough samples, they do show measurable ^{131}I activity.

3.4. Benthic trawls

3.4.1. Methods

In order to better assess the spatial extent of Milwaukee-sourced ^{131}I into the offshore zone, benthic trawling surveys were performed with an epibenthic sled. Sampling was carried out on 20 October and 5 November 2014 at the stations shown in **Figure 10**. The epibenthic sled was created by modifying a stream drift net (45.4cm wide by 12.2 cm tall, **Figure 11**). The net was fortified with a pipe on the bottom edge, was fitted with runners to guide it in the correct position across the lake bottom, and had a piece of nylon fabric attached to protect the net bottom from tearing.

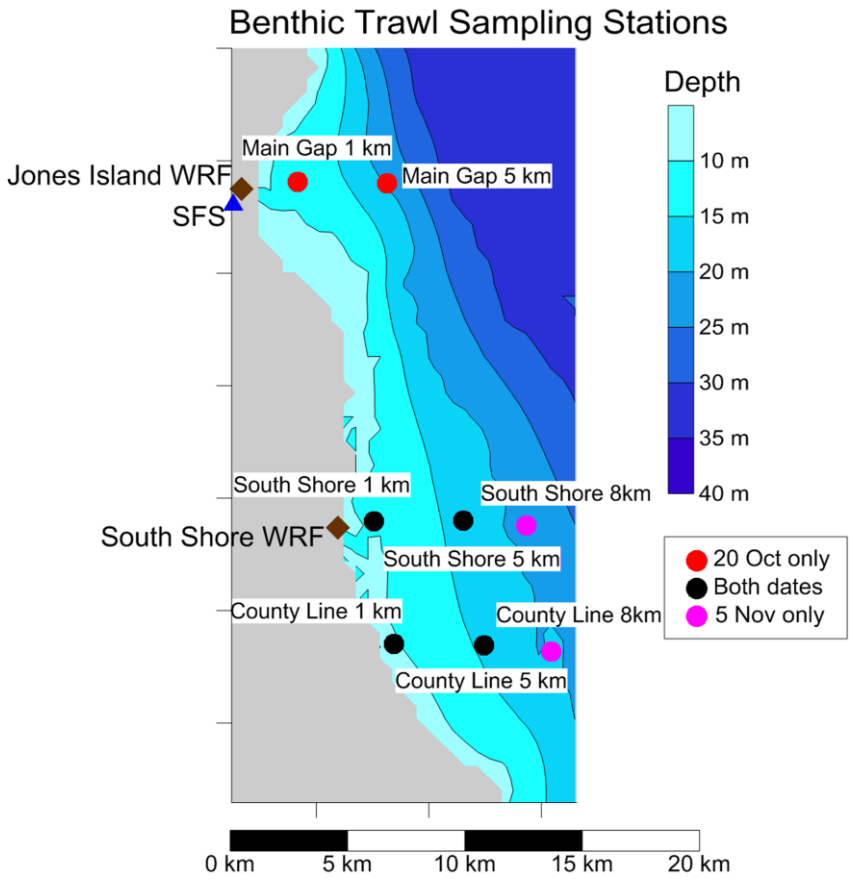

Figure 10 Benthic trawl sampling stations in the Milwaukee area of Lake Michigan on 20 October and 5 November 2014.

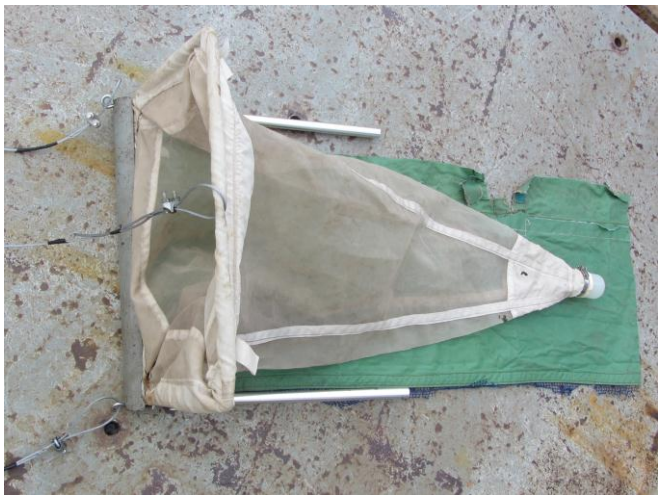

Figure 11 Epibenthic sled used for benthic trawl sampling.

The epibenthic sled was then lowered to the bottom and towed at 1 knot for 5 minutes before retrieval. This was repeated until at least ~1L of benthic material (determined visually) was collected at each station. The benthic material was then stored in plastic bags. In the lab, samples were mixed by hand and transferred to Marinelli beakers and analyzed by gamma spectroscopy (chapter 2.). The samples were then separated into *Cladophora*, dreissenid mussels, and abiotic material (which combined to comprise all collected material), and were dried and weighed. For one selected sample, these dried subsamples were analyzed separately to compare ^{131}I activity by material. This process took too much time to be carried out on other samples, due to the short half-life of ^{131}I. Activities were calculated per unit dry weight, area and material (where possible), and the composition of each full sample by weight was also calculated. An example calculation is shown below in Example 4.

Example 4 *Calculation of sample activity for an example benthic trawl sample.*

Sample	South Shore 1km Example
Time collected	10/20/14 15:06
Time of gamma analysis start	10/23/14 17:38
Time elapsed after collection (t_c)	3.11 d
Condition	Whole, wet
Container	Marinelli beaker
^{131}I peak energy (E)	365.61 keV
^{131}I counts (ct)	1260
Live time (t_L)	178114 s
^{131}I half-life ($t_{1/2}$)	8.0233 d
^{131}I branching fraction (BF)	0.812
Detector	2
Sample Dry Weight (DW)	0.607 kg
Sampled Area	493 m^2

Calculation of counts per second (cps):

$$cps = \frac{ct}{t_L}$$

$$cps = \frac{1260}{178114\ s} = 0.000707 s^{-1}$$

^{131}I decay constant (λ):

$$\lambda = \frac{ln\,2}{t_{\frac{1}{2}}}$$

$$\lambda = \frac{ln\,2}{8.0233\ d} = 0.0864\ d^{-1}$$

Correction factor for decay during counting (CF) after converting t_L from seconds to days:

$$CF = \frac{t_L \lambda}{1 - e^{-t_L \lambda}}$$

$$CF = \frac{2.06d \times 0.0864 d^{-1}}{1 - e^{-2.06d \times 0.0864 d^{-1}}} = 1.09$$

Sample counting efficiency (Eff) for a Marinelli beaker on Detector 2:

$$Eff = 0.0065 + 0.054 \times e^{-0.0040E}$$

$$Eff = 0.0065 + 0.054 \times e^{-0.0040 \times 365.61 keV} = 0.0190$$

^{131}I activity at time of analysis (A'):

$$A' = \frac{cps \times CF}{BF \times Eff}$$

$$A' = \frac{0.000707s^{-1} \times 1.09}{0.812 \times 0.0190} = 0.497Bq$$

^{131}I activity at time of collection (A_0):

$$A_0 = \frac{A'}{e^{-\lambda t_c}}$$

$$A_0 = \frac{0.497Bq}{e^{-0.0864d^{-1} \times 3.11d}} = 0.650Bq$$

^{131}I activity per unit dry weight:

$$\frac{A_0}{DW} = \frac{0.650Bq}{0..607kg} = 1.07Bq/kg = 1070mBq/kg$$

^{131}I activity per unit area:

$$\frac{A_0}{Area} = \frac{0.650Bq}{493m^2} = 0.00479Bq/m^2 = 4.79mBq/m^2$$

3.4.2. Results and Discussion

^{131}I was found in every benthic trawl sample taken. Sample activities per unit dry weight ranged from 49±87 mBq/kg to 1071±83 mBq/kg, with a mean activity of 288±81 mBq/kg. In general, ^{131}I activity per unit dry weight decreased with increasing distance from the shoreline, and was highest along the South Shore transect, extending from the SS WRF (**Table 6**). The notable exception to this trend is at the 8 km stations, where ^{131}I activity at County Line 8km exceeded (albeit within one standard deviation) that of the South Shore 8km station. In either case, ^{131}I was detected up to 8km from shore and up to 10km from the SS WRF outfall.

Table 6 Mean ^{131}I activities per kilogram dry weight in benthic trawl samples in Lake Michigan near Milwaukee.

Station	Mean ^{131}I mBq/kg DW			*n*
Main Gap 1km	188	±	66	1
Main Gap 5km	49	±	48	1
South Shore 1km	637	±	54	2
South Shore 5km	233	±	67	2
South Shore 8km	49	±	87	1
County Line 1km	456	±	328	2
County Line 5km	278	±	86	2
County Line 8km	94	±	52	1

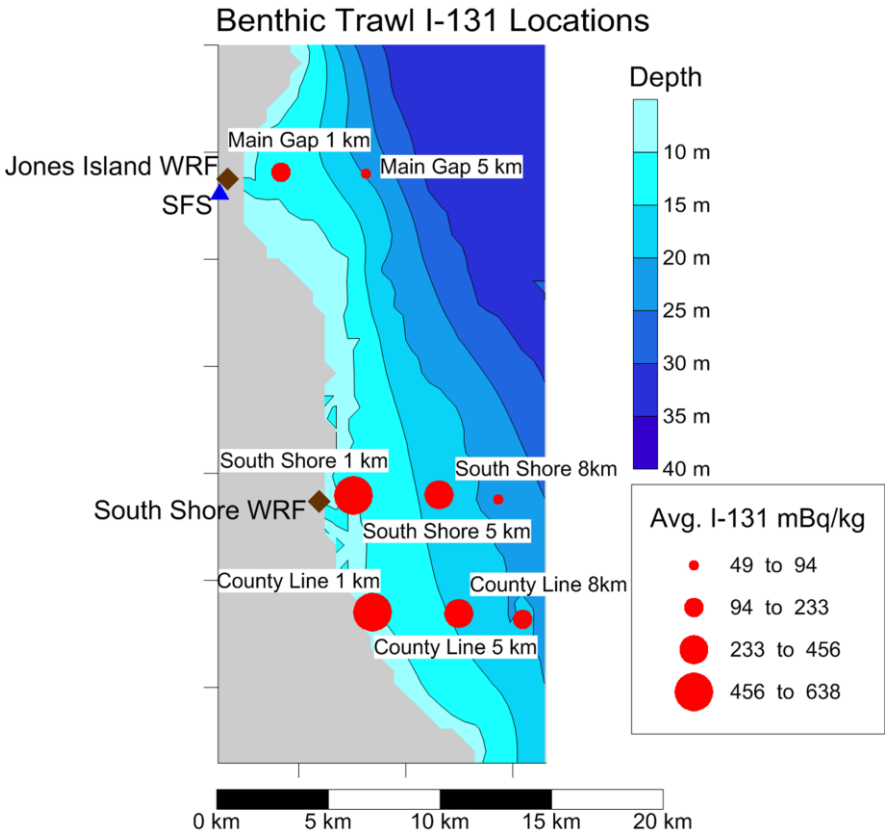

Figure 12 Mean ^{131}I activities per kg dry weight in benthic trawl sampling in Lake Michigan near Milwaukee.

The benthic trawl samples contained three main components: *Cladophora*, dreissenid mussels (and their empty shells), and abiotic material (e.g. sand and rock). The samples consisted

of, by mean dry weight, mostly abiotic material or mussels, with a small amount of *Cladophora*. However, the ^{131}I activity per unit dry weight in each material from the selected sample (South Shore 1km, 20 October 2014), behaved in the opposite manner. *Cladophora* contained the highest ^{131}I activity, followed by mussels and, finally, abiotic material (**Table 7**).

Table 7 Composition of the South Shore 1km sample from 20 October 2014. Activity per kilogram dry weight (Bq/kg), percent composition by dry weight (DW) and the percent of the sample's ^{131}I activity found in each material are shown. The right column also shows the mean percent of dry weight of each material among all samples.

Material	Bq/kg	Sample % DW	% Activity	Mean % DW
Abiotic	0.0091	74%	8%	46%
Dreissenids	1.1	20%	26%	48%
Cladophora	9.7	6%	66%	6%

These results give valuable insight into the ^{131}I enrichment of the different materials collected from the lakebed. In the South Shore 1km sample from 20 October 2014, shown in **Table 7**, dreissenid mussels contain an order of magnitude higher ^{131}I per kg than abiotic material, and *Cladophora* in turn contains an order of magnitude higher ^{131}I per kg than dreissenid mussels. This further reinforces my findings that *Cladophora* has an enhanced ability to concentrate ^{131}I from its surrounding environment. This finding is supported in the literature, which highlights macroalgae as effective concentrators of iodine through their active uptake of the micronutrient (e.g. Amachi 2008, Kleinschmidt 2009, Martinelango et al. 2006, Ullman and Aller 1985, Valentin 2004, Veliscek Carolan et al. 2011). The ^{131}I activity per unit dry weight in *Cladophora* and mussels in the South Shore 1km sample from 20 October 2014 (shown in **Table 7** above) is also remarkably similar to the mean activities per unit dry weight in these two organisms compared in chapter 3.3.2.

Perhaps most notably the benthic trawl results show the furthest measured extent of ^{131}I activity and sewage-derived material in Lake Michigan. This finding is discussed further in chapter 5.1.

3.5. Milwaukee outer harbor sediment

3.5.1. Methods

To determine the bed sediment inventory of ^{131}I in the Milwaukee outer harbor, sediment samples were collected from the outer harbor lakebed. Six sampling sites were chosen in the Milwaukee outer harbor and were numbered "1-6 H". Their locations are shown in **Figure 2**, (for specific coordinates see Appendix J). Sampling took place every 2-4 weeks from June-October 2014, for a total of six sampling dates: 20 June, 16 July, 29 July, 26 August, 24 September and 8 October. Sediment was collected from the outer harbor by PONAR grab during the 20 June and 24 September sampling events and by gravity core during the 16 July, 29 July, 26 August and 8 October sampling events.

PONAR grab sampling (Wildlife Supply Co., volume = 8200mL, grab area: 22.9cm × 22.9cm = 524cm^2) collects the most accessible surface sediment (grab depth ~7-17 cm in this study). This sediment is the most recently deposited, or the entirety of soft sediment above a hard substrate, and therefore is assumed to contain all activity of ^{131}I (due to its short half-life). Upon collection, the volume of the entire grab sample was measured and then the sample was homogenized in order to obtain more accurate areal radionuclide activities. If less than one liter of sediment was collected, additional PONAR grabs were performed and samples were added together until the sample contained at least one liter of sediment. The sediment was then transferred to a Marinelli beaker and analyzed by gamma spectroscopy to obtain the ^{131}I activity

of the sample. The ratio of the volume of sediment in the Marinelli beaker to the volume taken in the PONAR grab(s) was used to calculate the activity of the entire grab sample. ^{131}I activity of the grab sample was calculated per unit area, volume and dry weight. The sampling area was defined as the number of grabs multiplied by the PONAR grab area. The volume of wet total samples and counted samples was measured, along with wet weights. A smaller subsample of wet sediment was also taken to calculate the ratio of wet volume to dry weight. To do this, volume and wet weight were measured and then the subsample was dried for 48 hours at 60ºC and dry weight was measured. The ratio of wet volume to dry weight was used to calculate the dry weight of the counted sample.

Sediment was also collected by gravity coring. After collection, sediment cores (core area = 36.32cm^2) were extruded and the top 10cm (or the entire core if less than 10cm were collected) were sliced and stored for analysis. For the 16 July and 29 July sampling events, the cores were further sliced into 0-5cm and 5-10cm sections. We assume that activities of these short-lived radionuclides are negligible below 10cm. Core samples were then homogenized, placed in 89mm diameter plastic jars (Parkway Plastics, Inc.), and placed on gamma detectors for analysis. After counting, core samples were dried for 48 hours at 60ºC. Volume, wet weight (after collection and before counting) and dry weight were recorded. ^{131}I activity per units area, volume and dry weight were calculated. An example calculation is shown below in Example 5.

Example 5 *Calculation of sample activity for an example gravity core sample.*

Sample	3 H Core Example
Time collected	10/8/14 11:43
Time of gamma analysis start	10/14/14 17:16
Time elapsed after collection (t_c)	6.23 d
Container	Jar
^{131}I peak energy (E)	366.58 keV
^{131}I counts (ct)	226
Live time (t_L)	171113 s
^{131}I half-life ($t_{1/2}$)	8.0233 d
^{131}I branching fraction (BF)	0.812
Detector	2
Sample area	0.00363 m^2
Sample dry weight (DW)	0.202 kg
Sample volume (V)	0.242 L
Milwaukee outer harbor area ($Area_{OH}$)	4.43×10^6 m^2

Calculation of counts per second (cps):

$$cps = \frac{ct}{t_L}$$

$$cps = \frac{226}{171113\ s} = 0.00132 s^{-1}$$

^{131}I decay constant (λ):

$$\lambda = \frac{ln\,2}{t_{\frac{1}{2}}}$$

$$\lambda = \frac{ln\,2}{8.0233\ d} = 0.0864\ d^{-1}$$

Correction factor for decay during counting (CF) after converting t_L from seconds to days:

$$CF = \frac{t_L \lambda}{1 - e^{-t_L \lambda}}$$

$$CF = \frac{1.98d \times 0.0864 d^{-1}}{1 - e^{-1.98d \times 0.0864 d^{-1}}} = 1.09$$

Sample counting efficiency (Eff) for a jar on Detector 2:

$$Eff = 0.0073 + 0.060 \times e^{-0.0042E}$$

$$Eff = 0.0073 + 0.060 \times e^{-0.0042 \times 366.58 keV} = 0.0202$$

^{131}I activity at time of analysis (A'):

$$A' = \frac{cps \times CF}{BF \times Eff}$$

$$A' = \frac{0.00132s^{-1} \times 1.09}{0.812 \times 0.0202} = 0.0871Bq$$

^{131}I activity at time of collection (A_0):

$$A_0 = \frac{A'}{e^{-\lambda t_c}}$$

$$A_0 = \frac{0.0871Bq}{e^{-0.0864d^{-1} \times 6.23d}} = 0.149Bq$$

^{131}I activity per unit dry weight:

$$\frac{A_0}{DW} = \frac{0.149Bq}{0.202kg} = 0.739Bq/kg$$

I-31 activity per unit volume:

$$\frac{A_0}{V} = \frac{0.149Bq}{0.242L} = 0.618Bq/L$$

^{131}I activity per unit area:

$$\frac{A_0}{Area} = \frac{0.149Bq}{0.00363m^2} = 57.4Bq/m^2$$

The mean ^{131}I activity per unit area for all stations at this sampling date was 18.8Bq/m^2. This was used along with the Milwaukee outer harbor area to calculate the outer harbor ^{131}I inventory ($I_{I131,OH}$):

$$I_{I131,OH} = \left(\frac{\mathrm{A_0}}{\mathrm{Area}}\right)_{Avg} \times Area_{OH}$$

$$I_{I131,OH} = 18.8Bq/m^2 \times 4.43 \times 10^6 m^2 = 8.34 \times 10^7 Bq$$

3.5.2. Sediment collection comparison

PONAR grab sampling was compared to gravity coring to determine which method was the most precise. This was determined by taking three samples from the same area using both methods and comparing the standard deviation in the sample activities of ^{7}Be, an atmospheric-sourced radionuclide discussed in chapter 4. The sampling location was the slip next to the School of Freshwater Sciences, on the Kinnickinnic River in the Milwaukee inner harbor (**Figure 13**). All samples were processed and counted as described in 3.5.1. above.

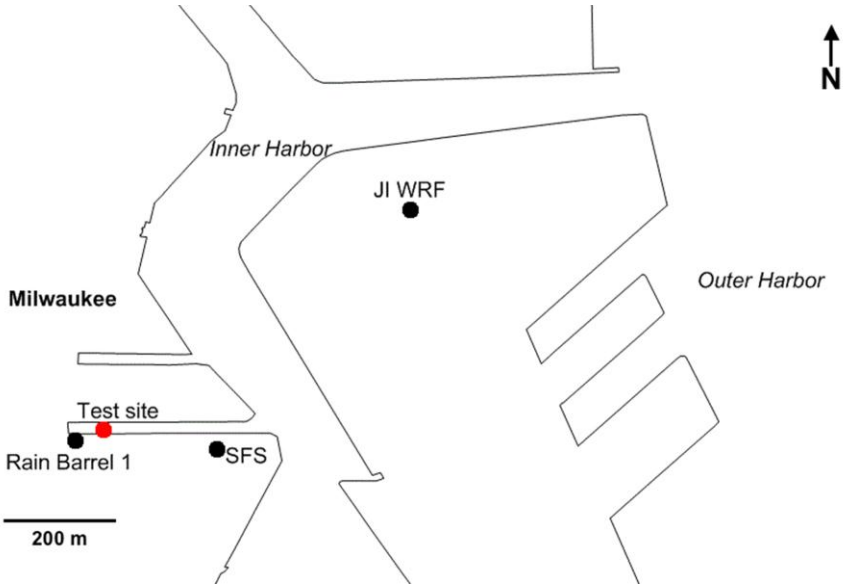

Figure 13 Area of the test site and rain barrel in the Milwaukee inner harbor relative to the School of Freshwater Sciences (SFS) and the Jones Island Water Reclamation Facility (JI WRF).

Gravity coring proved to have lower percent standard error between samples (**Figure 14**, **Table 8**, Appendix D). However, the ^{7}Be activity per unit area was unexpectedly higher in the gravity core samples than the PONAR grab samples by a factor of ~5.

Table 8 (Top) Test samples collected by gravity coring (GC) and PONAR grab (P) and their ^{7}Be activity per unit area. (Bottom) Comparison of gravity core and PONAR samples' mean and standard deviation (SD), and a comparison of the ^{7}Be flux needed to sustain that ^{7}Be activity with the mean (±SD) measured ^{7}Be rainfall flux from 19 June - 2 July, 2014. The test samples were collected 1 July, 2014.

Sample	^{7}Be (Bq/m^{2})		
GC 1	538	±	68
GC 2	590	±	236
GC 3	492	±	222
P 1	104	±	64
P 2	111	±	44
P 3	143	±	101

Gear	Mean ^{7}Be (Bq/m^{2})	SD	% SD	^{7}Be flux (Bq/m^{2}/d)			Mean ^{7}Be rain flux (Bq/m^{2}/d)		
GC	540	49	9%	7.00	±	0.64	10.5	±	4.3
P	119	21	18%	1.55	±	0.27	10.5	±	4.3

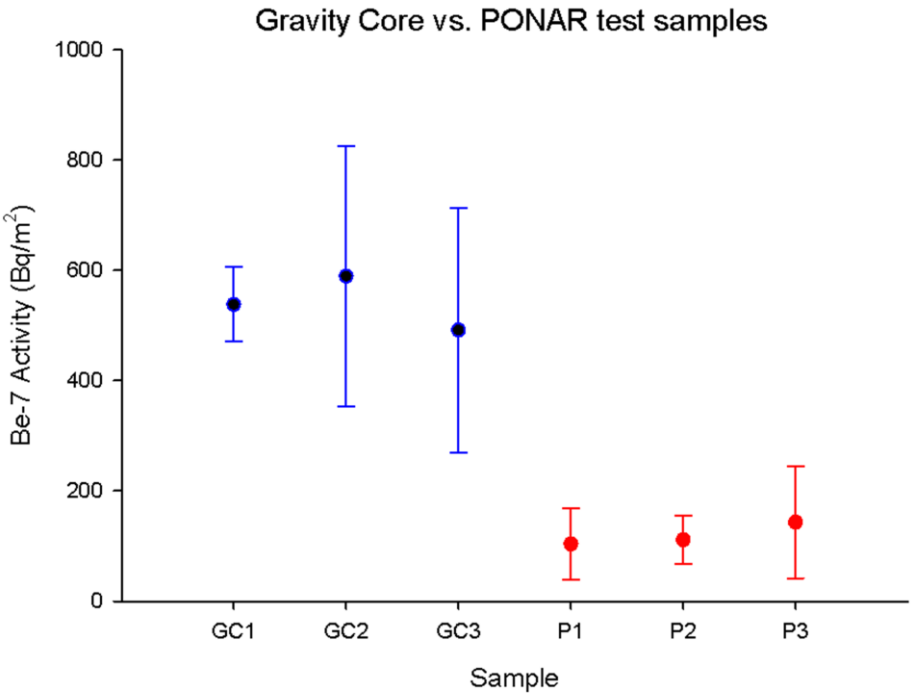

Figure 14 Comparison of ^{7}Be activity per unit area of triplicate gravity cores (left, blue) and PONAR grabs (red, right) taken from the same area.

Because of this large difference, it was unclear which method was more accurate and what the cause of the difference in ^{7}Be activity was. To determine which method was the most accurate, the ^{7}Be activities per unit area were compared with the flux of ^{7}Be from the atmosphere through rainfall (measured in chapter 4, below). The flux of ^{7}Be needed to sustain the ^{7}Be activity per unit area measured by each method was calculated and compared with the measured rainfall flux of ^{7}Be per unit area (**Table 8**). The flux calculated from the gravity core samples was within one standard deviation of the rainfall flux, while that of the PONAR samples was much lower. Therefore, we conclude that the gravity core samples yielded accurate ^{7}Be activities, while the PONAR samples did not.

It was not readily apparent whether the source of the difference in ^{7}Be activity was in the collection of the samples or in their measurement, since all gravity core samples were analyzed

in jar containers and all PONAR samples were analyzed in Marinelli beakers. To test whether this difference in sample container may be the source of the difference in activity, a new sediment sample was taken on 12 October, 2015 and was analyzed for ^{7}Be activity in both the jar and Marinelli beaker containers. The sample was taken with a PONAR grab at station 6H in the Milwaukee outer harbor. The samples were found to have ^{7}Be activities per unit area within one standard deviation of each other (311±80 Bq/m^2 for the jar sample and 360±52 Bq/m^2 for the Marinelli beaker sample). This finding leads us to believe that the source of the difference in ^{7}Be activities between the gravity core and PONAR test samples above is not due to the containers they were analyzed in.

Therefore, the difference in ^{7}Be activity must be due to the collection method. When a gravity core sample is collected, a plastic tube, fitted with a one-way valve at the top, is lowered straight into the sediment, and then lifted up and sealed at the bottom. In this way, the sediment-water interface is maintained relatively undisturbed. A PONAR grab, however, seals at the bottom during collection, and has a metal screen above the sample. The sediment-water interface is not protected. We have observed fine sediment leaking from the top of the PONAR grab during sample retrieval, especially in soft sediment like that of the test sample location. Surface sediment consists of the most newly deposited sediment. For radionuclides like ^{7}Be and ^{131}I, which are buried into the sediment bed from the water column and are enriched at the sediment-water interface, the top layer of newly deposited sediment contains the particles of the highest activity. Activity then usually drops off with sediment depth. Since PONAR grabs lose some surface sediment and effectively keep more deeper, lower activity sediment, they artificially lower the measured radionuclide activity. We expect that this sampling error is the source of the difference in ^{7}Be activity between the test sample triplicates shown above.

To test this hypothesis, we compared the ^{131}I and ^{7}Be inventories calculated in 3.5.3. and 4.3. below. If material from the sediment-water interface is indeed being lost during PONAR grab sampling, this should affect ^{131}I activity more than ^{7}Be activity. This is because ^{7}Be has a longer half-life (53.22 d) than ^{131}I (8.0233 d). With a longer half-life, ^{7}Be should have greater relative activity than ^{131}I in the deeper, older sediment which is not lost by the PONAR grab. Therefore we compared the ^{7}Be to ^{131}I ratios in the sediment inventories calculated below. The dates sampled by PONAR grab have higher $^{7}Be/^{131}I$ ratios (**Table 9**). This supports the hypothesis that the PONAR grab loses some newly buried sediment from the sediment-water interface, while gravity cores do not.

Table 9 Comparison of $^{7}Be/^{131}I$ ratio of bed sediment inventories between dates sampled by PONAR grab and gravity coring.

Date	Gear	$^{7}Be/^{131}I$ Ratio
6/20/14	PONAR	139
7/16/14	Gravity Core	21
7/29/14	Gravity Core	11
8/26/14	Gravity Core	4
9/24/14	PONAR	56
10/8/14	Gravity Core	16
Mean	**Gravity Core**	**13**
Mean	**PONAR**	**97**

Therefore, gravity coring is a more accurate and precise method of sediment collection than the PONAR grab. Because of this, we used gravity coring for the majority of our sampling events and exclusively to calculate the results of our sediment sampling. However, during some sampling events time or equipment limitations necessitated the use of the PONAR grab over gravity coring. The results of these events are shown below as well, but are denoted as such and should be interpreted while noting the method's limitations, described above.

3.5.3. Results and Discussion

Bed sediment ^{131}I inventories were calculated from the activity per unit area of gravity cores taken at each station. These station activities varied from 0 to 68±33 Bq/m^2 with a mean station ^{131}I activity of 21.6±4.3 Bq/m^2. ^{131}I inventories for the whole outer harbor were calculated in two ways: multiplying the mean of all stations' activities per unit area by the outer harbor area, and calculating the inventory by creating a contour map in the mapping program Surfer (Golden Software, Inc.). We will report the mean of the stations due to the lack of error calculation from the Surfer inventories, but the Surfer inventories are listed in **Table 10** for comparison. All Surfer inventories are within one standard deviation of the station mean method.

The inventories of ^{131}I in the outer harbor bed sediment vary over time, but within an order of magnitude. The ^{131}I bed sediment inventory of the entire outer harbor fluctuated around ~10^7-10^8 Bq, with a mean of (9.6±1.7)×10^7Bq. The individual inventories of ^{131}I at each of the four gravity coring sampling dates plus the two PONAR sampling dates are presented in **Figure 15** and **Table 10**. When sampling was done by gravity core, ^{131}I inventory was high for the first two dates and lower for the last two. The ^{131}I inventory was at its highest [(1.26±0.31)×10^8Bq] on 29 July, 2014 (28±17 Bq/m^2), and decreased to its lowest value [(5.2±1.4)×10^7Bq] on 26 August, 2014 (12±8 Bq/m^2). The spatial distribution of ^{131}I in the outer harbor bed sediment also changed over time, with varying stations showing high and low activities on each sampling date (**Figure 16**).

Table 10 Outer harbor inventories of ^{131}I in bed sediment at each sampling event in 2014, calculated by taking the mean of the activities per unit area at each station (left) and by the mapping program Surfer (right).

Sampling event	^{131}I (Mean) ($\times 10^7$ Bq)	^{131}I (Surfer) ($\times 10^7$ Bq)	Mean/Area (Bq/m^2)
Ponar 20 June	2.3 ± 1.1	3.1	5.1 ± 4.9
Gravity core 16 July	12.1 ± 2.9	12.4	27 ± 16
Gravity core 29 July	12.6 ± 3.1	15.4	28 ± 17
Gravity core 26 August	5.2 ± 1.4	5.9	11.8 ± 7.5
Ponar 24 September	2.67 ± 0.77	2.57	6.0 ± 3.5
Gravity core 8 October	8.34 ± 0.76	8.88	18.8 ± 4.2

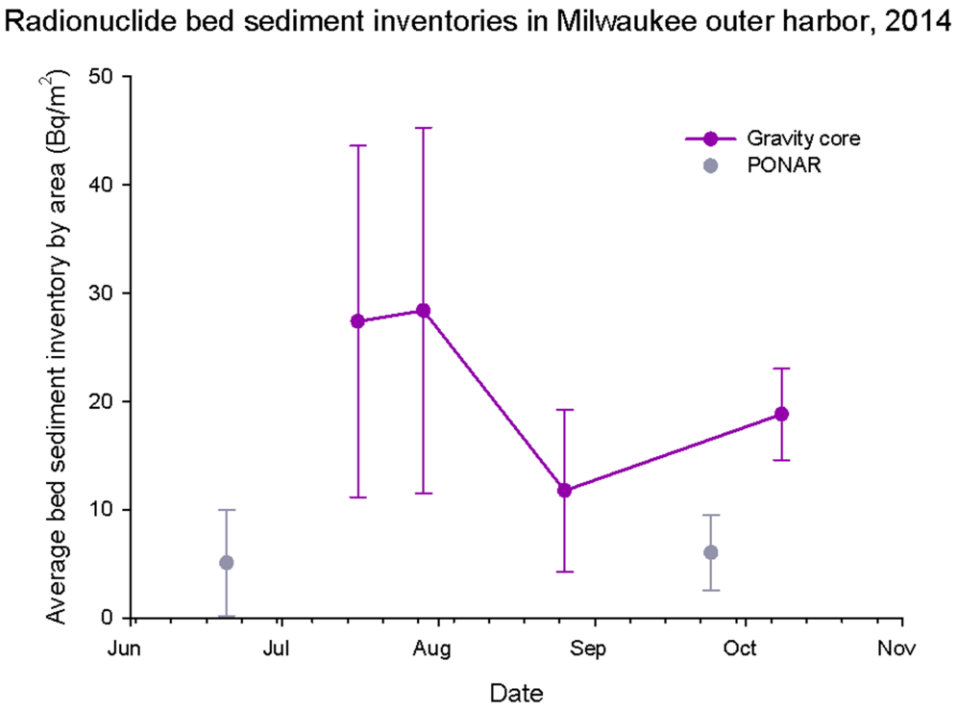

Figure 15 Bed sediment inventories per unit area of ^{131}I over four gravity core sampling dates in 2014. Inventories are means ± standard error. ^{131}I inventories from PONAR sampling dates are shown in gray.

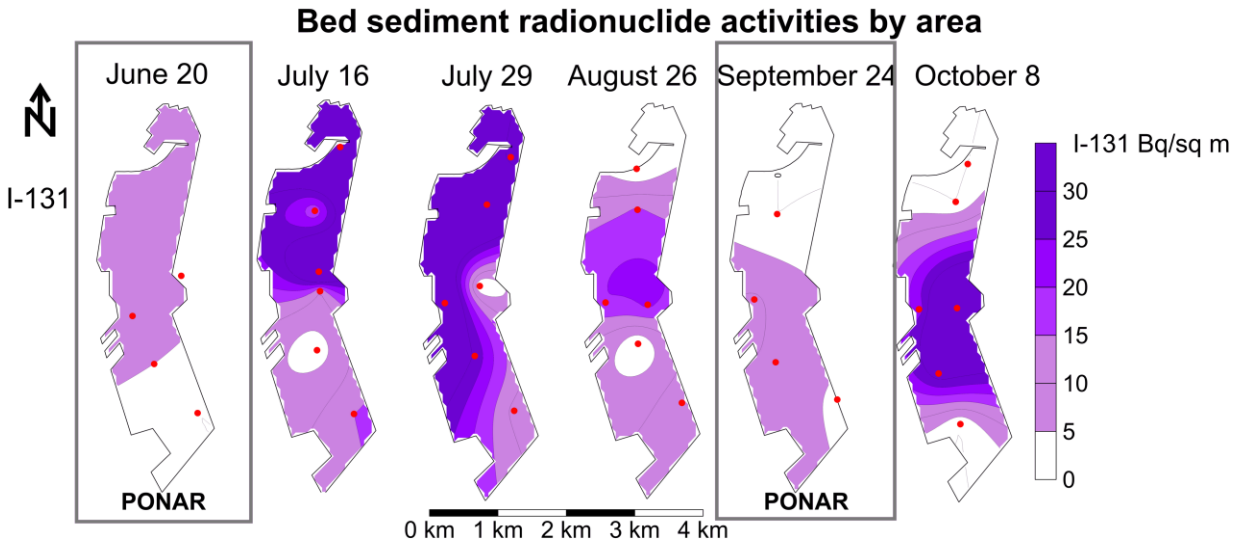

Figure 16 Contour maps of ^{131}I activity per unit area (Bq/m^2) in the Milwaukee outer harbor for different sampling dates in 2014, progressing from left to right in chronological order. Boxed maps show dates when samples were collected by PONAR grab, and activities are expected to be artificially low.

On all six sampling dates, ^{131}I was detected at at least several points in the Milwaukee outer harbor bed sediment. This suggests that ^{131}I, and by proxy, recent sewage effluent-derived material, is always present in the Milwaukee outer harbor. This, of course, is expected, since the outer harbor receives sewage effluent from Jones Island WRF and is partially enclosed. However, this finding is still important to note, because the Milwaukee outer harbor is a high traffic urban waterway important for transportation, industry, and recreation, including sailing and fishing.

^{131}I bed sediment inventories in the Milwaukee outer harbor change over time, but are relatively consistent compared to the ^{131}I flux from Jones Island WRF (**Figure 17**). These results also suggest that as long as ^{131}I be discharged from Jones Island WRF, new ^{131}I activity will continue to be added to the inventory in the outer harbor bed sediment.

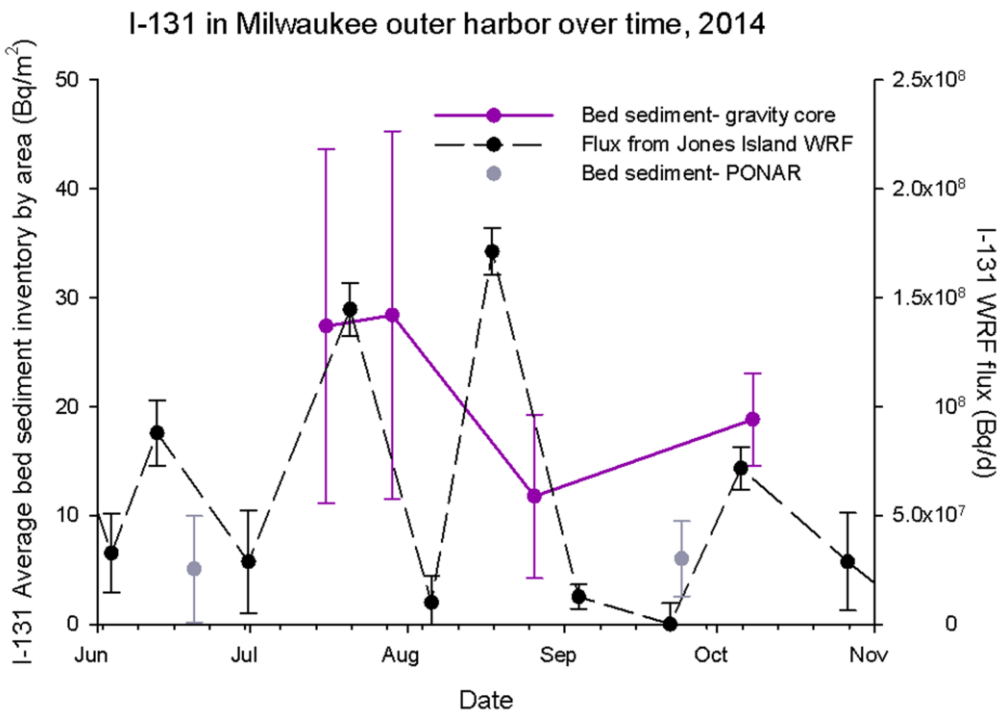

Figure 17 ^{131}I bed sediment inventory per unit area (mean± standard error) in the Milwaukee outer harbor and ^{131}I flux into the outer harbor from Jones Island Water Reclamation Facility (WRF) over the sampling season in 2014. Gray points represent dates sampled by PONAR grab.

The spatial distribution of ^{131}I activity per unit area in the outer harbor bed sediment did not stay constant over time, despite the fixed location of the Jones Island WRF outfall. Although ^{131}I was always detected near the outfall, little else remained constant over time in the ^{131}I spatial distributions. These changes could be due to differing current patterns or possibly the movement and deposition of surface sediment throughout the outer harbor during the sampling season.

3.6. Milwaukee outer harbor water

3.6.1. Methods

Water from the Milwaukee outer harbor was also examined for the presence of ^{131}I. Outer harbor water was collected during the 16 July, 29 July, 26 August and 8 October sampling events. Approximately 180L were collected from harbor stations 2H, 3H and 4H in total, during

each sampling event (**Figure 2**). Water was collected using a 30L Niskin bottle (General Oceanics, Inc.) and stored in 20L plastic carboys (Nalgene, Thermo Fisher Scientific Inc.). At each of the three stations, two carboys were filled with water from just below the surface, and one was filled with water taken from approximately 5m deep. The exception is the 16 July sampling date, when all water was taken from the surface. Outer harbor water sampling and analysis for each sampling date is summarized in **Table 11**.

Table 11 Outer harbor water sampling summary. X's indicate which sampling and analyses were carried out on each harbor sampling date, 2014.

Date	Surface water	Deep water	Particulate ^{131}I /TSM	Dissolved ^{131}I	Anion resin 2x
16 July	X		X		
29 July	X	X	X	X	
26 August	X	X	X	X	X
8 October	X	X	X	X	X

After collection, water samples were combined and filtered through glass fiber filters (142mm, 0.7µm pore size) for particulate matter (**Figure 18**). These filters were analyzed by gamma spectroscopy to determine particulate fraction activity of ^{131}I. They were then dried and weighed to calculate total suspended material (TSM; reported in Appendix E). The flow-through water was kept in three 75L plastic drums for further analysis.

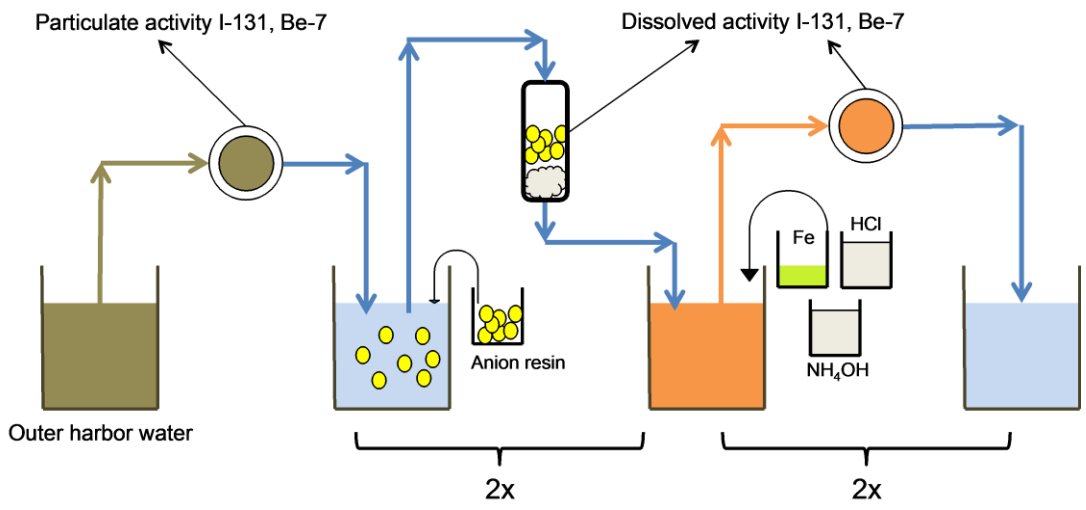

Figure 18 Filtering process to determine particulate and dissolved activities of ^{131}I and ^{7}Be in the outer harbor water column: filtering for particles (left), anion resin filtering for dissolved ^{131}I activity (center), and iron precipitate reaction and filtering for dissolved ^{7}Be activity (right).

For the 29 July harbor sampling events, three different types of filter media were used to capture dissolved ^{131}I. The water sample was pumped through three columns containing one filtering medium in each and glass wool in the bottom to keep any of the filter medium from leaving the column. The first column contained activated carbon (Sigma-Aldrich DARCO Activated Charcoal), the second anion resin (Baker Dowex 1-X8 anion exchange resin), and the third Mn-impregnated fiber (Scientific Computer Instruments). These filter media were then emptied into jars and were analyzed by gamma spectroscopy. The anion resin captured the most dissolved ^{131}I, therefore subsequent sampling dates discontinued the use of activated carbon and Mn-impregnated fiber.

For the 26 August and 8 October sampling events, the dissolved activity of ^{131}I was analyzed by adding the anion resin to the water and stirring for five minutes (Parekh et al. 2003). The anion resin was then filtered from the water through a column containing glass wool, and analyzed in jars by gamma spectroscopy (**Figure 18**). For the 26 August and 8 October sampling

events this was then repeated to capture any remaining ^{131}I and calculate the yield efficiency. The yield efficiency, or fraction of radionuclide activity captured by the anion resin, is calculated using an equation adapted from Rutgers van der Loeff et al. (2006):

$$A_{total} = A_1/(1 - A_2/A_1) \quad (6)$$

where A_{total} is the total activity of the radionuclide, A_1 is the measured activity from the first anion resin treatment and A_2 is the measured activity from the second anion resin treatment. The sources of inaccuracy in this calculation noted by Rutgers van der Loeff et al. (2006) are addressed here by adding anion resin in excess and using long contact times. On the 29 July sampling event, only one anion resin measurement was taken, so the mean A_2/A_1 ratio from the subsequent sampling dates was used to calculate A_{total}. An example calculation is shown in Example 6 below.

Example 6 *Calculation of sample activity for an example water column sample.*

Sample	Anion resin filter example
Time collected	10/8/14 11:07
Time of gamma analysis start	10/10/14 18:02
Time elapsed after collection (t_c)	2.29 d
Treatment #	1 of 2
Container	Jar
^{131}I peak energy (E)	364.75 keV
^{131}I counts (ct)	2949
Live time (t_L)	182786 s
^{131}I half-life ($t_{1/2}$)	8.0233 d
^{131}I branching fraction (BF)	0.812
Detector	3
Water Volume	212 L

Calculation of counts per second (cps):

$$cps = ct/t_L$$

$$cps = \frac{2949}{182786\ s} = 0.0161 s^{-1}$$

^{131}I decay constant (λ):

$$\lambda = ln\,2\,/t_{1/2}$$

$$\lambda = \frac{ln\,2}{8.0233\,d} = 0.0864\,d^{-1}$$

Correction factor for decay during counting (CF) after converting t_L from seconds to days:

$$CF = \frac{t_L\lambda}{1 - e^{-t_L\lambda}}$$

$$CF = \frac{2.12d \times 0.0864d^{-1}}{1 - e^{-2.12d \times 0.0864d^{-1}}} = 1.09$$

Sample counting efficiency (Eff) for a jar on Detector 3:

$$Eff = 0.0094 + 0.11 \times e^{-0.0044E}$$

$$Eff = 0.0094 + 0.11 \times e^{-0.0044 \times 364.75keV} = 0.0320$$

^{131}I activity at time of analysis (A'):

$$A' = \frac{cps \times CF}{BF \times Eff}$$

$$A' = \frac{0.0161s^{-1} \times 1.09}{0.812 \times 0.0320} = 0.675Bq$$

^{131}I activity at time of collection (A_0):

$$A_0 = \frac{A'}{e^{-\lambda t_c}}$$

$$A_0 = \frac{0.675Bq}{e^{-0.0864d^{-1} \times 2.29d}} = 0.822Bq$$

^{131}I activity per unit volume (A_0/V):

$$\frac{A_0}{V} = \frac{0.822Bq}{212L} = 0.00389Bq/L = 3.89mBq/L$$

Using A_0/V above as A_1 in equation (6), and A_2=1.88mBq/L, A_{total} is calculated below. In this case, A_{total} is the total ^{131}I activity per unit volume:

$$A_{total} = A_1/(1 - A_2/A_1)$$

$$A_{total} = \frac{3.89mBq/L}{1 - \frac{1.88mBq/L}{3.89mBq/L}} = 7.53mBq/L$$

3.6.2. Results and Discussion

^{131}I was found in the water column of the outer harbor on all three sampling dates. The total ^{131}I activity per unit volume in the outer harbor water column increased over time (**Figure 19**). No correlation was apparent with ^{131}I flux from the Jones Island WRF, however. Within the water column, the overwhelming majority of ^{131}I activity was found in the dissolved phase. However, ^{131}I was still detected in the particulate phase at each sampling event (**Table 12**). The mean particulate ^{131}I activity was 0.231±0.046 mBq/L, and the mean dissolved ^{131}I activity was 3.86±0.15 mBq/L. The mean total water column activity of ^{131}I in the outer harbor was 4.15±0.16 mBq/L.

Table 12 ^{131}I particulate and dissolved activities in the Milwaukee outer harbor water column on sampling dates in 2014, in units of mBq/L.

Date	^{131}I particulate activity			^{131}I dissolved activity		
16 July	0.043	±	0.053	No data		
29 July	0.208	±	0.079	1.48	±	0.24
26 August	0.022	±	0.081	2.56	±	0.34
8 October	0.65	±	0.14	7.53	±	0.15

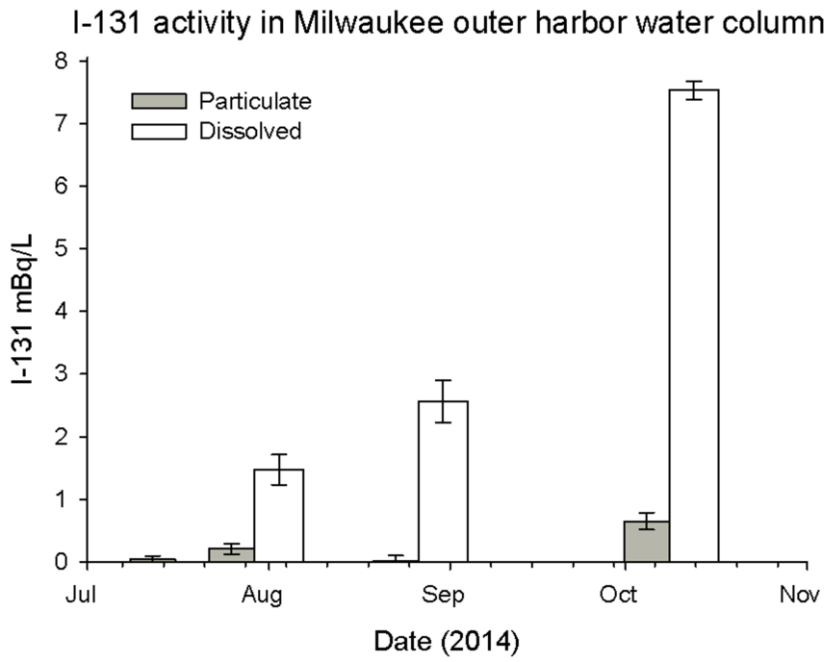

Figure 19 ^{131}I particulate and dissolved activities in the Milwaukee outer harbor on sampling dates in 2014.

The fact that ^{131}I was consistently found in the Milwaukee outer harbor water column indicates its potential for use as a tracer for processes taking place in the water column. So far in dealing with ^{131}I in Lake Michigan, we have only discussed its enrichment in the benthos. However, in environments such as the Milwaukee outer harbor, where ^{131}I is concentrated and enclosed enough, the detectability of ^{131}I in the water column in both the dissolved and particulate phase opens up several useful analyses.

Because the Milwaukee outer harbor not only receives sewage effluent, but also the combined mouth of Milwaukee's three rivers and all their suspended sediment, we focus on the uses of ^{131}I in tracing sediment dynamics in the Milwaukee outer harbor. This is discussed in depth below (5.3.).

4. Beryllium-7

In this chapter, I present time-series measurements of ^{7}Be activity in (*i*) sediment of the Milwaukee Outer Harbor, (*ii*) the water column of the Milwaukee Outer Harbor, with distinct measurements of both particle-bound and dissolved fractions, and (*iii*) atmospheric deposition (rainfall + dry deposition) at the School of Freshwater Sciences campus of the University of Wisconsin- Milwaukee. ^{7}Be activities in sediment and water are used, together with ^{131}I activities, to estimate sediment deposition rates in the Milwaukee Outer Harbor in chapter 5.

4.1. Background

Beryllium-7 (^{7}Be) is a relatively short-lived (half-life 53.22 d) gamma emitter (477.821 keV, 10.44% emissions; Nichols et al. 2008) that comes to Earth's surface through atmospheric deposition. In the atmosphere, ^{7}Be originates naturally from cosmic ray spallation of nitrogen and oxygen in the stratosphere and troposphere (Brost et al. 1991). ^{7}Be is a particle-reactive radionuclide that quickly sorbs to aerosols and other particles in the atmosphere. The main mode of deposition is in precipitation, although a small amount (~10%) descends via dry deposition (Doering and Akber 2008, Ioannidou and Papastefanou 2006). ^{7}Be adsorbs rapidly to solids when it enters freshwater systems (K_d [activity in sediment/activity in water]=10^5-10^6 L/kg; IAEA 2010; Blake et al. 1999, You et al. 1989, Hawley et al. 1986).

Like ^{131}I, ^{7}Be can be an effective tracer in freshwater systems. ^{7}Be shares the same benefits as ^{131}I from being a short-lived gamma emitter. ^{7}Be is also enriched in aquatic organisms like algae (Ishikawa et al. 2004, Karlander and Krauss 1972). Besides being found in biotic material, ^{7}Be is concentrated at the sediment-water interface (Ishikawa et al. 2004). Because of its atmospheric source, ^{7}Be can be found in the environment anywhere that has been recently

exposed to atmospheric fallout (Landis et al. 2014, Liu et al. 2001). ^{7}Be is therefore less specific than ^{131}I as a point-source tracer. However, ^{7}Be is usually found in the environment at much higher activities than ^{131}I. Due to these properties, ^{7}Be is a tracer of newly deposited sediment and can effectively be used to trace sediment dynamics in aquatic systems on the time scale of weeks to months. ^{7}Be has therefore been used to study river basins in the past (Fitzgerald et al. 2001, Dibb and Rice 1989, Olsen et al. 1986).

4.2. Methods

^{7}Be activity was measured simultaneously with ^{131}I in harbor bed sediment and the harbor water column (chapter 3.5.-3.6.). The only difference in measuring ^{7}Be was in the harbor water column dissolved phase, which required a different technique than ^{131}I.

For the outer harbor water column sampling events on 29 July, 26 August and 8 October, 2014, an iron precipitate reaction (e.g. Baskaran and Swarzenski 2006) was performed to adsorb dissolved ^{7}Be in the collected water. The reaction was carried out after the anion resin treatment (chapter 3.6.1.) by acidifying each drum of water with 250mL concentrated HCl, adding 1mL 25mg/L $FeSO_4$, then adding 250mL NH_4OH to raise the pH above 7 and create a precipitate. The drum was stirred throughout the process. The water sample was then filtered through glass fiber filters (142mm, 0.7µm pore size), and the filters (with precipitate) were analyzed by gamma spectroscopy (**Figure 18**). This was repeated, as with the anion resin above, to calculate yield efficiency on the 8 October sampling event. The resulting A_2/A_1 ratio from 8 October was then applied to the 29 July and 26 August sampling events to calculate dissolved ^{7}Be activity.

To measure the atmospheric ^{7}Be flux into the Milwaukee outer harbor, ^{7}Be activity was measured in rain samples. The flux of ^{7}Be atmospheric deposition was measured using a rain

barrel fit with a funnel (area = 0.22m^2) in an open space outside of the University of Wisconsin-Milwaukee School of Freshwater Sciences (**Figure 20**). Rainwater was collected every 1-14 days, depending on rainfall. Rainwater was collected by rinsing the funnel with 10% HCl to minimize the amount of ^{7}Be sorbed onto the funnel and barrel walls. The volume of rain and HCl were measured and the rain sample was homogenized. A homogenous 800 mL subsample was then poured into a 947 mL Marinelli beaker (GA-MA & Associates, Inc.) for gamma spectroscopy and analyzed (chapter 2.). The rain barrel location was changed mid-season due to construction activities in the initial location, but both locations were within 1 km from the outer harbor, and ^{7}Be atmospheric flux is assumed to be equal over both locations (Rain Barrel 1 moved to Rain Barrel 2 in **Figure 20**). For quality control, measured rainfall was compared to USGS hourly rainfall data taken from a rain gauge approximately 200m east of the School Freshwater Sciences.

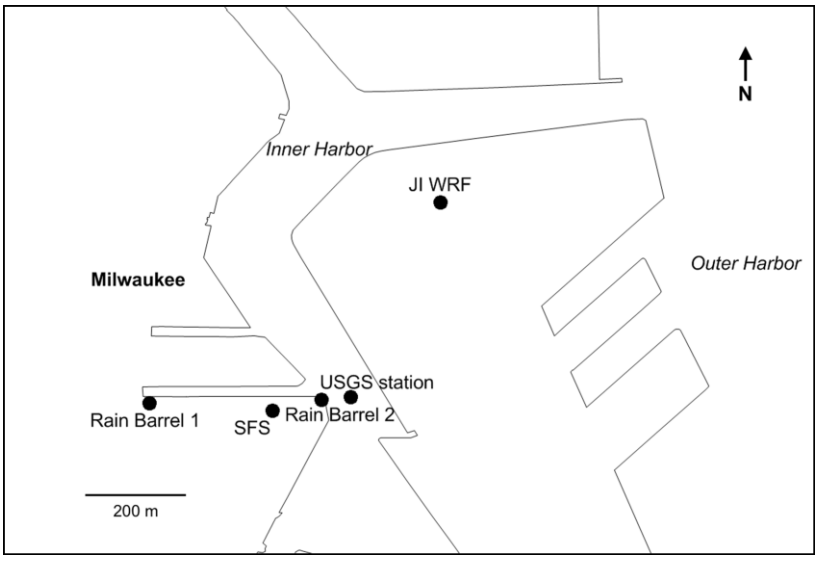

Figure 20 Location of rain barrels in relation to the University of Wisconsin-Milwaukee School of Freshwater Sciences (SFS), the USGS reference station and the Milwaukee inner and outer harbor.

For these rainwater samples, in addition to calculating the radionuclide activity at the time of collection (A_0) we also calculate the activity while still in the rain barrel (A_{barrel}). Due to

the often long barrel collection times and relatively short half-life of ^{7}Be, A_{barrel} is more representative of the radionuclide fluxes entering the system. A_{barrel} is calculated from A_0 using the following equation:

$$A_{barrel} = \frac{A_0 t_{barrel} \lambda}{1 - e^{-\lambda t_{barrel}}} \quad (7)$$

where t_{barrel} is the length of the collection period and λ is the decay constant. An example calculation of rainwater ^{7}Be activity and rainfall ^{7}Be flux is shown below in Example 7.

Example 7 *Calculation of sample activity for an example rainwater sample.*

Sample	Rainwater #4 Example
Time collected	6/27/14 11:00 to 7/2/14 10:26
Midpoint time	6/29/14 22:43
Time of barrel deployment (t_d)	4.98 d
Time of gamma analysis start	7/15/14 15:50
Time elapsed after collection (t_c)	15.7 d
Container	Marinelli beaker
^{7}Be peak energy (E)	478.83 keV
^{7}Be counts (ct)	341
Live time (t_L)	237821 s
^{7}Be half-life ($t_{1/2}$)	53.44 d
^{7}Be branching fraction (BF)	0.1044
Detector	3
Sample volume (V)	0.795 L
Rainwater volume	6.62 L
Rainwater + HCL volume (V_{barrel})	6.70 L
Funnel area ($Area_{funnel}$)	0.216 m^2
USGS rainfall	27.9 mm
Barrel rainfall	30.6 mm
Milwaukee outer harbor area ($Area_{OH}$)	4.43×10^6 m^2

Calculation of counts per second (cps):

$$cps = \frac{ct}{t_L}$$

$$cps = \frac{341}{237821\ s} = 0.00143 s^{-1}$$

^{7}Be decay constant (λ):

$$\lambda = \frac{ln\ 2}{t_{\frac{1}{2}}}$$

$$\lambda = \frac{ln\,2}{53.44\ d} = 0.01297 d^{-1}$$

Correction factor for decay during counting (CF) after converting t_L from seconds to days:

$$CF = \frac{t_L \lambda}{1 - e^{-t_L \lambda}}$$

$$CF = \frac{2.75d \times 0.01297 d^{-1}}{1 - e^{-2.75d \times 0.01297 d^{-1}}} = 1.02$$

Sample counting efficiency (Eff) for a Marinelli beaker on Detector 2:

$$Eff = 0.0047 + 0.046 \times e^{-0.0033E}$$

$$Eff = 0.0047 + 0.046 \times e^{-0.0033 \times 478.83} = 0.0141$$

[7]Be activity at time of analysis (A'):

$$A' = \frac{cps \times CF}{BF \times Eff}$$

$$A' = \frac{0.00143 s^{-1} \times 1.02}{0.1044 \times 0.0141} = 0.989 Bq$$

[7]Be activity at time of collection (A_0):

$$A_0 = \frac{A'}{e^{-\lambda t_c}}$$

$$A_0 = \frac{0.989 Bq}{e^{-0.01297 d^{-1} \times 15.7 d}} = 1.21 Bq$$

[7]Be activity per unit volume in sample (which contains HCl as well as rainwater):

$$\frac{A_0}{V} = \frac{1.21 Bq}{0.795 L} = 1.53 Bq/L$$

[7]Be activity of the rain barrel (A_{total}):

$$A_{total} = \frac{A_0}{V} \times V_{barrel}$$

$$A_{total} = 1.53 Bq/L \times 6.70 L = 10.2 Bq$$

[7]Be activity of the rain barrel corrected for decay before collection (A_{barrel}):

$$A_{barrel} = \frac{A_{total} t_{barrel} \lambda}{1 - e^{-\lambda t_{barrel}}}$$

$$A_{barrel} = \frac{10.2Bq \times 4.98d \times 0.01297d^{-1}}{1 - e^{-0.01297d^{-1}4.98d}} = 10.6Bq$$

^{7}Be rainfall flux ($J_{Be7,rain}$):

$$J_{Be7,rain} = \frac{A_{barrel}}{t_d \times Area_{funnel}}$$

$$J_{Be7,rain} = \frac{10.6Bq}{4.98d \times 0.216m^2} = 9.79Bq/m^2/d$$

^{7}Be rainfall flux to the Milwaukee outer harbor ($J_{Be7,rain,OH}$):

$$J_{Be7,rain,OH} = J_{Be7,rain} \times Area_{OH}$$

$$J_{Be7,rain,OH} = 9.79Bq/m^2/d \times 4.43 \times 10^6 m^2 = 4.34 \times 10^7 Bq/d$$

4.3. Results and Discussion

^{7}Be was found in nearly all outer harbor sediment samples, ranging in activity from 0 to 1157±249 Bq/m^2. The mean ^{7}Be activity per unit area in outer harbor sediment was 305±57 Bq/m^2. The ^{7}Be inventory in outer harbor bed sediment was calculated using the station means as well as by using contour mapping with the program Surfer, with the same techniques applied to calculating ^{131}I inventories. ^{7}Be bed sediment inventories fell over time before rising again for the last sampling date (**Table 13**, **Figure 21**). However, the inventories largely stayed within the 10^9 Bq order of magnitude, 1-2 orders of magnitude higher than those of ^{131}I. The PONAR results are surprisingly high in ^{7}Be, which may be due to sampling in areas of clayey sediment, but is beyond our scope to fully explain. When the inventories calculated from the means between the sampling stations are compared to those calculated by Surfer, the Surfer estimates are consistently higher, but both estimates follow the same trends over time. It should also be

noted that the spatial distribution of ^{7}Be activity in the outer harbor bed sediment is very similar to that of ^{131}I for each sampling date (**Figure 22**).

Table 13 Bed sediment inventories of ^{7}Be in the Milwaukee outer harbor in 2014, as estimated by mean between stations and the mapping program Surfer.

Sampling event	^{7}Be (Mean) ($\times 10^{9}$ Bq)	^{7}Be (Surfer Inventory) ($\times 10^{9}$)	^{7}Be Mean/Area (Bq/m^{2})
Ponar 20 June	3.133 ± 0.063	4.865	707 ± 28
Gravity core 16 July	2.53 ± 0.13	3.01	570 ± 70
Gravity core 29 July	1.33 ± 0.11	1.65	300 ± 59
Gravity core 26 August	0.233 ± 0.070	0.294	53 ± 39
Ponar 24 September	1.49 ± 0.10	1.74	337 ± 43
Gravity core 8 October	1.324 ± 0.067	1.67	299 ± 37

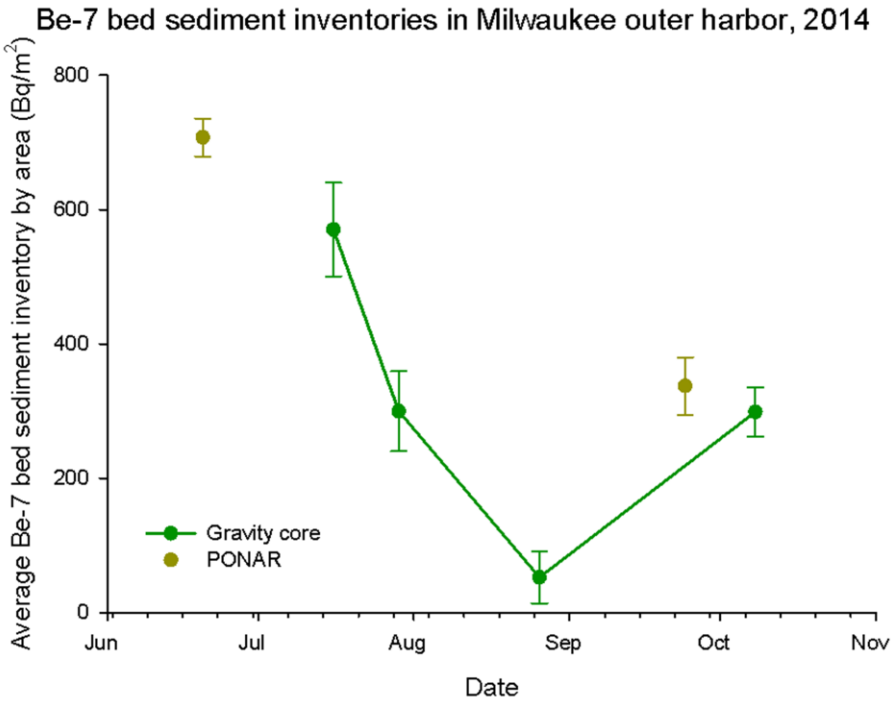

Figure 21 ^{7}Be bed sediment inventories per unit area (mean ± standard error) in the Milwaukee outer harbor at sampling dates in 2014. PONAR-sampled results are shown separately for the reasons explained in chapter 3.5.2.

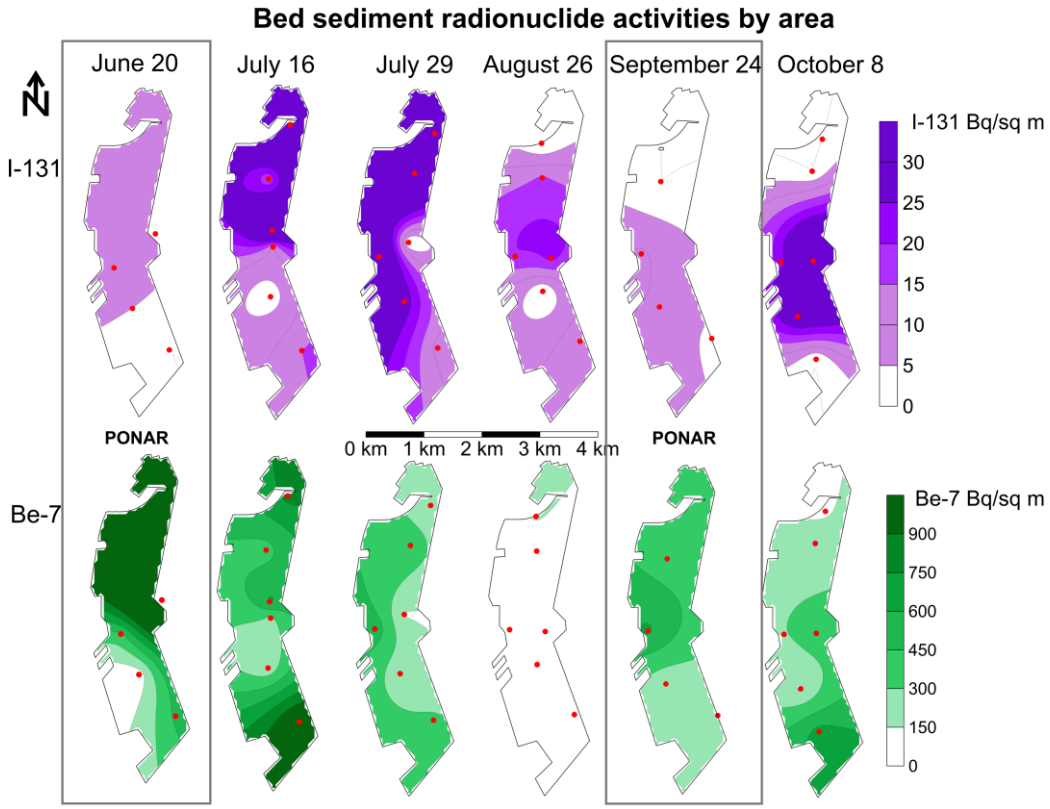

Figure 22 Spatial distribution of activity per m^2 of ^{7}Be (green, bottom) as compared to that of ^{131}I (purple, top) in the Milwaukee outer harbor at sampling dates in 2014.

In the outer harbor water column, ^{7}Be was consistently found in both the dissolved and particulate phases (**Table 14**, **Figure 23**). Unlike ^{131}I, the particulate phase dominated ^{7}Be water column activity. In general, ^{7}Be outer harbor water column activities decreased from July to October 2014. The mean particulate ^{7}Be activity was 4.98±0.63 mBq/L, and the mean dissolved ^{7}Be activity was 2.31±0.59 mBq/L. The mean total water column ^{7}Be activity was 6.67±0.84 mBq/L.

Table 14 ^{7}Be particulate and dissolved activities in the Milwaukee outer harbor water column on sampling dates in 2014, in mBq/L.

Date	^{7}Be particulate activity	^{7}Be dissolved activity
16 July	6.9 ± 1.8	No data
29 July	6.55 ± 0.80	1.4 ± 1.0
26 August	4.1 ± 1.4	3.5 ± 1.0
8 October	2.45 ± 0.74	2.0 ± 1.0

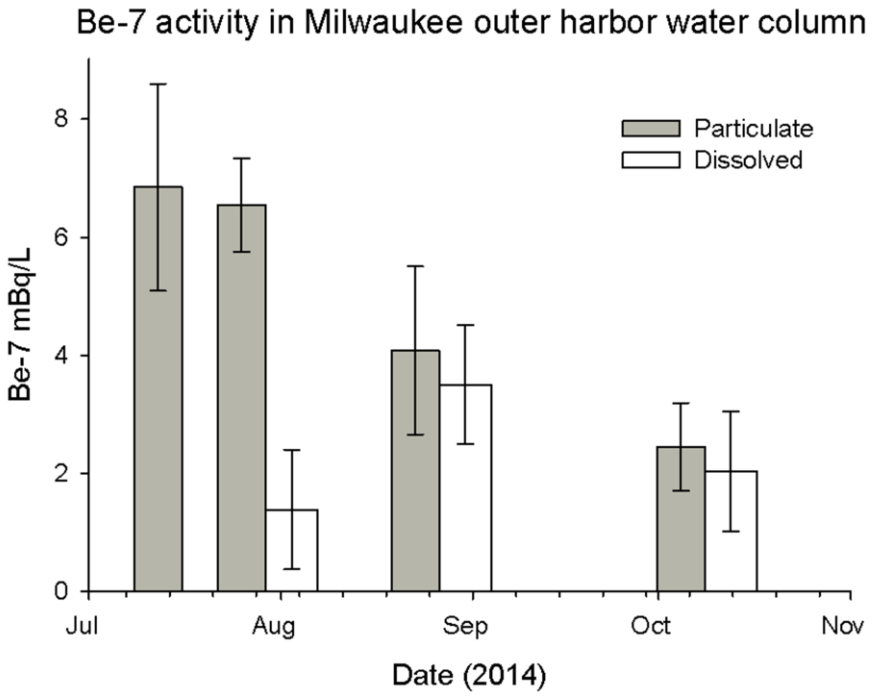

Figure 23 ^{7}Be particulate and dissolved water column activities in the Milwaukee outer harbor. No dissolved phase data was collected on the16 July, 2014 sampling date.

The ^{7}Be flux to the Milwaukee outer harbor through rainfall varied over time, but largely stayed within the 10^{7} Bq/d order of magnitude. This flux ranged from 1.86±0.10 Bq/m^{2}/d to 16.62±0.36 Bq/m^{2}/d, with a mean flux of 6.7±1.2 Bq/m^{2}/d (**Figure 24**). The ^{7}Be rainfall flux was very high during the early summer rains, then fell and leveled off in late summer and early fall. In the early summer, the ^{7}Be rainfall flux spikes with large rainfall events, but later in the season, rainfall and ^{7}Be deposition do not appear to be correlated.

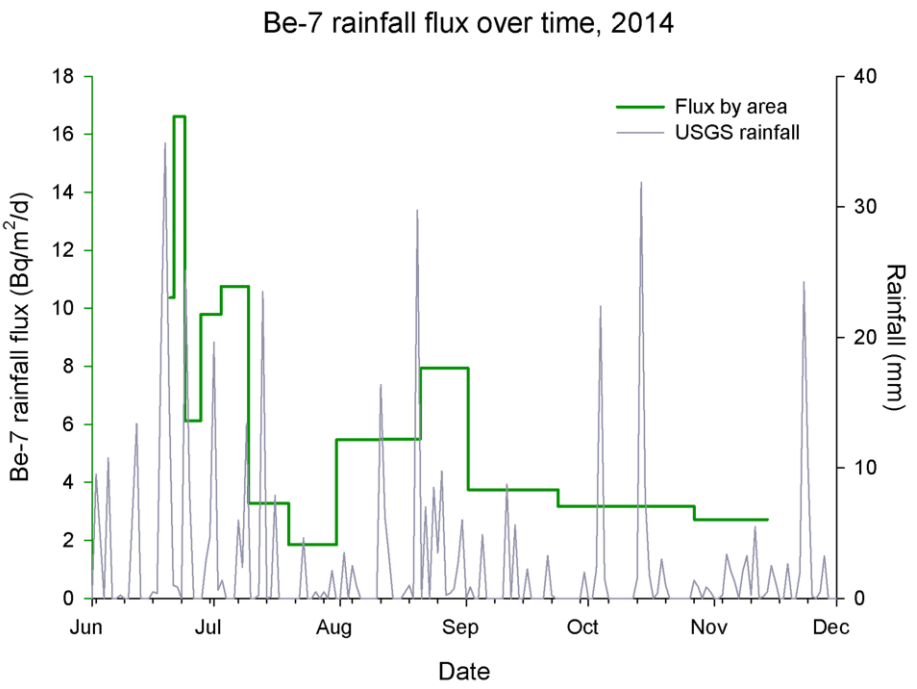

Figure 24 ^{7}Be flux per unit area to the Milwaukee outer harbor through atmospheric deposition ("rainfall") in 2014. The gray lines show nearby rainfall data for the same time period, taken from the United States Geological Survey (USGS).

^{7}Be is found everywhere that ^{131}I is in the environment, and shares the characteristics of relatively short half-life and enrichment in the sediment and biota. ^{7}Be has much higher inventories in the environment than ^{131}I, but the similar behavior of the two in the environment can be seen in their similar spatial distributions in the Milwaukee outer harbor bed sediment (**Figure 22**). This fact, along with the previous use of ^{7}Be as a tracer of recently deposited sediment, suggests that the hotspots of the two radionuclides in the outer harbor are also hotspots of recent sediment deposition (see chapter 5.3.).

^{7}Be also has a varying flux from the atmosphere. It appears to be roughly correlated to periods of frequent, heavy rains, but may also show seasonal differences. Unfortunately, our data do not cover enough to time to further support the apparent seasonal changes in ^{7}Be flux. Baskaran and Swarzenski (2007) report seasonal changes in ^{7}Be atmospheric flux in Tampa Bay,

Florida, with high ^{7}Be fluxes during heavy rains which diminish with more frequent summer rains, suggesting that frequent rain events deplete the atmospheric inventory of ^{7}Be. McNeary and Baskaran (2003) also reported similar trends in Michigan. Those results are supported in this study as well, despite the differences in study area.

One difficulty with using ^{7}Be as a tracer in the Milwaukee outer harbor system is its multiple sources. Although all ^{7}Be is originally sourced from atmospheric deposition, this is not necessarily what drives the changes in its inventory in the outer harbor. ^{7}Be is already present in all water and suspended sediment entering and leaving the harbor through the rivers as well as the interface with Lake Michigan. Evidence of this complex cycle can be seen in the poor correlation between the flux of ^{7}Be into the outer harbor through rainfall and the ^{7}Be inventory in the outer harbor bed sediment (**Figure 25**). Rather, the changes in bed sediment inventory over time more closely mirror those of ^{131}I (**Figure 26**). Since ^{131}I has a completely different source than ^{7}Be, this suggests that the changes in harbor inventory over time must be due to another factor, such as outer harbor water and sediment dynamics. The great difference in magnitude between the flux of ^{7}Be in through rainfall and the bed sediment inventory, for a relatively short-lived radionuclide, is also a testament to other sources of ^{7}Be to the outer harbor (i.e. river water). This makes ^{7}Be dynamics much more complex and difficult to understand than that of a radionuclide with a discrete, easily quantifiable source, such as ^{131}I.

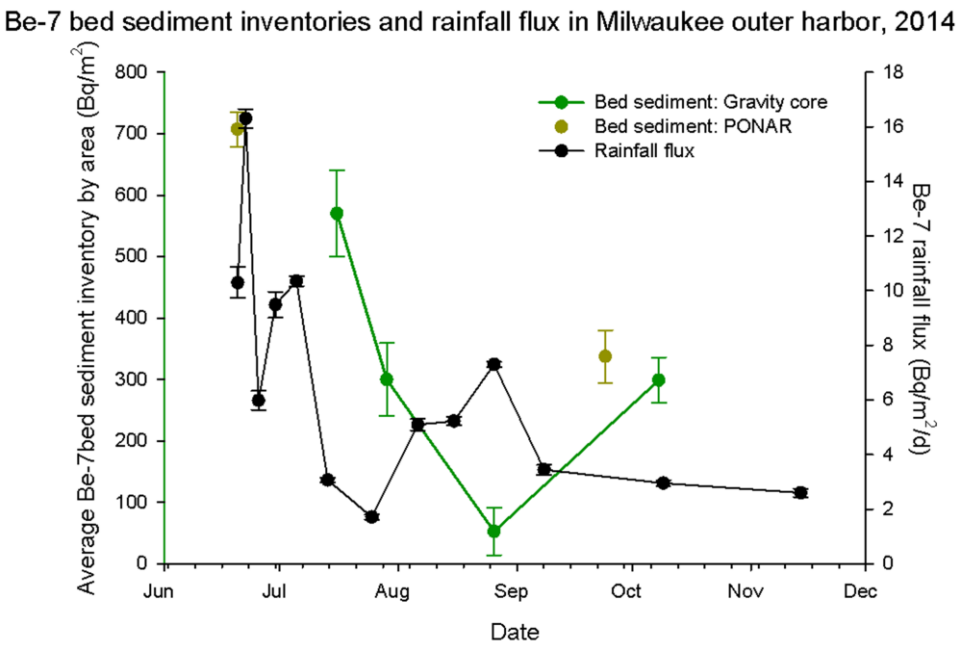

Figure 25 ^{7}Be bed sediment inventory per unit area in the Milwaukee outer harbor compared to ^{7}Be rainfall flux per unit area over time.

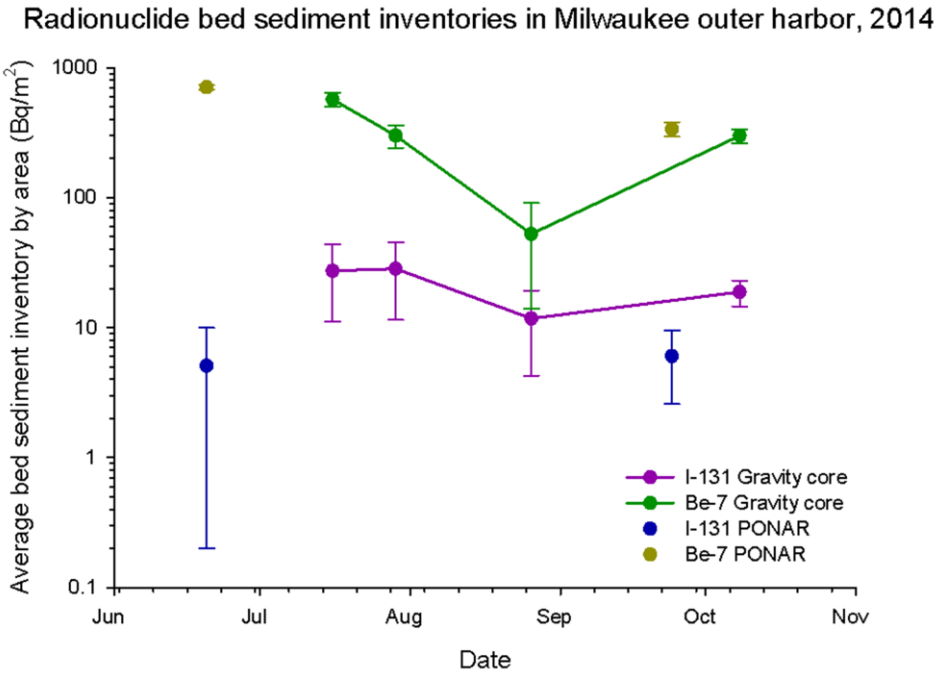

Figure 26 Comparison of mean bed sediment inventories (per unit area) of ^{7}Be and ^{131}I in the Milwaukee outer harbor on a log scale. Dates sampled by PONAR grab are shown separately.

5. Discussion: ^{131}I Applications

In this final chapter, I explore the potential applications of ^{131}I as a tracer of (*i*) recent exposure to treated sewage effluent in coastal Lake Michigan (section 5.1), (*ii*) benthic material transport in coastal Lake Michigan (section 5.2), and, in conjunction with ^{7}Be measurements, (*iii*) riverine sediment deposition in the Milwaukee outer harbor (section 5.3). The entire thesis is summarized and conclusions are drawn in section 5.4.

5.1. Sewage effluent tracer

The Milwaukee metropolitan area relies on Lake Michigan for drinking water and has numerous recreational beaches along its shoreline. Most drinking water intakes and beaches are located north of the MMSD WRFs. This is because average alongshore current near Milwaukee is north to south, year-round (Beletsky et al. 1999). However, a significant amount of across-shore transport has also been documented (Waples and Klump 2013), and day-to-day currents along the Milwaukee shoreline vary greatly from average currents and even Milwaukee's northern beaches suffer from high bacterial counts and algal blooms on occasion (Kleinheinz 2014).

The simplest and most obvious application of ^{131}I is as a short-term tracer of sewage-derived material. Smith et al. (2008) have suggested that ^{131}I would be useful for this purpose. Despite these observations, we are aware of only one study that has used ^{131}I as a tracer of sewage effluent-derived material (Rose et al. 2015).

Sewage effluent is the only source of ^{131}I in the Great Lakes, so any ^{131}I found in Lake Michigan must have been part of sewage effluent recently enough to not have decayed below the limit of detection according to its ~8 day half-life. Although the components of sewage effluent

may separate once released into Lake Michigan, the presence of ^{131}I nonetheless indicates the possibility of recent exposure to any other component of sewage effluent in the same location.

Although sewage effluent has been treated, some pathogens remain, as well as some *Escherichia coli*, a commonly used fecal indicator that informs beach closures. Treated or not, sewage effluent is also nutrient rich, fueling algal blooms which can produce toxins or incubate pathogens, as well as being aesthetically unpleasant at beaches. The fact that sewage effluent-sourced material makes its way to popular public beaches in a short time frame has negative economic and public health implications.

This study has found ^{131}I at or near the popular Milwaukee area recreational beaches at Atwater Park, Bradford Beach, South Shore Beach, Bay View Park, Grant Park and Bender Park. In 2014, these beaches were closed or showed a warning advisory to swimmers a combined 28 times due to concerns about elevated *E. coli* levels (Atwater 4, Bay View 3, Bender 5, Bradford 7, Grant 2, South Shore 7, Kleinheinz 2014). Blooms of *Cladophora* and blue-green algae can also make beaches unpleasant or incubate bacteria like *E. coli* while they decompose on the beach (Olapade et al. 2006). Elevated bacteria levels and algal blooms are often fueled by exposure to treated or untreated sewage (Barlie 2010, Mallin et al. 2007). The above problems, often fueled by sewage, not only endanger public health at beaches, but also reduce their economic value of beaches to nearby shops and restaurants (Rabinovici et al. 2004).

Traditional methods of testing for water quality at beaches typically take days to produce results and are expensive. However, if ^{131}I can be used as a tracer of sewage-derived material, critical results could be obtained in hours to days, and at little cost if a gamma detector is available.

^{131}I can also show the "footprint" of sewage-derived material along the Milwaukee shoreline and nearshore zone. This can inform future placement of beaches, recreational areas as well as infrastructure such as water intakes and breakwaters to avoid negative influence from sewage.

The benthic trawl surveys have found ^{131}I further offshore and further away from the nearest WRF outfall than ever before. ^{131}I was found 8km offshore on both the South Shore and County Line transects. Additionally, the finding of ^{131}I activity at the County Line 8km station is the furthest away from a WRF outfall we have found ^{131}I- at 10km from the South Shore WRF outfall.

Furthermore, these results have found a short-lived sewage indicator much further offshore in Lake Michigan than any Milwaukee sewage-derived material has been found before. The survey of sewage-derived PPCPs documented by Blair et al. (2013) found PPCPs in the Milwaukee area of Lake Michigan as far as 3.8km offshore and 3.2km from the nearest WRF outfall (South Shore). In contrast, this study more than doubles both of those distances. It should also be noted that beyond simply indicating the presence of sewage effluent-derived material, ^{131}I indicates the recent exposure to this material, while PPCPs are persistent in the environment and degrade according to poorly-known effective half-lives. These results suggest that the area of short-term sewage effluent influence from Milwaukee is much larger than previously understood.

5.2. Transport of benthic material in coastal Lake Michigan

5.2.1. Steady-state model

We believe that the results of our benthic trawl surveys above (chapter 3.4.2.) have potential applications beyond merely showing the presence of short-term sewage-derived

materials in the Lake Michigan benthos. Under certain conditions, the ^{131}I activities in the benthic trawl samples can be used to roughly estimate the transport speed and direction of mobile benthic material in nearshore Lake Michigan.

We have found ^{131}I in benthic trawl samples at every station sampled in our surveys above, and some on two separate cruises 16 days apart (20 October and 5 November 2014). The ^{131}I activities generally diminished as the stations moved further away from each WRF, and the majority of ^{131}I activity was contained in *Cladophora*, despite it only accounting for a small fraction of the samples' dry weight (chapter 3.4.2. above). The fact that ^{131}I was found at similar activities in the same place about two half-lives later and the importance of *Cladophora* in the sample activities leads us to the assumptions, listed below, upon which we build a steady-state model of benthic currents:

1. **^{131}I input is constant**- as shown above in chapter 3.1.2., this is not strictly true. However, the ^{131}I flux from both WRFs is always nonzero, and usually within the same order of magnitude, so for the purposes of this steady state model, it will be assumed to be constant.
2. **All ^{131}I activity in benthic trawl samples is contained in *Cladophora***- as shown above in chapter 3.4.2., *Cladophora* is responsible for the majority of ^{131}I activity in the benthic trawl sample. Additionally, ^{131}I activity found in the dreissenid mussel and abiotic sections of the sample could be largely due to the attachment of particles of finely ground *Cladophora* that had degraded due to its fall die-off and the physical action of waves and currents against benthic substrate.
3. **^{131}I is fixed in *Cladophora* by the start of each transect**- we assume that any ^{131}I found in *Cladophora* was sorbed in an area closest to the WRF outfalls, that no

additional ^{131}I sorbs to sloughed *Cladophora* as it moves away from a WRF outfall, and that ^{131}I does not leave the *Cladophora* tissue through means other than radioactive decay.

4. ***Cladophora* is sloughed and moves with the speed and direction of benthic currents**- at this time of year, most *Cladophora* is sloughing off of the lakebed and dying, being moved by the current as it decomposes (Dodds and Gudder 1992, Higgins et al. 2005). We assume that is the case for all *Cladophora* near the WRF and at the benthic trawl stations, and that it is carried efficiently, making the speed and direction of *Cladophora* movement approximately proportional to that of the benthic currents.

If these assumptions are valid, this means that each station is receiving a continuous flux of sloughed *Cladophora* tagged with the same ^{131}I activity near the WRF outfalls. The difference in ^{131}I activity at each station is only due to the decay during the time it takes the *Cladophora* to get there. The time to cover the distance between the stations can be easily expressed as a velocity.

5.2.2. Calculations

The ^{131}I activities used in our calculations are those of the whole counted sample, without normalizing for mass. Since we have assumed that all ^{131}I activity is contained in *Cladophora*, the dry weight of which is nearly negligible, and each sample is the same volume of well-mixed benthic material, this is more accurate than using the activity per unit dry weight. For stations sampled more than once, mean activities were calculated.

To calculate the travel time of the *Cladophora* between any two stations (e.g. Station 1 and Station 2), Station 2 was treated simply as the activity at Station 1 after a time of decay, using a modification of Equation 5 from chapter 2.4 above:

$$A_0 = \frac{A'}{e^{-\lambda t}} \quad (5)$$

This time, however, we are solving for t, the time it takes to transport *Cladophora* from Station 1 to Station 2. The ^{131}I activity at Station 1 is A_0 and the activity at Station 2 is A'. Solving for t, the equation becomes:

$$t = \frac{\ln(A'/A_0)}{-\lambda} \quad (8)$$

Dividing the distance between stations (d) by t, we can calculate the current velocity (v):

$$v = \frac{d}{t} \quad (9)$$

5.2.3. Benthic material transport velocities

We calculated the benthic current velocity between all logical stations to show the movement of material away from the two WRFs (**Figure 27**). Analysis of the Main Gap transect shows an offshore (easterly) current of 220±300 m/d away from Jones Island WRF. Analysis of currents moving material away from South Shore WRF is more complex, but shows currents moving in both the alongshore (southerly) and offshore (easterly) directions, with the strongest current moving southeasterly at 830±310 m/d from the South Shore 1km station to the County Line 5km station. The specific current velocities between stations are shown in **Table 15** below. The finding of a strong westerly current from County Line 5km to County Line 1km will not be considered valid due to its high standard deviation and the finding of a low-standard deviation

easterly current from both County Line 1km to County Line 8km and County Line 5km to County Line 8km.

Table 15 Current velocities from Station 1 to Station 2 based on ^{131}I found in benthic trawl sampling.

Station 1	Station 2	Velocity (m/d)
Main Gap 1km	Main Gap 5km	220 ± 300
South Shore 1km	South Shore 5km	165 ± 30
South Shore 5km	South Shore 8km	300 ± 740
South Shore 1km	South Shore 8km	210 ± 140
South Shore 1km	County Line 1km	560 ± 110
South Shore 1km	County Line 5km	830 ± 310
South Shore 1km	County Line 8km	390 ± 100
County Line 1km	County Line 5km	-2900 ± 7800
County Line 5km	County Line 8km	188 ± 81
County Line 1km	County Line 8km	460 ± 200

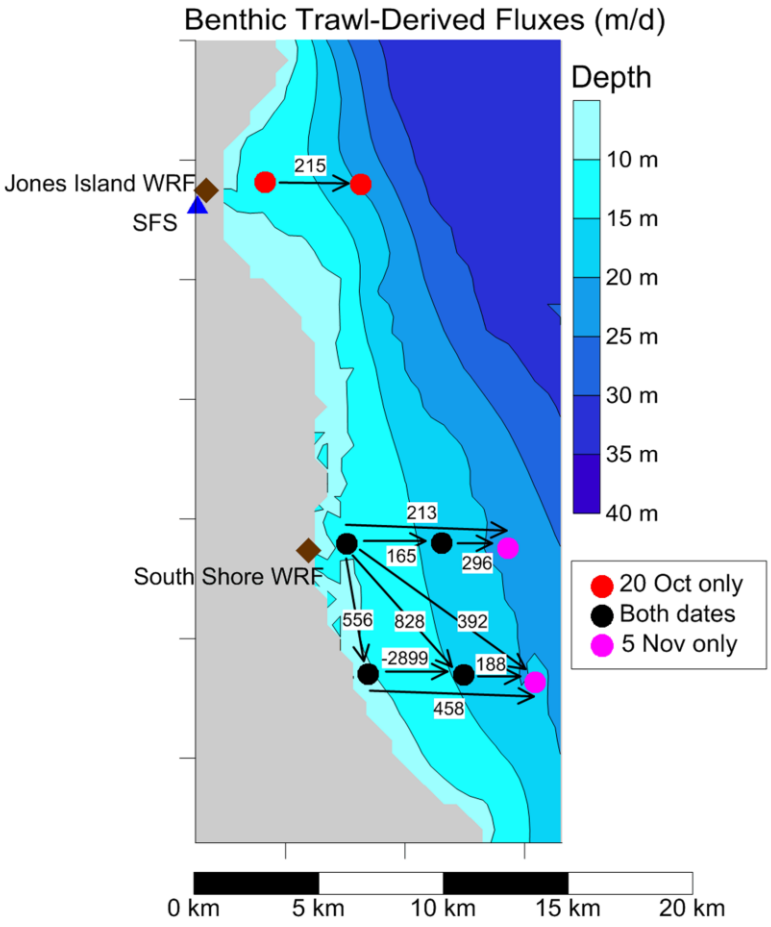

Figure 27 Calculated transport of benthic material (i.e. sloughed *Cladophora*) between stations in m/d based on the ^{131}I activities of benthic trawl samples.

The second fastest current velocity is from South Shore 1km to County Line 1km, 560±110 m/d alongshore in the southerly direction. This implies that the current from South Shore 1km has a greater alongshore than offshore component. However, the offshore current is still significant, as it can be found along all three transects, as fast as 460±200 m/d along the County Line transect. The significance of the offshore component of the current is most clearly shown by the finding that the current flows faster from South Shore 1km to County Line 5km than County Line 1km.

Current meter measurements were not taken concurrently with the benthic trawl surveys. Waples, however, took water column current meter data at the nearby Green Can Station (depth: 22m; **Figure 28**) in the late summer and fall of 2007 and 2009 (Waples 2009, unpublished data). These data show a prevailing easterly and southerly current at the deepest depths (**Figure 29**). This is consistent with the strongest directions of benthic material transport calculated above.

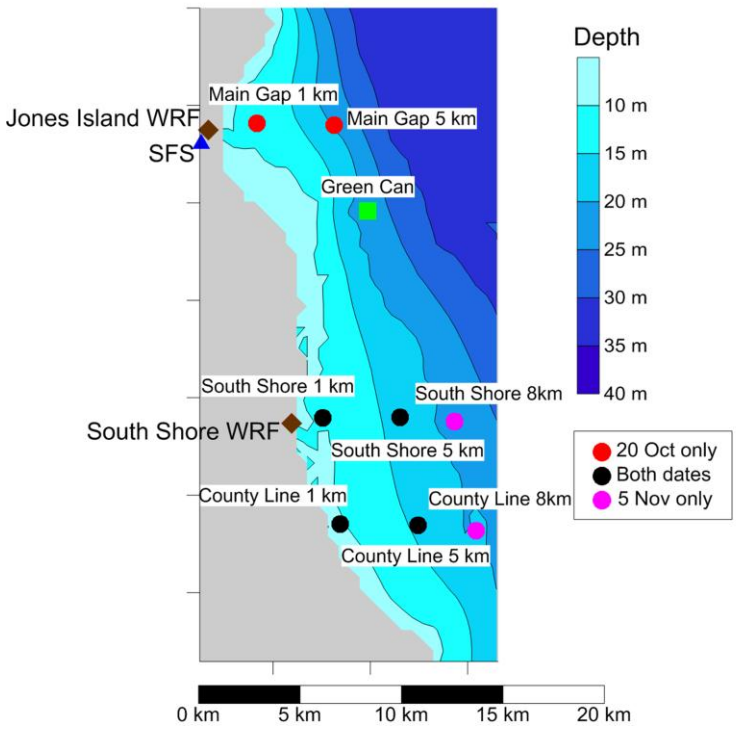

Figure 28 Milwaukee shoreline of Lake Michigan and benthic trawl sampling stations, plus the Green Can Station (green square) where current meter measurements were taken (Waples 2009, unpublished data).

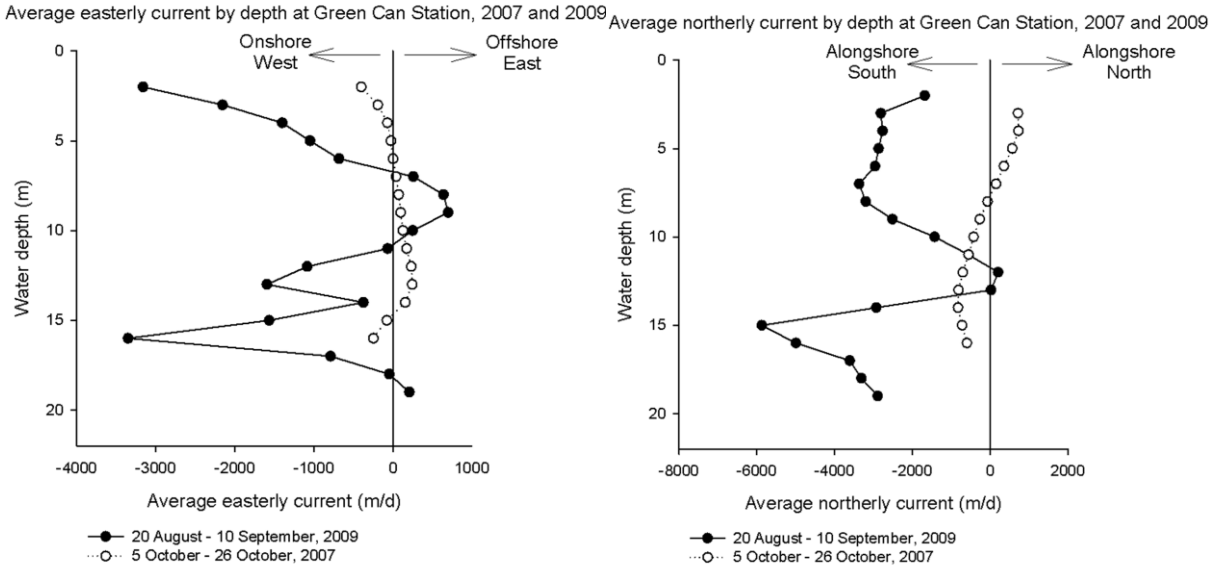

Figure 29 Magnitude and direction of mean currents by depth at Green Can Station in Lake Michigan (depth: 22m). Easterly currents are shown on the left and northerly currents are shown on the right. Data taken from Waples (2009 unpublished data).

The finding of a prevailing southeasterly current from the Milwaukee shoreline of Lake Michigan is in line with conventional thought on generalized current flow in southern Lake Michigan. Beletsky et al. (1999) documented a prevailing year-round alongshore (southerly) current in the nearshore zone of Lake Michigan near Milwaukee as part of a large-scale current model for the Great Lakes. Easterly (offshore) flow has also been recognized, however, as an important component of particle transport in the nearshore, as discussed in Eadie et al. (2008) and shown in **Figure 30**. Moreover, Waples and Klump (2013) have also documented significant easterly (offshore) transport of particles from nearshore Lake Michigan using ^{234}Th as a particle tracer.

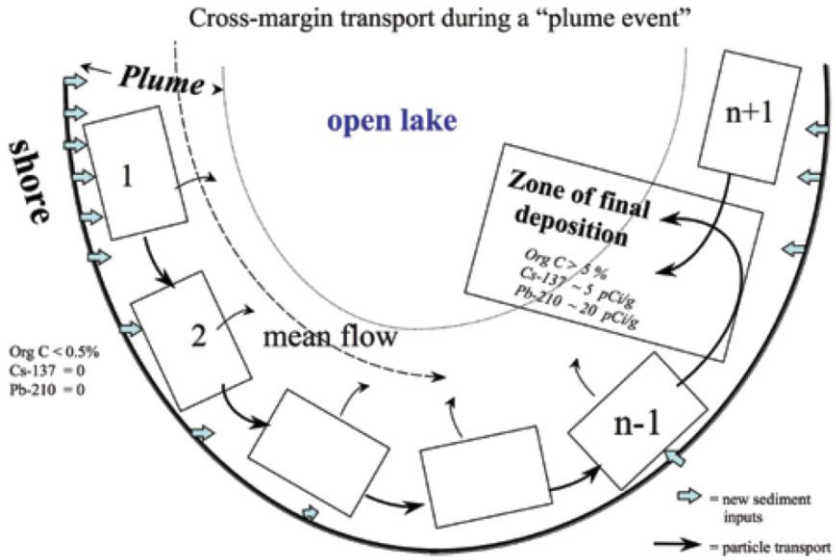

Figure 30 Conceptual model of sediment transport in southern Lake Michigan from the Episodic-Events-Great- Lakes Experiment (EEGLE). Figure from Eadie et al. 2008.

The average southeasterly transport of particulate material on the lake bottom near Milwaukee, however, should not be confused with "potential" transport of suspended and dissolved material in the water column. Recreational beaches and drinking water intake sites

north of Milwaukee WRF outfalls are not immune to occasional exposure to treated sewage effluent carried by northerly currents.

The benthic "particle trajectories" shown above are both a simplified model and a snapshot of the actual conditions in Lake Michigan. Additional research is needed to confirm these results in a systematic study. However, the fact that this simple snapshot conforms to conventional views of currents in this area of Lake Michigan coupled with the relative ease with which ^{131}I can be used to calculate this information should encourage further study.

5.3. Outer harbor sediment deposition

Sediment pollution is one of the largest sources of pollution in aquatic and marine systems around the world (Alongi 2002, Kennish 2002, Ockenden et al. 2012, Short and Wyllie-Echeverria 1996), and is of special concern in the Great Lakes (Great Lakes Commission 2000). Riverine sediment loads are increased from their natural levels by anthropogenic disturbances such as agriculture and land development. This decreases water quality for recreational use, degrades aquatic habitats, limits phytoplankton growth and increases the need for maintenance dredging, causing considerable economic, ecological and aesthetic costs (Ouyang and Bartholic 2003).

Additionally, nutrients and pollutants sorb to sediment and are carried along with it, including industrial toxins, pesticides and pharmaceuticals and personal care products (PPCPs), all of which affect the Milwaukee harbor (Great Lakes Commission 2008, Luthy et al. 1997). These ubiquitous pollutants are concentrated in areas with high sediment loading and burial, where they enter the food web, bioaccumulate, and persist for many years, causing endocrine disruption and other toxic effects throughout the ecosystem (e.g. Brodin et al. 2013, Crago and

Klaper 2012, Fent et al. 2006, Santos et al. 2010). As a result, fisheries and aquatic ecosystems are disrupted and human populations are exposed to potentially harmful contaminants.

This is especially true for the Milwaukee harbor, due to its location at the intersection of riverine sediment loading and heavy human use. The Milwaukee inner harbor experiences all of these issues, but is upstream of the Jones Island WRF. According to sediment traps we deployed in the Kinnickinnic river (detailed in Appendix F), the inner harbor does receive some sewage, as evidenced by the presence of ^{131}I. However, ^{131}I activity in the inner harbor sediment traps was inconsistent. It is likely that ^{131}I inventories in the inner harbor rely on ephemeral fluxes from backflow from the outer harbor or chance exposure to raw sewage from leaking infrastructure (e.g. Sauer et al. 2011). However, the above occurrences are difficult to predict and therefore we do not focus on the inner harbor. The Milwaukee outer harbor, however, experiences the same impacts as the inner harbor, but also directly receives sewage effluent (and with it ^{131}I) from the Jones Island WRF. Although the sewage is treated, it is still a large source of PPCPs, which are not efficiently removed by conventional treatment processes (Blair et al. 2013). The Milwaukee outer harbor thereby receives sediment and contaminants from its entire watershed, as well as a consistent flux of ^{131}I. ^{131}I has the potential to trace non-sewage-related process as well, the most useful of which, in this system, is short-term sediment deposition.

In the Milwaukee outer harbor, ^{131}I is present in the bed sediment and the water column. Logically, the ^{131}I activity in the water column must be feeding the inventory in the bed sediment. By combining that flux of ^{131}I from the water column to the bed sediment with the outer harbor TSM, the flux of suspended material to the bed sediment, or sediment deposition can be calculated. These calculations can also be done using ^{7}Be instead of ^{131}I. Sediment deposition

estimates for a high-traffic, dredged area like the Milwaukee outer harbor are otherwise difficult to obtain.

5.3.1. Calculations

The steady state sediment burial calculation starts with the bed sediment ^{131}I inventory calculated in chapter 3.5. above (chapter 4.3. for ^{7}Be). That inventory (I_{sed}) is multiplied by the decay constant to find the flux of the radionuclide to the bed sediment ($J_{bed\ sed}$) in Bq/d:

$$J_{bed\ sed} = I_{sed} \times \lambda \tag{10}$$

Next, the total (dissolved + particle-bound) water column radionuclide activity per liter (A_T/L) is divided by TSM (in g/L) to calculate the outer harbor radionuclide activity per gram of suspended material present (A/mass) in Bq/g:

$$\frac{A_T}{mass} = \frac{\frac{A_T}{L}}{TSM} \tag{11}$$

Finally, to calculate the steady state sediment deposition ($J_{sed\ dep}$) in g/d (later converted to metric tonnes per day), the radionuclide flux to the sediment is divided by the radionuclide activity per gram:

$$J_{sed\ dep} = J_{bed\ sed} / \frac{A_T}{mass} \tag{12}$$

These calculations could also be carried out based on the radionuclide activity on suspended particles only, rather than the total water column activity shown above (by using the particulate radionuclide activity as A_T/mass in equation 10). However, recent research leads us to believe that using the total water column activity leads to a more accurate calculation of sediment flux. This is because Waples (2015, in press) reports that activity in the bed sediment is not only due to the deposition of suspended particles sorbed with radionuclides, but also due to

convective (advective and turbulent diffusive) mixing of the water column with the surface of the bed sediment, allowing radionuclides in the dissolved fraction to bind with bed sediment particles directly. The Milwaukee outer harbor is relatively shallow and well-mixed, and should also follow this convective model.

In order to test this assumption, we compared the $^{7}Be/^{131}I$ ratios of particulate material from the water column and the bed sediment in the Milwaukee outer harbor on our four (gravity core) sampling dates. The $^{7}Be/^{131}I$ ratio can be used to show the relative age of sediment (see chapter 3.5.2.). The $^{7}Be/^{131}I$ ratio is almost always higher for particulate material than for bed sediment (**Table 16**). Because the half-life of ^{7}Be is longer than that of ^{131}I, without an input of new radionuclides, this ratio will only increase over time. This means that in order for the bed sediment to have a lower $^{7}Be/^{131}I$ ratio than the particulate material, it must not be receiving radionuclides exclusively from the burial of particulate material. Additionally, the bed sediment $^{7}Be/^{131}I$ ratio is much more similar to that of the total water column than that of the particulate fraction. This supports the idea that the bed sediment is also receiving a flux of radionuclides in the dissolved phase from the water column through mixing. The mode of sorbtion of radionuclides to bed sediment was not studied here, but could involve diagenetic processes that preferentially remove ^{131}I from the water column.

Table 16 Comparison of the $^{7}Be/^{131}I$ ratio of Milwaukee outer harbor bed sediment, particulate material filtered from the Milwaukee outer harbor water column and the total (particulate plus dissolved) water column activities.

Date	Bed sediment $^{7}Be/^{131}I$	Particulate $^{7}Be/^{131}I$	Total Water Column $^{7}Be/^{131}I$
7/16/14	21	135	-
7/29/14	11	31	5
8/26/14	4	189	3
10/8/14	16	4	0.5
Mean	**13**	**90**	**3**

We can also compare the $^{7}Be/^{131}I$ ratios of the radionuclide flux to the bed sediment (i.e. $J_{bed\ sed}$, above) to those of the particulate and total water column activities. These ratios, shown in **Table 17**, show that the $^{7}Be/^{131}I$ ratio for radionuclide flux to the bed sediment is much closer to that of the total water column activity than that of the particulate fraction activity, providing additional evidence that bed sediment radionuclide inventories are sourced from total water column activities, and not simply by the settling particulate fraction alone. Additional evidence that radionuclides from the water column are removed by bottom scavenging and vertical convection rather than particle settling is provided below where we calculate sediment burial based on only particulate radionuclide activities for comparison.

Table 17 Comparison of the $^{7}Be/^{131}I$ ratio of Milwaukee outer harbor radionuclide flux to bed sediment ($J_{bed\ sed}$), particulate material filtered from the Milwaukee outer harbor water column and the total (particulate plus dissolved) water column activities. Shaded dates were sampled by PONAR grab, and are not included in the mean.

Date	$J_{bed\ sed}$ $^{7}Be/^{131}I$	Particulate $^{7}Be/^{131}I$	Total Water Column $^{7}Be/^{131}I$
6/20/14	21		
7/16/14	3	135	-
7/29/14	2	31	5
8/26/14	1	189	3
9/24/14	8		
10/8/14	2	4	0.5
Mean	**2**	**90**	**3**

In addition to the steady-state sediment deposition calculations detailed above, we also calculate non-steady state flux estimates. In these estimates, instead of calculating the radionuclide flux to the bed sediment from the inventory on each sampling date separately, the bed sediment inventory on the previous sampling date is taken into account. Because each sampling date is within a few half-lives of the previous date, some of the inventory measured on the previous date is still there:

$$I_{old} = I_{prev} \times e^{-\lambda t} \quad (13)$$

where I_{old} is the remaining inventory from the previous date, I_{prev} is the inventory on the previous date, λ is the decay constant, and t is the time between sampling dates. The new inventory added between sampling dates (I_{new}), then, is the difference between the measured inventory at the current sampling date ($I_{current}$) and the old inventory remaining from the previous sampling date:

$$I_{new} = I_{current} - I_{old} \quad (14)$$

However, I_{new} is also decaying during the time between sampling dates. This decay is not unlike the decay that occurs while a sample is being counted on a gamma detector. Therefore, the correction factor (CF) used to account for this decay is the same one used for decay during sample analysis (equation 3, chapter 2.4.):

$$CF = \frac{\lambda t}{1 - e^{-\lambda t}} \quad (3)$$

The decay-corrected new inventory ($I_{new,corr}$), then, is:

$$I_{new,corr} = I_{new} \times CF \quad (15)$$

In this non-steady state scenario, the radionuclide flux to the bed sediment ($J_{bed\ sed,NSS}$) is the flux needed to support this new inventory:

$$J_{bed\ sed,NSS} = \frac{I_{new,corr}}{\Delta t} \quad (16)$$

where Δt is the time elapsed (days) between sampling dates. From here, the calculations are the same as in the steady state, using equations 10 and 11, above:

$$J_{sed\ dep,NSS} = J_{bed\ sed,NSS} / \frac{A}{mass} \quad (17)$$

where $J_{sed\ dep,NSS}$ is the non-steady state sediment deposition to the outer harbor, and A/mass represents either A_P/mass for mass flux estimates based on nuclide scavenging due to particle settling only, or A_T/mass for mass flux estimates based on bottom scavenging and vertical convection.

5.3.2. Sediment deposition estimates

The time-weighted mean steady state sediment deposition estimates using the convective mixing model (i.e. total water column activities) was 8.2±1.3 metric tonnes (MT) per day for ^{131}I and 6.0±2.3 MT/d for ^{7}Be (**Table 18**). Using the non-steady state model, the weighted mean sediment deposition estimate was 5.48±0.93 MT/d for ^{131}I. For ^{7}Be, the weighted mean was 10.2±3.0 MT/d (**Table 19**). However, this included one negative deposition (i.e. erosion) estimate. If we assume the estimate of negative deposition is not representative of the true conditions in the outer harbor, a long-term mean (i.e. using only the first and last sampling dates of 29 July and 8 October) gives an estimate of 7.6±1.3 MT/d. This long-term mean is what we report hereafter. Sediment deposition estimates using the particulate model (i.e. particulate fraction activities) are also shown in **Table 18** and **Table 19**.

Table 18 Steady state estimates of sediment deposition for each sampling date in 2014 and the time-weighted mean of all sampling dates. Estimates are calculated using either particulate radionuclide activities (particulate) or the total water column radionuclide activities (convective). Sediment deposition is in units of metric tonnes per day.

Date	^{131}I particulate	^{7}Be particulate	^{131}I convective	^{7}Be convective
16 July	390 ± 410	9.6 ± 3.7	-	-
29 July	128 ± 58	6.50 ± 0.95	15.9 ± 4.6	5.37 ± 0.97
26 August	1000 ± 3700	3.5 ± 1.6	8.3 ± 2.4	1.90 ± 0.72
8 October	37.7 ± 8.6	24.0 ± 7.4	3.00 ± 0.28	13.1 ± 3.7
Wt. Mean	**500 ± 1200**	**10.0 ± 3.8**	**9.2 ± 1.3**	**6.0 ± 2.3**

Table 19 Non-steady state estimates of sediment deposition between each sampling date in 2014 and the mean of all sampling dates. Estimates are calculated using either particulate radionuclide activities (particulate) or the total water column radionuclide activities (convective). Negative values imply erosion. Sediment deposition is in units of metric tonnes per day.

Date	^{131}I particulate	^{7}Be particulate	^{131}I convective	^{7}Be convective
16-29 July	200 ± 110	-22.1 ± 6.5	-	-
29 Jul- 26 Aug	87 ± 46	-16.7 ± 3.2	6.3 ± 2.2	-12.2 ± 2.4
26 Aug- 8 Oct	38.1 ± 9.1	50 ± 12	4.94 ± 0.49	24.8 ± 4.7
Wt. Mean	**94 ± 23**	**19.9 ± 6.5**	**5.48 ± 0.93**	10.2 ± 3.0
Long term Mean				**7.6 ± 1.3**

5.3.3. Comparison

Comparison of sediment deposition in the Milwaukee outer harbor results to published data presents a challenge, as no previous studies have directly reported this figure. However, the United States Army Corps of Engineers (US ACE) is charged with the maintenance dredging of federal navigation channels, which include much of the Milwaukee inner and outer harbor. In their 2008 dredged material maintenance plan (US ACE 2008), they list the estimated amount of sediment removal needed to keep the harbor at the designated federal depths over the next 23 years. This figure is 70,000 cubic yards of dredging every four years for the areas US ACE maintains in the Milwaukee harbor. This volume was converted to dry weight using the mean ratio of dry weight to (wet) volume of outer harbor sediment collected by gravity coring in this study, and scaled to outer harbor portion of the dredged area (calculation process described in detail in Appendix K). Assuming that the goal of US ACE dredging is to maintain constant depth (i.e. only remove newly buried sediment), 25 metric tonnes/d of sediment burial in the outer harbor must be occurring to motivate this amount of dredging.

We assume that sediment deposition rates outside of the dredged area in the outer harbor area negligible. This is because our bed sediment radionuclide results above suggest that bed

sediment in the outer harbor regularly moves and shifts (e.g. **Figure 22**). If this is the case, most newly deposited sediment should be eventually deposited in the deepest areas of the outer harbor, which are the dredged areas (shown in **Figure 33**). This US ACE sediment deposition estimate is higher than the deposition rates estimated in this study (**Figure 31**). However, some of the differences in sediment deposition rate estimates could be due to temporal factors or the inherent lack of precision in the US ACE dredging estimate. For example, the US ACE estimate is simply a prediction of anticipated future dredging needs, and past volumes of sediment dredging have varied. Additionally, the US ACE estimate takes into account the entire year, while the estimates from this study only show time points from July-October 2014. However, both sources give sediment deposition rates largely within the same order of magnitude. Therefore, we consider the two estimates to be reasonably close to one another for the purposes of comparing sediment deposition measured by different methods, and that the US ACE dredging estimate supports the possibility of ^{131}I and ^{7}Be being viable tools to estimate sediment deposition in this system.

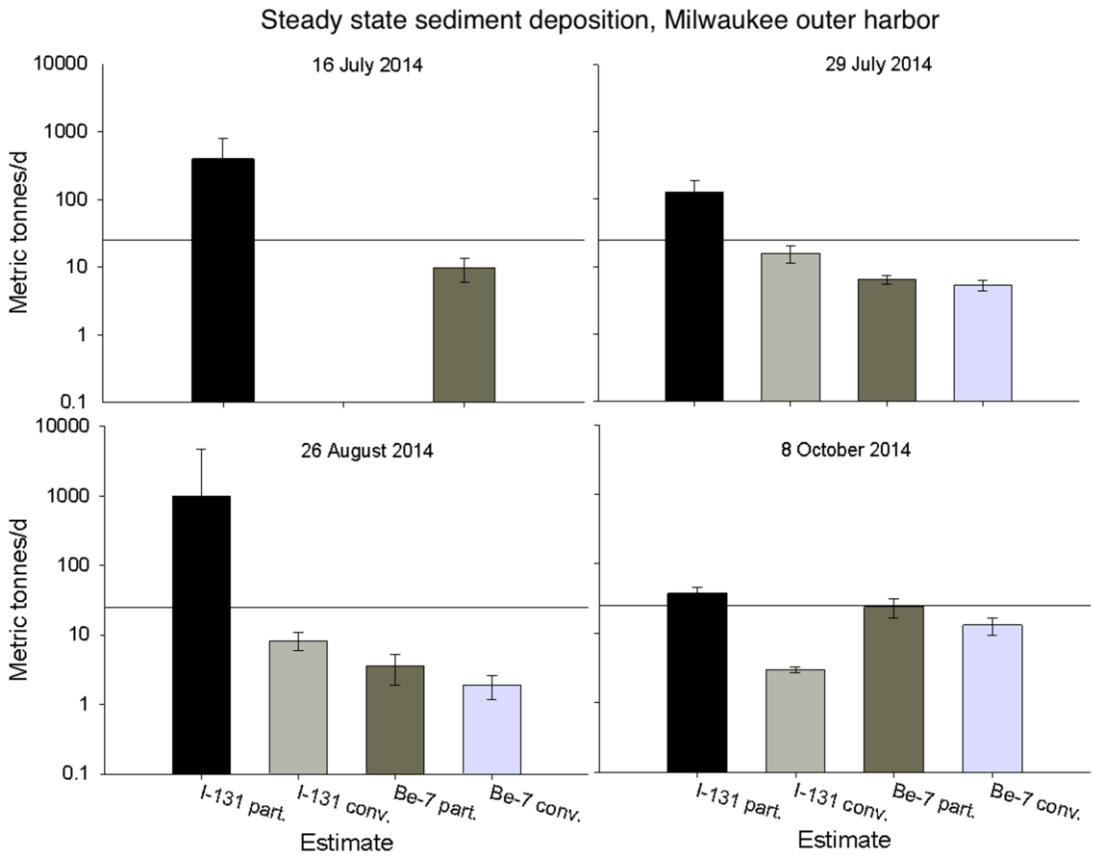

Figure 31 Steady state sediment deposition in the Milwaukee outer harbor on four dates according to the particulate and total water column activities of ^{131}I and ^{7}Be. These are compared to a sediment deposition estimate of ~25 metric tonnes/d based on an U.S. Army Corps of Engineers dredging report (US ACE 2008, reference line).

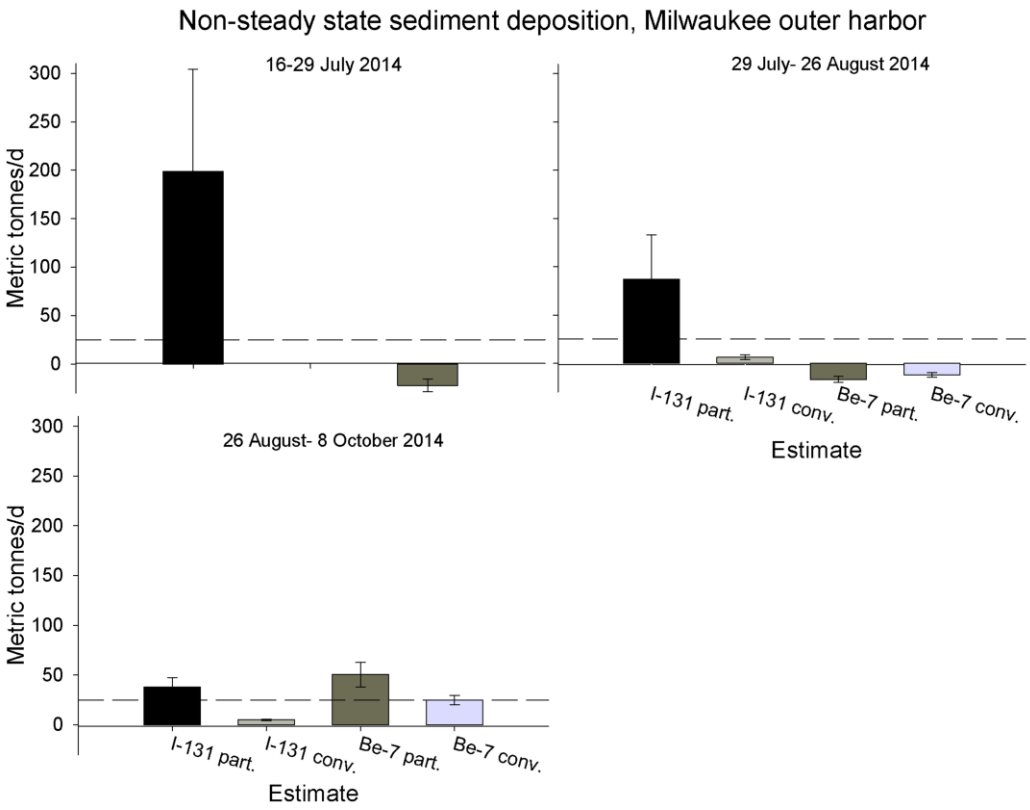

Figure 32 Non-steady state sediment deposition in the Milwaukee outer harbor on four dates according to the particulate and total water column activities of ^{131}I and ^{7}Be. These are compared to a sediment deposition estimate of ~25 metric tonnes/d based on an U.S. Army Corps of Engineers dredging report (US ACE 2008, reference line).

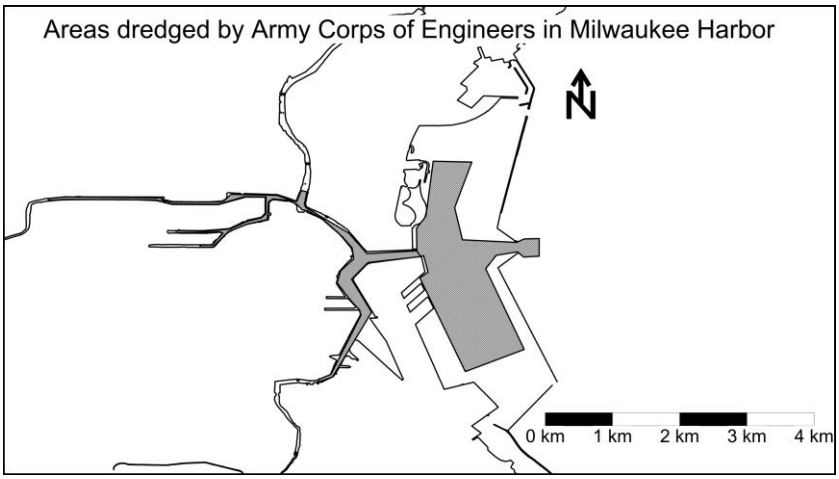

Figure 33 Milwaukee inner and outer harbors. Shaded areas are those dredged by the US Army Corps of Engineers. Dredged material figures have been scaled to the outer harbor portion of the dredging for comparison with outer harbor sediment burial estimated in this study.

The United States Geological Survey (USGS) takes daily measurements of river discharge, surface turbidity and bottom turbidity at the mouth of the Milwaukee River (after it has combined with the Menomonee and Kinnickinnic Rivers; USGS station 04087170). These data were used to calculate sediment loading to the Milwaukee outer harbor. This was accomplished by taking the mean of the surface and bottom turbidity measurements (assuming 1 Formazin Nephelometric Unit = 1 g/m^3) and multiplying it by the river discharge. On dates when discharge data was not available (1 October – 8 October, or 7% of total data), discharge from the next station upstream was substituted, which had consistently showed discharges very close to that of the Milwaukee river mouth. On other dates, bottom turbidity data was not available. To account for this, the mean ratio of the measured mean of bottom turbidity to surface turbidity versus surface turbidity (1.3; 75% of complete data record) was used to convert surface turbidity (100% of complete data record) to an mean of surface and bottom turbidity. The mean of these USGS sediment loading estimates over 29 July- 8 October, 2014 was 9.1±1.0 MT/d. Our sediment deposition estimates are consistently lower than this estimate of sediment loading (**Figure 34**). A comparison of our sediment deposition estimates to USGS data over time can be seen in **Figure 35**.

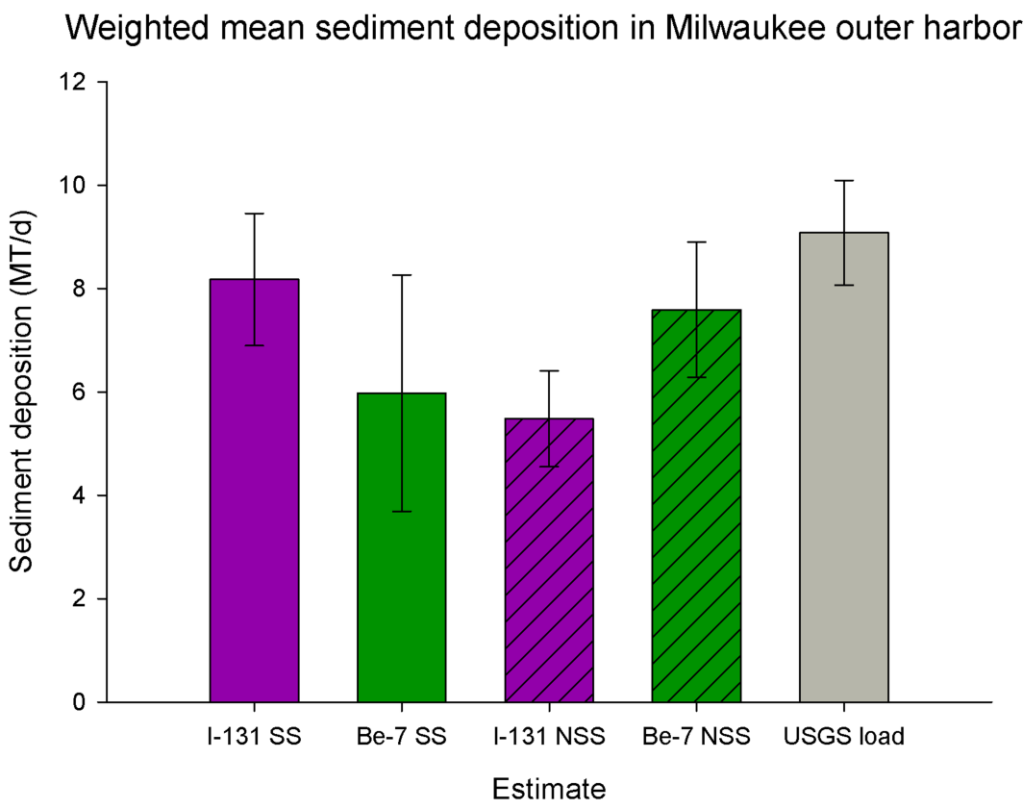

Figure 34 Steady state (SS) and non-steady state (NSS) weighted mean sediment deposition in the Milwaukee outer harbor in 2014 following the convective model using the short-lived radionuclides ^{131}I and ^{7}Be. An estimate of sediment loading to the harbor (9.1±1.0 MT/d) using United States Geological Survey (USGS) data is also shown.

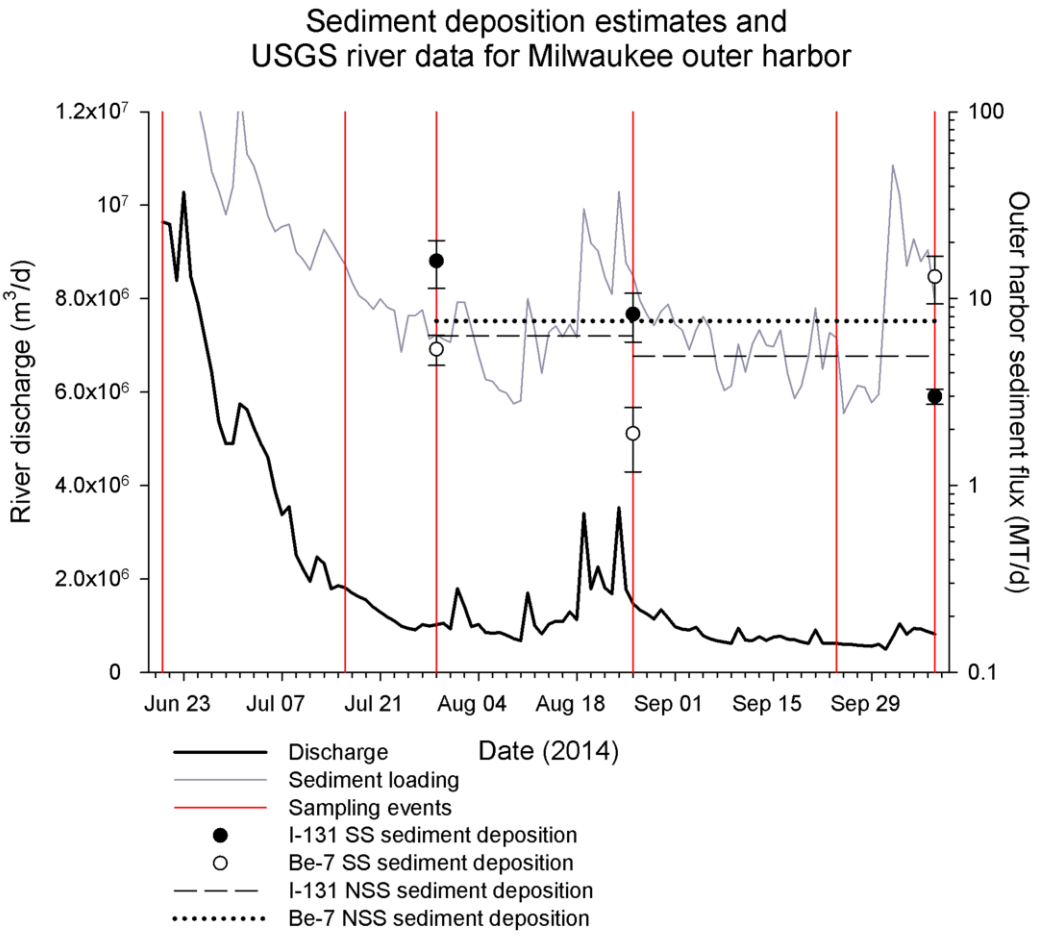

Figure 35 Sediment deposition estimates by date according to the steady state (SS) and non-steady state (NSS) models using the short-lived radionuclides ^{131}I and ^{7}Be. Convective mixing is assumed. River discharge and sediment loading into the outer harbor from the combined Milwaukee, Menomonee and Kinnickinnic Rivers are also shown, using data from the United States Geological Survey (USGS).

Additionally, the United States Environmental Protection Agency (US EPA) studied sediment in the Milwaukee outer harbor as part of its 1979 study on the effect of the Menomonee River on pollutants in Lake Michigan (Bannerman et al. 1979). The study calculated sediment loading to the outer harbor using total and suspended solids and discharge measurements in a similar manner as we have done with the USGS data above. In addition to carrying out these measurements at the mouth of the Milwaukee River, Bannerman et al. (1979) also performed them at the interfaces between the outer harbor and Lake Michigan. By comparing these

calculations of sediment loading to the outer harbor and sediment loading to Lake Michigan, they estimated that the difference between the two figures was the sediment deposition in the outer harbor. In this way, they estimated that the average yearly sediment deposition in the outer harbor was 55% of the sediment load entering the outer harbor.

By comparing the sediment deposition estimates from this study to the sediment loads estimated from USGS data, we can also calculate the percent of sediment loading contained in the outer harbor for comparison with Bannerman et al. (1979). Our estimates of percent sediment deposition range from 60%±12% to 90%±17%, with a mean of 75%±9% (using the estimates from the convective model only). The percent sediment deposition from each estimate is shown in **Table 20**. While the sediment deposition estimates from this study are higher than that of Bannerman et al. (1979), these differences may be a result of the low river discharge conditions during our study period (29 July to 8 October, 2014). The average combined river discharge during the (annual) study period of Bannerman et al. (1979) was 14.4 m^3/s, while it was only 11.9 m^3/s during our study period. This difference is equal to the entire average discharge of the Menomonee River in the study period of Bannerman et al. (1979). Additionally, Bannerman et al. (1979) describe a rain event which occurred on July 18, 1977 that produced a visible plume of suspended sediment extending into the lake as much as 5km from the gaps in the outer harbor for up to two days. Differences in river discharge such as these may not have allowed as much suspended sediment to settle out and be deposited in the outer harbor as during the low flow conditions of our study. These factors as well as the limited precision inherent in each study lead us to believe that our findings are reasonable when compared to those of Bannerman et al. (1979).

Table 20 Estimated percent of sediment loading deposited in the Milwaukee outer harbor from 29 July- 8 October, 2014 according to steady state (SS) and non-steady state (NSS) models of sediment deposition and assuming convective mixing. Sediment loading estimates are derived from United States Geological Survey data. An estimate from the United States Environmental Protection Agency (US EPA) is also shown (Bannerman et al. 1979).

Estimate	Percent sediment deposition
^{131}I SS	90 ± 17
^{7}Be SS	66 ± 26
^{131}I NSS	60 ± 12
^{7}Be NSS	84 ± 9
Mean	**75 ± 9**
US EPA	**55**

5.3.4. Implications

Sediment pollution comes with myriad ecological, economic and public health consequences. However, there are no previously published studies directly measuring sediment deposition in the Milwaukee outer harbor, an indication of the difficulty in obtaining this measurement. This study provides a feasible method for obtaining this information with relative ease and reliability.

The method described above has produced rough estimates for sediment deposition in the Milwaukee outer harbor. This sediment deposition estimate could be put to a variety of uses. These include predicting when and how much maintenance dredging needs to be done, and how expensive it will be. Additionally, if sediment burial is monitored concurrently with upstream restoration, development or dredging projects, it can be used to assess the effect of such activities on the amount of sediment being deposited in the outer harbor.

This method gives scientists and managers a tool to perform the difficult task of measuring sediment deposition in harbors and other somewhat enclosed areas through the use of ^{131}I and/or ^{7}Be. This method could conceivably be used with any radionuclide found in both the

water column and the bed sediment in significant activities, provided enough is known about the radionuclide's dynamics and biogeochemistry. It is preferable, however, to use a radionuclide like ^{131}I, due to the simplicity provided by its clear point source.

5.4. Summary and Conclusions

To summarize, this study has found the short-lived, sewage-derived radionuclide ^{131}I in sewage effluent from the two major Milwaukee WRFs, in *Cladophora* algae and dreissenid mussels in nearshore and offshore Lake Michigan, and in the bed sediment and water column of the Milwaukee outer harbor.

In Milwaukee sewage effluent from the Jones Island WRF, ^{131}I had a mean activity of ~0.25 Bq/L and a mean flux of $(6.64\pm0.12)\times10^{7}$ Bq/d to the Milwaukee outer harbor. From the South Shore WRF, sewage effluent had a mean ^{131}I activity of ~0.74 Bq/L and a mean flux of $(2.07\pm0.68)\times10^{8}$ Bq/d to nearshore Lake Michigan. Sewage effluent samples were taken from June 2013 to December 2014.

Cladophora containing ^{131}I was found along the Milwaukee area shoreline and Lake Michigan nearshore zone in samples collected between July 2013 and July 2014. Mean site ^{131}I activities ranged from below the limit of detection to 38.84±0.75 Bq/g DW. ^{131}I was found in *Cladophora* both north and south of both MMSD WRFs, and was highest near South Shore WRF.

Several opportunistic samples of invasive dreissenid mussels collected between July 2013 and July 2014 were also found to contain ^{131}I. Mean site ^{131}I activities ranged from below the detection limit to 0.55±0.29 Bq/m^2 and 0.70±0.26 Bq/g DW and were highest near the Milwaukee harbor. However, at sites where *Cladophora* and dreissenid mussels were both sampled, *Cladophora* almost always contained higher ^{131}I activities per unit dry weight.

Benthic trawl surveys using an epibenthic sled were used to systematically study ^{131}I in benthic material at eight stations in the nearshore and offshore zones of Lake Michigan on 20 October and 5 November, 2014. The collected material was mostly abiotic (e.g. sand and pebbles), but also contained dreissenid mussels and usually a small amount of *Cladophora*. Each sample contained ^{131}I, including the furthest station, which was 8km offshore and 10km from the South Shore WRF outfall. ^{131}I activities were highest near the South Shore WRF. Most ^{131}I activity was found in *Cladophora*, despite it only making up a small fraction of each sample's dry weight. This activity was about ten times the activity found in dreissenid mussels, which in turn was about ten times the activity found in abiotic material.

Bed sediment samples were taken by gravity core in the Milwaukee outer harbor on four dates in the summer and fall of 2014. On each date, ^{131}I was found in sediment taken from several stations. Outer harbor bed sediment ^{131}I inventories ranged from 11.8±7.5 Bq/m^2 to 18.8±4.2 Bq/m^2. The spatial distribution of ^{131}I varied over time, but ^{131}I was always detected near the Jones Island WRF outfall.

The water column of the Milwaukee outer harbor was also sampled and tested for ^{131}I. The particulate fraction was sampled four times and the dissolved fraction was sampled three times in the summer and fall of 2014. ^{131}I was consistently detected, and had much higher activities in the dissolved fraction than the particulate fraction. Dissolved ^{131}I activities varied from 1.48±0.24 mBq/L to 7.53±0.15 mBq/L, and particulate ^{131}I activities varied from 0.022±0.081 mBq/L to 0.65±0.14 mBq/L.

^{7}Be, an atmospherically-sourced radionuclide, was also measured. The flux of ^{7}Be from the atmosphere was measured using a rain barrel to collect rainwater from June to November

2014. The flux of ^{7}Be through atmospheric deposition ranged from 1.71±0.10 Bq/m^2/d to 16.30±0.35 Bq/m^2/d, with a mean of 6.4±1.2 Bq/m^2/d. As other studies have also reported, the ^{7}Be flux was higher earlier in the season. ^{7}Be was also always found in the Milwaukee outer harbor, and at activities much higher than that of ^{131}I. The mean bed sediment activity of ^{7}Be was 305±57 Bq/m^2. In the water column, ^{7}Be activities were higher in the particulate fraction (mean: 4.98±0.63 mBq/) than the dissolved fraction (2.31±0.59 mBq/L).

^{131}I was measured in *Cladophora* algae at popular Milwaukee-area beaches as well as offshore, as far as 8km offshore and 10km from the nearest WRF outfall, indicating that sewage effluent-derived material can travel to these locations in a matter of days to weeks. We applied a steady state model to show the movement of *Cladophora* with measurable ^{131}I both offshore to the east and alongshore to the south at speeds of ~200 to ~500 m/d- an indication of a net southeasterly current moving material away from Milwaukee. We also use ^{131}I along with ^{7}Be to provide steady and non-steady state estimates of sediment deposition in the Milwaukee outer harbor. Calculated fluxes assuming radionuclide scavenging by settling particles resulted in significant disagreement between both radionuclide-derived mass fluxes, with ^{131}I-derived mass fluxes as high as three orders of magnitude larger than ^{7}Be-derived mass fluxes. Concordance between both radionuclide derived mass fluxes was achieved, however, when bottom scavenging and vertical convection of water column material was assumed. Our mean (July to October, 2014) ^{131}I-derived sediment deposition estimates for the Milwaukee outer harbor range from 5.5±0.9 MT/d (using non-steady state assumptions) to 9.2±1.3 MT/d (using steady state assumptions), and compare well with our mean (July to October, 2014) ^{7}Be-derived sediment deposition estimates of 7.6±1.3 MT/d (using non-steady state assumptions) and 6.0±2.3 MT/d (using steady state assumptions). Both sets of radionuclide derived sediment flux estimates are in

reasonable concordance with sediment loading and deposition estimates made by the United States Army Corps of Engineers, Geological Survey and Environmental Protection Agency.

In conclusion, our work positively identifies the presence of ^{131}I in Milwaukee sewage effluent and in the environment in Lake Michigan. While future refinements to the methods and applications explored here are needed, we show that ^{131}I has great potential to serve as a valuable tool for scientists and managers to trace sewage-derived material, benthic transport and sediment deposition near cities like Milwaukee.

References

(1) Alongi, D. M. (2002) Present state and future of the world's mangrove forests. *Environ. Conserv. 29*, 331–349.

(2) Amachi, S. (2008) Microbial Contribution to Global Iodine Cycling: Volatilization, Accumulation, Reduction, Oxidation, and Sorption of Iodine. *Microbes Environ. 23*, 269–276.

(3) Apfelbaum, S., Dephilip, M., and Hinz, L. (2007) Identifying and Valuing Restoration Opportunities and Resource Improvements at Watershed and Subwatershed. Broadhead, WI. *Great Lakes Protection Fund Grant 758 Report.*

(4) Bannerman, R., Konrad, J. G., and Becker, D. (1979) Effects of Tributary Inputs On Lake Michigan During High Flows. Chicago, IL. *United States Environmental Protection Agency Report.*

(5) Barci-Funel, G., Dalmasso, J., Magne, J., and Ardisson, G. (1993) Simultaneous detection of short-lived 201Tl, 99Tcm and 131I isotopes in sewage sludge using low energy photon spectrometry. *Sci. Total Environ. 130-131*, 37–42.

(6) Baskaran, M., and Swarzenski, P. W. (2007) Seasonal variations on the residence times and partitioning of short-lived radionuclides (234Th, 7Be and 210Pb) and depositional fluxes of 7Be and 210Pb in Tampa Bay, Florida. *Mar. Chem. 104*, 27–42.

(7) Beletsky, D., Saylor, J. H., and Schwab, D. J. (1999) Mean Circulation in the Great Lakes. *J. Great Lakes Res. 25*, 78–93.

(8) Benotti, M. J., and Brownawell, B. J. (2009) Microbial degradation of pharmaceuticals in estuarine and coastal seawater. *Environ. Pollut. 157*, 994–1002.

(9) Blair, B., Crago, J., Hedman, C., and Klaper, R. (2013) Pharmaceuticals and personal care products found in the Great Lakes above concentrations of environmental concern. *Chemosphere*.

(10) Bojanowski, R., and Paslawska, S. (1970) On the occurrence of iodine in bottom sediments and interstitial waters of the Southern Baltic Sea. *Acta Geophys. 18*, 277–286.

(11) Brodin, T., Fick, J., Jonsson, M., and Klaminder, J. (2013) Dilute concentrations of a psychiatric drug alter behavior of fish from natural populations. *Science 339*, 814–5.

(12) Chapman, E. M. (1946) The Treatmant of Hyperthyroidism with Radioactive Iodine. *J. Am. Med. Assoc. 131*, 86.

(13) Cochran, J. K., and Masque, P. (2003) Short-lived U/Th Series Radionuclides in the Ocean: Tracers for Scavenging Rates, Export Fluxes and Particle Dynamics. *Rev. Mineral. Geochemistry 52*, 461–492.

(14) Cosenza, A., Rizzo, S., Sansone Santamaria, A., and Viviani, G. (2015) Radionuclides in wastewater treatment plants: monitoring of Sicilian plants. *Water Sci. Technol. 71*, 252.

(15) Dodds, W. K., and Gudder, D. A. (1992) The Ecology of Cladophora. *J. Phycol. 28*, 415–427.

(16) Eadie, B. J., Robbins, J. A., Klurnp, J. V, Schwab, D. J., and Edgington, D. N. (2008) Winter-Spring Storms and Their Influence on Sediment Resuspension, Transport, and Accumulation Patterns in Southern Lake Michigan. *Oceanography 21*, 118–135.

(17) Erlandsson, B., and Mattsson, S. (1978) Medically used radionuclides in sewage sludge. *Water. Air. Soil Pollut. 9*, 199–206.

(18) Fent, K., Weston, A. a, and Caminada, D. (2006) Ecotoxicology of human pharmaceuticals. *Aquat. Toxicol. 76*, 122–59.

(19) Fischer, H. W., Ulbrich, S., Pittauerová, D., and Hettwig, B. (2009) Medical radioisotopes in the environment - following the pathway from patient to river sediment. *J. Environ. Radioact. 100*, 1079–85.

(20) Fitzgerald, S. a., Klump, J. V., Swarzenski, P. W., Mackenzie, R. a., and Richards, K. D. (2001) Beryllium-7 as a Tracer of Short-Term Sediment Deposition and Resuspension in the Fox River, Wisconsin. *Environ. Sci. Technol. 35*, 300–305.

(21) Gomez, E., Bachelot, M., Boillot, C., Munaron, D., Chiron, S., Casellas, C., and Fenet, H. (2012) Bioconcentration of two pharmaceuticals (benzodiazepines) and two personal care products (UV filters) in marine mussels (Mytilus galloprovincialis) under controlled laboratory conditions. *Environ. Sci. Pollut. Res. 19*, 2561–2569.

(22) Great Lakes Commission. (2008) The Economics of Soil Erosion and Sedimentation in the Great Lakes Basin. *GLC Report to US ACE*.

(23) Higgins, S. N., Todd Howell, E., Hecky, R. E., Guildford, S. J., and Smith, R. E. (2005) The Wall of Green: The Status of Cladophora glomerata on the Northern Shores of Lake Erie's Eastern Basin, 1995–2002. *J. Great Lakes Res. 31*, 547–563.

(24) IAEA (International Atomic Energy Agency). (2010) Handbook of Parameter Values for the Prediction of Radionuclide Transfer in Terrestrial and Freshwater. Vienna, Austria. *IAEA Technical Report no. 472*.

(25) International Joint Commission. (1987) Revised Great Lakes Water Quality Agreement of 1978 as Amended by Protocol Signed November 18, 1987. Ottawa, United States, Canada. *International Joint Commission Agreement.*

(26) Ishikawa, Y., Kagaya, H., and Saga, K. (2004) Biomagnification of 7Be, 234Th, and 228Ra in marine organisms near the northern Pacific coast of Japan. *J. Environ. Radioact. 76*, 103–12.

(27) Jiang, M., Wang, L., and Ji, R. (2010) Biotic and abiotic degradation of four cephalosporin antibiotics in a lake surface water and sediment. *Chemosphere 80*, 1399–405.

(28) Jiménez, F., Debán, L., Pardo, R., López, R., and García-Talavera, M. (2011) Levels of 131I and six natural radionuclides in sludge from the sewage treatment plant of valladolid, Spain. *Water. Air. Soil Pollut. 217*, 515–521.

(29) Karlander, E. P., and Krauss, R. W. (1972) Absorption and Toxicity of Beryllium and Lithium in Chlorella vannielii. *Chesap. Sci. 13*, 245.

(30) Kennish, M. J. (2002) Environmental threats and environmental future of estuaries. *Environ. Conserv. 29*, 78–107.

(31) Kleinheinz, G. T. (2014) Wisconsin Beach Health. *Lake Michigan Beach Advis.*

(32) Kleinschmidt, R. (2009) Uptake and depuration of 131I by the macroalgae Catenella nipae--potential use as an environmental monitor for radiopharmaceutical waste. *Mar. Pollut. Bull. 58*, 1539–43.

(33) Küpper, F. C., Schweigert, N., Gall, E. a., Legendre, J. M., Vilter, H., and Kloareg, B. (1998) Iodine uptake in Laminariales involves extracellular, haloperoxidase-mediated oxidation of iodide. *Planta 207*, 163–171.

(34) Landis, J. D., Renshaw, C. E., and Kaste, J. M. (2014) Quantitative retention of atmospherically deposited elements by native vegetation is traced by the fallout radionuclides 7Be and 210Pb. *Environ. Sci. Technol. 48*, 12022–30.

(35) Liu, H., Jacob, D. J., Bey, I., and Yantosca, R. M. (2001) Constraints from 210 Pb and 7 Be on wet deposition and transport in a global three-dimensional chemical tracer model driven by assimilated meteorological fields. *J. Geophys. Res. Atmos. 106*, 12109–12128.

(36) Luthy, R. G., Aiken, G. R., Brusseau, M. L., Cunningham, S. D., Gschwend, P. M., Pignatello, J. J., Reinhard, M., Traina, S. J., Weber, W. J., and Westall, J. C. (1997) Sequestration of Hydrophobic Organic Contaminants by Geosorbents. *Environ. Sci. Technol. 31*, 3341–3347.

(37) Mackin, J. E., Aller, R. C., and Ullman, W. J. (1988) The effects of iron reduction and nonsteady-state diagenesis on iodine, ammonium, and boron distributions in sediments from the Amazon continental shelf. *Cont. Shelf Res. 8*, 363–386.

(38) Mallin, M. A., Cahoon, L. B., Toothman, B. R., Parsons, D. C., McIver, M. R., Ortwine, M. L., and Harrington, R. N. (2007) Impacts of a raw sewage spill on water and sediment quality in an urbanized estuary. *Mar. Pollut. Bull. 54*, 81–8.

(39) Martin, J. E., and Fenner, F. D. (1997) Radioactivity in municipal sewage and sludge. *Public Health Rep. 112*, 308–318.

(40) Martin, J. B., Gieskes, J. M., Torres, M., and Kastner, M. (1993) Bromine and iodine in Peru margin sediments and pore fluids: Implications for fluid origins. *Geochim. Cosmochim. Acta 57*, 4377–4389.

(41) Martinelango, P. K., Tian, K., and Dasgupta, P. K. (2006) Perchlorate in seawater: Bioconcentration of iodide and perchlorate by various seaweed species. *Anal. Chim. Acta 567*, 100–107.

(42) Mcneary, D., and Baskaran, M. (2003) Depositional characteristics of 7 Be and 210 Pb in southeastern Michigan *108*.

(43) Milliman, J., and Meade, R. (1983) World-Wide Delivery of River Sediment to the Oceans. *J. Geol. 91*, 1–21.

(44) Mohiuddin, K. M., Zakir, H. M., Otomo, K., Sharmin, S., and Shikazono, N. (2010) Geochemical distribution of trace metal pollutants in water and sediments of downstream of an urban river. *Int. J. Environ. Sci. Technol. 7*, 17–28.

(45) Mortimer, C. H. (1988) Discoveries and testable hypotheses arising from Coastal Zone Color Scanner imagery of southern Lake Michigan. *Limnol. Oceanogr. 33*, 203–226.

(46) Moss, C. E. (1973) Control of radioisotope releases to the environment from diagnostic isotope procedures. *Health Phys. 25*, 197–8.

(47) Nalepa, T. F., Fanslow, D. L., and Pothoven, S. a. (2010) Recent changes in density, biomass, recruitment, size structure, and nutritional state of Dreissena populations in southern Lake Michigan. *J. Great Lakes Res. 36*, 5–19.

(48) Newton, R. J., Vandewalle, J. L., Borchardt, M. a, Gorelick, M. H., and McLellan, S. L. (2011) Lachnospiraceae and Bacteroidales alternative fecal indicators reveal chronic human sewage contamination in an urban harbor. *Appl. Environ. Microbiol. 77*, 6972–81.

(49) Nichols, A. L., Aldama, D. L., and M., V. (2008) Handbook of Nuclear Data for Safeguards. Vienna, Austria. *International Atomic Energy Agency Handbook.*

(50) Ockenden, M. C., Deasy, C., Quinton, J. N., Bailey, A. P., Surridge, B., and Stoate, C. (2012) Evaluation of field wetlands for mitigation of diffuse pollution from agriculture: Sediment retention, cost and effectiveness. *Environ. Sci. Policy 24*, 110–119.

(51) Olapade, O. A., Depas, M. M., Jensen, E. T., and McLellan, S. L. (2006) Microbial communities and fecal indicator bacteria associated with Cladophora mats on beach sites along Lake Michigan shores. *Appl. Environ. Microbiol. 72*, 1932–8.

(52) Parekh, P., Bari, A., and Harris, P. (2003) Rapid radiochemical analysis of 131I in environmental samples using a well-type Ge-detector. *J. Radioanal. Nucl. … 256*, 225–230.

(53) Pimenova, M. E., Shelepova, O. V., Kostenko, N. S., Safronova, L. M., and Konkova, P. D. (2004) Content of iodine in some species of medicinal plants of Kara-Dag nature reserve and in seaweeds of its aqua territory (South-Eastern Crimea). *Rastitelnye resursy. 40*, 3-17.

(54) Price, N. B., and Calvert, S. E. (1973) The geochemistry of iodine in oxidised and reduced recent marine sediments. *Geochim. Cosmochim. Acta 37*, 2149–2158.

(55) Price, N. B., and Calvert, S. E. (1977) The contrasting geochemical behaviours of iodine and bromine in recent sediments from the Namibian shelf. *Geochim. Cosmochim. Acta 41*, 1769–1775.

(56) Rabinovici, S. J. M., Bernknopf, R. L., Wein, A. M., Coursey, D. L., and Whitman, R. L. (2004) Economic and Health Risk Trade-Offs of Swim Closures at a Lake Michigan Beach. *Environ. Sci. Technol. 38*, 2737–2745.

(57) Rasmuson, T. (2006) Radioactive iodine in thyroid medicine. *Acta Oncol. (Madr). 45*, 1011–1012.

(58) Rose, P. S., Smith, J. P., Cochran, J. K., Aller, R. C., and Swanson, R. L. (2013) Behavior of medically-derived 131I in the tidal Potomac River. *Sci. Total Environ. 452-453*, 87–97.

(59) Rose, P. S., Swanson, R. L., and Cochran, J. K. (2012) Medically-derived 131I in municipal sewage effluent. *Water Res. 46*, 5663–71.

(60) Rose, P. S., Smith, J. P., Aller, R. C., Cochran, J. K., Swanson, R. L., and Coffin, R. B. (2015) Medically-Derived ^{131} I as a Tool for Investigating the Fate of Wastewater Nitrogen in Aquatic Environments. *Environ. Sci. Technol. 49*, 10312–10319.

(61) Rose, P. (2011) Medically-derived ^{131}I as a tracer in aquatic environments. Stony Brook University. *PhD Dissertation.*

(62) Rutgers van der Loeff, M., Sarin, M. M., Baskaran, M., Benitez-Nelson, C., Buesseler, K. O., Charette, M., Dai, M., Gustafsson, Ö., Masque, P., Morris, P. J., Orlandini, K., Rodriguez y Baena, A., Savoye, N., Schmidt, S., Turnewitsch, R., Vöge, I., and Waples, J. T. (2006) A review of present techniques and methodological advances in analyzing 234Th in aquatic systems. *Mar. Chem. 100*, 190–212.

(63) Santos, L. H. M. L. M., Araújo, a N., Fachini, A., Pena, a, Delerue-Matos, C., and Montenegro, M. C. B. S. M. (2010) Ecotoxicological aspects related to the presence of pharmaceuticals in the aquatic environment. *J. Hazard. Mater. 175*, 45–95.

(64) Sauer, E. P., Vandewalle, J. L., Bootsma, M. J., and McLellan, S. L. (2011) Detection of the human specific Bacteroides genetic marker provides evidence of widespread sewage contamination of stormwater in the urban environment. *Water Res. 45*, 4081–91.

(65) Shishkina, O. V., and Pavlova, G. A. (1965) Iodine distribution in marine and oceanic bottom muds and in their pore fluids. *Geochem. Intern.* 559–565.

(66) Short, F., and Wyllie-Echeverria, S. (1996) Natural and human-induced disturbance of seagrasses. *Environ. Conserv. 23*, 17–27.

(67) Smith, J. P., Oktay, S. I., Kada, J., and Olsen, C. R. (2008) Iodine-131: a potential short-lived, wastewater-specific particle tracer in an urbanized estuarine system. *Environ. Sci. Technol. 42*, 5435–40.

(68) Sodd, V. J., Velten, R. J., and Saenger, E. L. (1975) Concentrations of the Medically Useful Radionuclides, Technetium-99m and Iodine-131 at a Large Metropolitan Waste Water Treatment Plant. *Health Phys. 28*, 355–359.

(69) Stetar, E. A., Boston, H. L., Larsen, I. L., and Mobley, M. H. (1993) The removal of radioactive cobalt , cesium , and iodine in a conventional municipal wastewater treatment plant. *Water Environ. Res. 65*, 630–639.

(70) Ullman, W. J. (1982) The Sedimentary Geochemistry of Iodine and Bromine. University of Chicago. *PhD Dissertation.*

(71) Ullman, W. J., and Aller, R. C. (1985) The geochemistry of iodine in near-shore carbonate sediments. *Geochim. Cosmochim. Acta 49*, 967–978.

(72) Valentin, J. (2004) Release of patients after therapy with unsealed radionuclides. *Ann. ICRP 34*.

(73) Veliscek Carolan, J., Hughes, C. E., and Hoffmann, E. L. (2011) Dose assessment for marine biota and humans from discharge of 131I to the marine environment and uptake by algae in Sydney, Australia. *J. Environ. Radioact. 102*, 953–963.

(74) Verdel, E., Kline, P., Wani, S., and Woods, A. (2000) Purification and partial characterization of haloperoxidase from Cladophora glomerata. *Comp. Biochem. …*.

(75) Waller, E. J., and Cole, D. (1999) An Environmental Radionuclide Baseline Study Near Three Canadian Naval Ports. *Health Phys. 77*, 37–42.

(76) Waples, J. T. (2009) Water column current data at Green Can Station, 2007-2009, Lake Michigan. Milwaukee, WI. *[Unpublished data]*.

(77) Waples, J. T. (2015, in press) Particle delivery to the benthos of coastal Lake Michigan. *J. Geophys. Res. Ocean*.

(78) Waples, J. T., Benitez-Nelson, C., Savoye, N., Rutgers van der Loeff, M., Baskaran, M., and Gustafsson, Ö. (2006) An introduction to the application and future use of ^{234}Th in aquatic systems. *Mar. Chem. 100*, 166–189.

(79) Waples, J. T., and Klump, J. V. (2013) Vertical and horizontal particle transport in the coastal waters of a large lake: An assessment by sediment trap and thorium-234 measurements. *J. Geophys. Res. Ocean. 118*, 5376–5397.

(80) Zou, Y. H., and Christensen, E. R. (2012) Phosphorus Loading to Milwaukee Harbor from Rivers, Storm Water, and Wastewater Treatment. *J. Environ. Eng. 138*, 143–151.

Appendices

Appendix A: Sewage Effluent Samples

This appendix contains the raw data used to calculate ^{131}I fluxes from water reclamation facilities operated by the Milwaukee Metropolitan Sewerage District (MMSD) from June 2013 to December 2014. All samples were counted in Marinelli beakers. The column descriptions are as follows. The location of the two water reclamation facilities (WRFs) in relation to the University of Wisconsin-Milwaukee School of Freshwater Sciences (SFS) is shown below the raw data. The results (^{131}I activities) for each individual sample are listed below that, followed finally by an example comparison examining the effect of bleach on sample ^{131}I activity.

1. **Sample date**: date of composite sample prepared by MMSD. Midpoint of composite is always 17:00 on date.
2. **WRF**: sampled water reclamation facility: Jones Island (JI) or South Shore (SS). Also included are the test samples taken from the small WRFs in Cedarburg (C), West Bend (WB), South Milwaukee (SM) and Racine (R).
3. **V eff**: volume of effluent in counted sample (mL).
4. **V samp**: volume of total counted sample (mL). Differences between V samp and V eff are attributed to the addition of bleach and/or deionized water.
5. **Det**: gamma detector used.
6. **Counting start**: start date and time of gamma analysis.
7. **Live time**: live time of gamma analysis (s).
8. **^{131}I Peak**: energy of the ^{131}I peak (keV).
9. **^{131}I Counts**: ^{131}I counts recorded, ± one standard deviation.
10. **Flow**: mean effluent discharge from the water reclamation facility during sampling period, reported by MMSD ($10^5 m^3/d$, or $10^8 L/d$).

Sample date	WRF	V eff	V samp	Det	Counting Start	Live time	^{131}I Peak	^{131}I Counts	Flow
7/16/13	JI	840	930	1	7/18/13 10:14	100792	363.92	406 ± 43	2.99
7/29/13	JI	800	890	1	7/30/13 13:37	172800	364.00	56 ± 26	2.63
8/6/13	JI	710	800	1	8/8/13 10:57	107531	364.56	207 ± 49	2.44
8/14/13	JI	800	890	1	8/15/13 11:46	90840	364.09	1210 ± 57	2.40
11/7/13	JI	655	745	1	11/11/13 10:04	172800	364.00	172 ± 46	4.05
12/5/13	JI	435	525	1	12/6/13 11:07	172800	364.00	1210 ± 66	2.27
12/18/13	JI	800	890	1	12/19/13 11:19	94319	364.18	301 ± 51	2.23
12/29/13	JI	770	860	1	1/2/14 14:14	172800	363.75	180 ± 54	2.10
1/21/14	JI	800	890	1	1/22/14 11:08	172800	364.01	623 ± 68	2.42
2/5/14	JI	800	890	1	2/6/14 13:45	172800	363.97	576 ± 61	2.44
2/18/14	JI	800	890	1	2/19/14 10:39	172800	364.17	457 ± 66	2.85
3/5/14	JI	220	890	1	3/8/14 11:40	172800	364.42	127 ± 50	2.44
3/25/14	JI	800	890	1	3/26/14 10:53	172800	364.12	380 ± 66	3.07
4/10/14	JI	800	890	1	4/13/14 8:12	172800	364.00	147 ± 47	3.02
4/23/14	JI	800	890	1	4/24/14 11:46	172800	364.33	253 ± 51	3.22
5/8/14	JI	800	890	1	5/9/14 10:53	172800	364.41	1410 ± 72	3.43
6/3/14	JI	255	890	1	6/4/14 10:34	172800	364.00	84 ± 46	2.89
6/12/14	JI	800	890	1	6/17/14 12:03	170447	364.22	269 ± 46	5.28
6/30/14	JI	470	560	1	7/3/14 18:42	172800	364.00	56 ± 46	5.73
7/20/14	JI	800	800	2	7/22/14 13:13	100702	365.63	612 ± 52	2.40
8/5/14	JI	800	800	3	8/6/14 16:37	79268	365.70	36 ± 44	2.35
8/17/14	JI	800	800	3	8/18/14 13:29	159046	364.60	949 ± 59	2.97
9/3/14	JI	810	810	3	9/8/14 8:03	179689	364.32	69 ± 30	2.48
9/21/14	JI	800	800	3	9/22/14 10:16	191110	363.51	1 ± 74	2.56
10/5/14	JI	670	800	3	10/6/14 11:37	192607	364.67	558 ± 76	2.13
10/26/14	JI	800	800	3	11/2/14 13:01	78020	366.08	54 ± 42	2.66
11/2/14	JI	800	800	2	11/4/14 9:21	121930	365.88	67 ± 56	2.89
11/18/14	JI	428	800	2	11/19/14 10:39	168669	365.93	219 ± 64	2.16
12/9/14	JI	800	800	3	12/12/14 9:58	257524	364.39	123 ± 82	2.33
6/20/13	SS	670	720	1	6/21/13 11:42	172800	364.31	451 ± 65	2.65
7/16/13	SS	840	930	1	7/22/13 11:40	172800	364.00	119 ± 27	2.65
7/29/13	SS	800	890	1	8/1/13 17:15	84292	364.25	849 ± 55	2.42
8/6/13	SS	800	890	1	8/9/13 16:50	172800	364.25	1090 ± 73	2.52
8/14/13	SS	580	670	1	8/16/13 13:03	172800	364.16	1120 ± 71	2.50
11/7/13	SS	800	890	1	11/8/13 10:58	172800	364.00	68 ± 47	3.10
12/5/13	SS	800	890	1	12/9/13 9:47	172800	364.00	197 ± 47	2.73
12/18/13	SS	285	890	1	12/20/13 13:34	172800	364.16	614 ± 68	2.23
12/29/13	SS	800	890	1	12/30/13 11:16	172800	364.16	121 ± 47	2.40
1/21/14	SS	790	880	1	1/24/14 11:48	172800	364.08	371 ± 64	2.62
2/5/14	SS	800	890	1	2/10/14 9:36	172800	364.00	142 ± 47	2.29
2/18/14	SS	800	890	1	2/21/14 15:13	172800	364.20	553 ± 61	2.27
3/5/14	SS	670	890	1	3/6/14 10:49	172800	364.00	191 ± 48	2.43
3/25/14	SS	800	890	1	3/28/14 11:02	172800	364.23	233 ± 50	3.22
4/10/14	SS	800	890	1	4/11/14 11:50	159671	364.00	118 ± 46	3.75
4/23/14	SS	800	890	1	4/26/14 12:24	172800	364.30	2820 ± 82	3.60
5/8/14	SS	800	890	1	5/12/14 9:45	172800	364.41	8140 ± 109	3.54
6/3/14	SS	800	890	1	6/6/14 10:53	172800	364.48	836 ± 69	3.90
6/12/14	SS	800	890	1	6/19/14 11:26	168352	363.90	195 ± 46	4.28
6/30/14	SS	800	890	3	7/3/14 18:45	192494	364.55	382 ± 148	4.27
7/20/14	SS	800	800	3	7/22/14 13:21	99954	364.52	1123 ± 120	2.78
8/5/14	SS	800	800	2	8/6/14 16:34	89648	364.86	181 ± 47	2.73
8/17/14	SS	800	800	2	8/18/14 13:28	82437	365.66	3312 ± 75	2.51

Sample date	WRF	V eff	V samp	Det	Counting Start	Live time	^{131}I Peak	^{131}I Counts	Flow
9/3/14	SS	800	800	2	9/8/14 8:02	179555	365.64	676 ± 69	2.65
9/21/14	SS	680	800	2	9/22/14 10:20	190694	365.66	7011 ± 109	2.46
10/5/14	SS	552	800	2	10/6/14 11:40	192265	365.59	202 ± 67	2.47
10/26/14	SS	790	790	2	10/29/14 11:05	167334	364.97	75 ± 63	2.38
11/2/14	SS	800	800	3	11/3/14 10:44	203170	364.75	180 ± 72	2.16
11/18/14	SS	800	800	3	11/24/14 9:34	175014	364.72	49 ± 68	2.33
12/9/14	SS	800	800	2	12/12/14 9:59	257514	364.18	1606 ± 83	2.69
7/8/14	WB	800	800	1	7/10/14 10:26	104175	364.00	0 ± 0	0.21
7/8/14	C	800	890	3	7/9/14 16:14	170537	364.47	0 ± 0	0.09
7/8/14	SM	800	852	2	7/9/14 16:17	170166	363.71	52 ± 58	0.14
7/10/14	R	800	800	1	7/11/14 15:32	172800	364.48	2610 ± 82	0.62

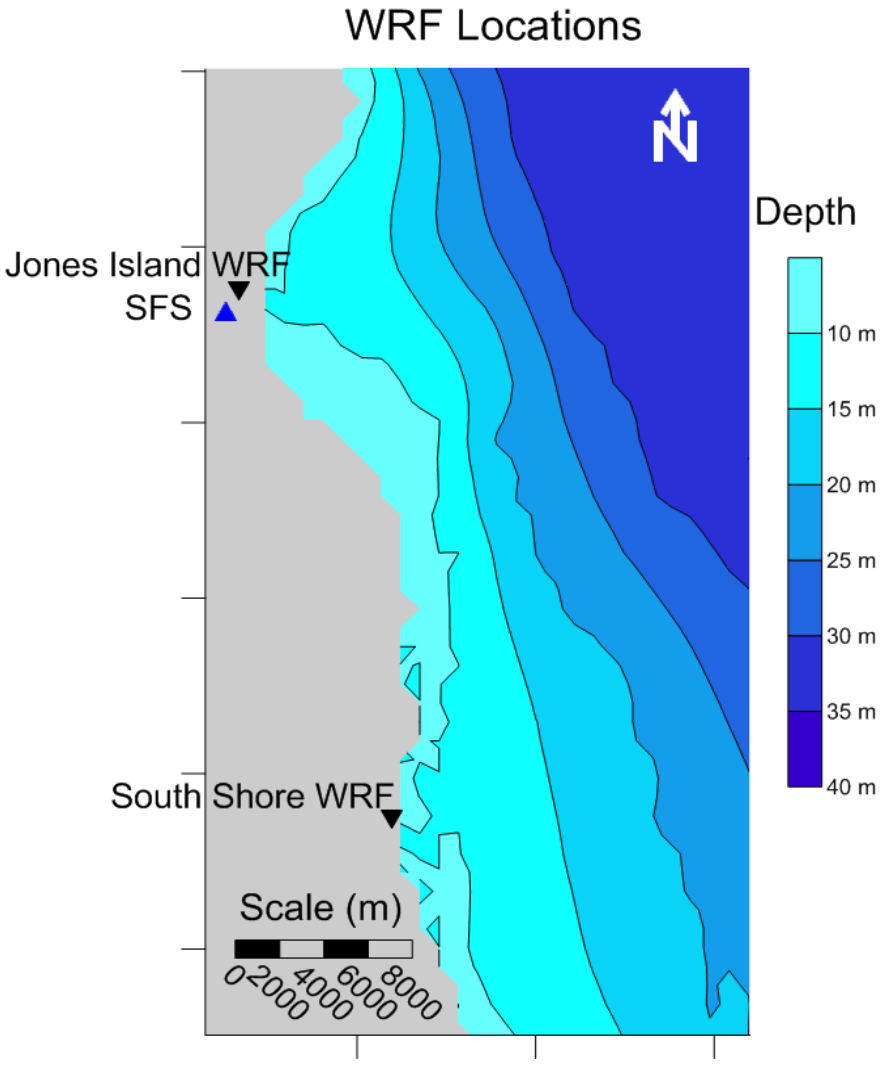

Sample date	WRF	^{131}I A_0 (Bq)			^{131}I A_0/V (Bq/L)			^{131}I J (Bq/d)		
7/16/13	JI	0.252	±	0.027	0.299	±	0.032	8.96E+07	±	9.48E+06
7/29/13	JI	0.019	±	0.009	0.024	±	0.011	6.40E+06	±	2.92E+06
8/6/13	JI	0.121	±	0.029	0.170	±	0.041	4.16E+07	±	9.92E+06
8/14/13	JI	0.764	±	0.036	0.955	±	0.045	2.29E+08	±	1.09E+07
11/7/13	JI	0.076	±	0.020	0.117	±	0.031	4.73E+07	±	1.26E+07
12/5/13	JI	0.417	±	0.023	0.958	±	0.053	2.18E+08	±	1.20E+07
12/18/13	JI	0.183	±	0.031	0.229	±	0.039	5.10E+07	±	8.59E+06
12/29/13	JI	0.081	±	0.025	0.105	±	0.032	2.22E+07	±	6.69E+06
1/21/14	JI	0.215	±	0.024	0.268	±	0.029	6.51E+07	±	7.12E+06
2/5/14	JI	0.200	±	0.021	0.250	±	0.026	6.11E+07	±	6.46E+06
2/18/14	JI	0.157	±	0.023	0.196	±	0.028	5.59E+07	±	8.11E+06
3/5/14	JI	0.052	±	0.020	0.237	±	0.093	5.79E+07	±	2.26E+07
3/25/14	JI	0.131	±	0.023	0.164	±	0.028	5.02E+07	±	8.73E+06
4/10/14	JI	0.060	±	0.019	0.074	±	0.024	2.25E+07	±	7.13E+06
4/23/14	JI	0.087	±	0.018	0.109	±	0.022	3.51E+07	±	7.06E+06
5/8/14	JI	0.486	±	0.025	0.607	±	0.031	2.08E+08	±	1.06E+07
6/3/14	JI	0.029	±	0.016	0.113	±	0.062	3.28E+07	±	1.80E+07
6/12/14	JI	0.133	±	0.023	0.166	±	0.029	8.79E+07	±	1.51E+07
6/30/14	JI	0.024	±	0.019	0.050	±	0.041	2.87E+07	±	2.36E+07
7/20/14	JI	0.482	±	0.041	0.602	±	0.051	1.45E+08	±	1.23E+07
8/5/14	JI	0.034	±	0.042	0.043	±	0.052	1.00E+07	±	1.23E+07
8/17/14	JI	0.461	±	0.029	0.576	±	0.036	1.71E+08	±	1.06E+07
9/3/14	JI	0.041	±	0.018	0.051	±	0.022	1.27E+07	±	5.53E+06
9/21/14	JI	0.000	±	0.030	0.001	±	0.037	1.30E+05	±	9.59E+06
10/5/14	JI	0.226	±	0.031	0.337	±	0.046	7.17E+07	±	9.77E+06
10/26/14	JI	0.086	±	0.067	0.108	±	0.084	2.88E+07	±	2.24E+07
11/2/14	JI	0.043	±	0.036	0.054	±	0.045	1.57E+07	±	1.31E+07
11/18/14	JI	0.097	±	0.028	0.226	±	0.066	4.90E+07	±	1.43E+07
12/9/14	JI	0.045	±	0.030	0.057	±	0.038	1.32E+07	±	8.79E+06
6/20/13	SS	0.063	±	0.015	0.075	±	0.017	2.00E+07	±	4.60E+06
7/16/13	SS	0.698	±	0.045	0.872	±	0.056	2.11E+08	±	1.35E+07
7/29/13	SS	0.456	±	0.030	0.570	±	0.038	1.44E+08	±	9.58E+06
8/6/13	SS	0.424	±	0.027	0.730	±	0.046	1.83E+08	±	1.16E+07
8/14/13	SS	0.023	±	0.016	0.029	±	0.020	9.08E+06	±	6.29E+06
11/7/13	SS	0.088	±	0.021	0.109	±	0.026	2.98E+07	±	7.17E+06
12/5/13	SS	0.233	±	0.026	0.816	±	0.090	1.82E+08	±	2.01E+07
12/18/13	SS	0.042	±	0.016	0.052	±	0.020	1.25E+07	±	4.87E+06
12/29/13	SS	0.152	±	0.026	0.193	±	0.033	5.06E+07	±	8.68E+06
1/21/14	SS	0.069	±	0.023	0.086	±	0.028	1.97E+07	±	6.46E+06
2/5/14	SS	0.230	±	0.025	0.287	±	0.032	6.52E+07	±	7.19E+06
2/18/14	SS	0.066	±	0.017	0.098	±	0.025	2.38E+07	±	6.03E+06
3/5/14	SS	0.095	±	0.020	0.119	±	0.025	3.84E+07	±	8.19E+06

Sample date	WRF	^{131}I A_0 (Bq)	^{131}I A_0/V (Bq/L)	^{131}I J (Bq/d)
3/25/14	SS	0.044 ± 0.017	0.055 ± 0.021	2.06E+07 ± 7.93E+06
4/10/14	SS	1.160 ± 0.034	1.450 ± 0.042	5.22E+08 ± 1.52E+07
4/23/14	SS	3.617 ± 0.048	4.522 ± 0.060	1.60E+09 ± 2.14E+07
5/8/14	SS	0.342 ± 0.028	0.428 ± 0.035	1.67E+08 ± 1.37E+07
6/3/14	SS	0.116 ± 0.027	0.145 ± 0.034	6.19E+07 ± 1.47E+07
6/12/14	SS	0.189 ± 0.073	0.236 ± 0.091	1.01E+08 ± 3.90E+07
6/30/14	SS	0.918 ± 0.098	1.147 ± 0.123	3.19E+08 ± 3.41E+07
7/20/14	SS	0.148 ± 0.038	0.184 ± 0.048	5.04E+07 ± 1.31E+07
8/5/14	SS	2.899 ± 0.066	3.624 ± 0.082	9.09E+08 ± 2.06E+07
8/17/14	SS	0.395 ± 0.040	0.493 ± 0.050	1.31E+08 ± 1.34E+07
9/3/14	SS	2.766 ± 0.043	4.067 ± 0.063	1.00E+09 ± 1.55E+07
9/21/14	SS	2.766 ± 0.043	4.067 ± 0.063	1.00E+09 ± 1.55E+07
10/5/14	SS	0.079 ± 0.026	0.144 ± 0.048	3.55E+07 ± 1.18E+07
10/26/14	SS	0.040 ± 0.033	0.050 ± 0.042	1.20E+07 ± 1.00E+07
11/2/14	SS	0.069 ± 0.028	0.086 ± 0.035	1.87E+07 ± 7.48E+06
11/18/14	SS	0.033 ± 0.046	0.041 ± 0.057	9.63E+06 ± 1.34E+07
12/9/14	SS	0.573 ± 0.030	0.716 ± 0.037	1.93E+08 ± 9.96E+06
7/8/14	WB	0.000 ± 0.000	0.000 ± 0.000	0.0 ± 0.0
7/8/14	C	0.000 ± 0.000	0.000 ± 0.000	0.0 ± 0.0
7/8/14	SM	0.023 ± 0.026	0.029 ± 0.032	3.90E+05 ± 4.35E+05
7/10/14	R	0.931 ± 0.029	1.163 ± 0.036	7.22E+07 ± 2.27E+06

Effect of bleach on sample ^{131}I activity

Sample	South Shore Effluent with Bleach
Time collected	9/21/14 17:00
Time of gamma analysis start	10/4/14 11:04
Time elapsed after collection (t_c)	12.75 d
Container	Marinelli beaker
^{131}I peak energy (E)	364.67 keV
^{131}I counts (ct)	1963
Count uncertainty	159
Live time (t_L)	174589
^{131}I half-life ($t_{1/2}$)	8.0233 d
^{131}I branching fraction (BF)	0.812
Detector	3
Efficiency (Eff)	0.0185
Effluent volume (V)	0.604 L
Bleach volume	0.090 L
DI water volume	0.196 L
Total volume	0.800 L
Counts per second (cps)	0.0112 s^{-1}
Counting correction factor (CF)	1.09
Activity at time of analysis (A')	0.812 Bq
Activity at time of collection (A_0)	2.44±0.20 Bq
Activity per L effluent	**4.05±0.33 Bq/L**

Appendix B: Rainfall Samples

This appendix contains the raw data for the rain barrel rainfall samples used to calculate the atmospheric ^{7}Be flux, followed by the activity results for each sample. The rain barrel was fitted with a funnel collecting from a circular surface area of 2165cm^2. The area of the Milwaukee outer harbor is 4434510 m^2. See **Figure 20** for barrel locations. All samples were counted in Marinelli beakers. The column descriptions for the raw data table are as follows.

1. **Collection start**: date and time of rain barrel deployment.
2. **Collection end**: date and time of sample collection from rain barrel.
3. **Latitude**: latitude of rain barrel (DD).
4. **Longitude**: longitude of rain barrel (DD).
5. **V rain**: volume of rain collected from barrel (L).
6. **V total**: volume of rain collected from barrel plus the volume of HCl used to rinse the funnel (L).
7. **Det**: gamma detector used.
8. **V samp**: volume of total counted sample (rainfall/HCl mixture) (L).
9. **Counting start**: start date and time of gamma analysis.
10. **Live time**: live time of gamma analysis (s).
11. **^{7}Be Peak**: energy of the ^{7}Be peak (keV).
12. **^{7}Be Counts**: ^{7}Be counts recorded, ± one standard deviation.
13. **R m**: measured rainfall from rain barrel (mm).
14. **R o**: official rainfall, taken from the USGS rain gauge station (42.981ºN, 87.918ºW) (mm)

Collection start	Collection end	Latitude	Longitude	V rain	V total	Det	V samp	Counting start	Live time	^{7}Be peak	^{7}Be Counts	R m	R o
6/19/14 14:20	6/20/14 16:15	43.017643°	-87.907438°	4.05	4.07	1	0.900	6/24/14 10:00	172800	477.86	186 ± 46	18.7	15.5
6/20/14 16:15	6/23/14 15:27	43.017643°	-87.907438°	8.28	8.30	2	0.900	6/27/14 17:02	192424	478.09	303 ± 60	38.2	25.3
6/23/14 15:27	6/27/14 11:00	43.017643°	-87.907438°	1.68	2.00	2	0.740	7/3/14 18:47	192596	478.82	471 ± 63	7.8	8.4
6/27/14 11:00	7/2/14 10:26	43.017643°	-87.907438°	6.62	6.70	3	0.795	7/15/14 15:50	237821	478.83	341 ± 142	30.6	27.9
7/2/14 10:26	7/8/14 11:05	43.017643°	-87.907438°	4.66	4.76	2	0.795	7/15/14 15:52	237857	479.02	696 ± 71	21.5	23.0
7/8/14 11:05	7/18/14 16:45	43.017643°	-87.907438°	7.49	7.60	1	0.790	7/28/14 14:21	230798	477.69	285 ± 67	34.6	31.9
7/18/14 16:45	7/31/14 13:15	43.017643°	-87.907438°	1.64	1.74	1	0.791	8/5/14 13:08	92278	479.73	369 ± 43	7.6	7.8
7/31/14 13:15	8/11/14 15:00	43.017643°	-87.907438°	4.55	4.67	3	0.800	8/12/14 11:34	173879	477.51	489 ± 118	21.0	29.3
8/11/14 15:00	8/19/14 12:00	43.017730°	-87.902999°	6.82	6.92	2	0.800	8/19/14 12:25	169659	479.31	247 ± 60	31.5	34.8
8/19/14 12:00	9/1/14 12:00	43.017730°	-87.902999°	10.28	10.35	2	0.800	9/10/14 9:58	171609	479.19	332 ± 57	47.5	39.6
9/1/14 12:00	9/14/14 14:15	43.017730°	-87.902999°	3.42	3.49	3	0.800	9/14/14 15:07	177834	477.97	532 ± 121	15.8	20.1
10/3/14 16:00	10/14/14 15:30	43.017730°	-87.902999°	6.76	6.82	2	0.800	10/16/14 16:51	251014	479.11	277 ± 87	31.2	39.4
11/10/14 14:00	11/17/14 9:30	43.017730°	-87.902999°	1.57	1.65	3	0.800	11/17/14 9:53	171158	477.90	445 ± 52	7.3	9.5

Collection start	Collection end	^{7}Be A_0 (Bq)	^{7}Be A_0/V_{total} (Bq/L)	^{7}Be A_{total}	^{7}Be A_{barrel}	^{7}Be rain flux (Bq/m^2/d)	^{7}Be harbor flux (Bq/d)
6/19/14 14:20	6/20/14 16:15	0.53 ± 0.13	0.592 ± 0.032	2.406 ± 2.406	2.42 ± 0.13	10.37 ± 0.57	4.60E+07 ± 2.51E+06
6/20/14 16:15	6/23/14 15:27	1.14 ± 0.22	1.262 ± 0.027	10.468 ± 10.468	10.67 ± 0.23	16.62 ± 0.36	7.37E+07 ± 1.59E+06
6/23/14 15:27	6/27/14 11:00	1.83 ± 0.24	2.472 ± 0.145	4.937 ± 4.937	5.06 ± 0.30	6.13 ± 0.36	2.72E+07 ± 1.60E+06
6/27/14 11:00	7/2/14 10:26	1.21 ± 0.51	1.526 ± 0.076	10.215 ± 10.215	10.55 ± 0.53	9.79 ± 0.49	4.34E+07 ± 2.17E+06
7/2/14 10:26	7/8/14 11:05	2.25 ± 0.23	2.836 ± 0.049	13.499 ± 13.499	14.03 ± 0.24	10.76 ± 0.19	4.77E+07 ± 8.29E+05
7/8/14 11:05	7/18/14 16:45	0.71 ± 0.17	0.893 ± 0.022	6.787 ± 6.787	7.25 ± 0.18	3.27 ± 0.08	1.45E+07 ± 3.60E+05
7/18/14 16:45	7/31/14 13:15	2.16 ± 0.25	2.734 ± 0.153	4.758 ± 4.758	5.17 ± 0.29	1.86 ± 0.10	8.23E+06 ± 4.61E+05
7/31/14 13:15	8/11/14 15:00	2.09 ± 0.50	2.615 ± 0.111	12.212 ± 12.212	13.11 ± 0.56	5.47 ± 0.23	2.43E+07 ± 1.03E+06
8/11/14 15:00	8/19/14 12:00	1.03 ± 0.25	1.287 ± 0.037	8.901 ± 8.901	9.36 ± 0.27	5.49 ± 0.16	2.44E+07 ± 6.94E+05
8/19/14 12:00	9/1/14 12:00	1.59 ± 0.27	1.984 ± 0.026	20.544 ± 20.544	22.33 ± 0.30	7.93 ± 0.11	3.52E+07 ± 4.70E+05
9/1/14 12:00	9/14/14 14:15	2.23 ± 0.51	2.792 ± 0.149	9.753 ± 9.753	10.60 ± 0.56	3.74 ± 0.20	1.66E+07 ± 8.83E+05
10/3/14 16:00	10/14/14 15:30	0.82 ± 0.26	1.028 ± 0.038	7.009 ± 7.009	7.52 ± 0.28	3.16 ± 0.12	1.40E+07 ± 5.21E+05
11/10/14 14:00	11/17/14 9:30	1.86 ± 0.22	2.328 ± 0.138	3.836 ± 3.836	4.01 ± 0.24	2.72 ± 0.16	1.21E+07 ± 7.16E+05

Appendix C: PONAR sediment sampling

This appendix contains the raw data from PONAR sediment sampling used to calculate radionuclide activities in sediments. The column descriptions are as follows. The table of results for each sample is shown below, followed by a figure of site locations outside of the Milwaukee outer harbor (harbor sites shown in **Figure 2**).

1. **Site**: name of sampling station. H stands for harbor and L stands for lake.
2. **Collection time**: date and time of sample collection.
3. **V coll**: volume of sediment sample collected (L).
4. **V samp**: volume of counted sediment sample (L).
5. **Area**: area of lakebed sampled (m^2).
6. **DW samp**: dry weight of counted sediment sample (g).
7. **Cont**: sample container: Marinelli beaker (M) or jar (J).
8. **Det**: gamma detector used.
9. **Counting start**: start date and time of gamma analysis.
10. **Live time**: live time of gamma analysis (s).
11. **^{131}I Peak**: energy of ^{131}I peak (keV).
12. **^{7}Be Peak**: energy of ^{7}Be peak (keV).
13. **^{131}I Counts**: ^{131}I counts recorded, ± one standard deviation.
14. **^{7}Be Counts**: ^{7}Be counts recorded, ± one standard deviation.

Site	Collection time	V coll	V samp	Area	DW samp	Cont	Det	Counting start	Live time	^{131}I Peak	^{7}Be Peak	^{131}I Counts	^{7}Be Counts
2H	9/24/14 13:25	5.600	0.800	0.0524	482	M	3	9/26/14 15:05	175081	363.10	477.95	0 ± 0	680 ± 204
3H	6/20/14 14:26	2.155	0.945	0.0524	386	M	2	6/23/14 10:15	202707	364.70	477.82	341 ± 93	12406 ± 141
4H	6/20/14 11:46	5.955	0.945	0.0524	570	M	2	6/25/14 18:40	166568	363.96	477.48	63 ± 103	145 ± 97
4H	9/24/14 13:00	4.750	0.800	0.0524	553	M	3	9/28/14 15:47	171242	365.72	477.75	58 ± 117	379 ± 215
5H	6/20/14 12:05	4.655	0.945	0.0524	519	M	3	6/25/14 18:47	165992	362.86	477.41	0 ± 0	1170 ± 225
5H	9/24/14 12:19	5.800	0.800	0.0524	453	M	2	9/26/14 15:02	175092	366.42	478.95	142 ± 102	323 ± 90
6H	9/24/14 14:00	4.000	0.800	0.0524	235	M	3	9/24/14 15:24	171475	364.63	477.79	266 ± 100	1637 ± 179
6H 1/3	6/20/14 10:59	5.455	0.945	0.0524	599	M	3	6/23/14 10:31	202116	363.91	477.34	70 ± 285	1200 ± 241
6H 2/3	6/20/14 11:15	4.855	0.945	0.0524	676	M	1	6/26/14 10:27	172800	364.00	477.82	166 ± 93	1500 ± 114
6H 3/3	6/20/14 11:28	5.355	0.835	0.0524	561	M	1	6/30/14 13:34	172800	364.00	477.95	147 ± 87	931 ± 113
L3-2	6/20/14 13:41	1.655	0.945	0.1049	904	M	1	6/21/14 10:13	172800	364.00	477.78	0 ± 0	22500 ± 153
L4	6/20/14 13:23	3.555	0.945	0.1049	835	M	2	6/29/14 22:30	150496	365.98	477.77	0 ± 0	452 ± 98
L5	6/20/14 13:08	0.920	0.110	0.1573	122	J	2	6/20/14 15:57	237806	366.11	478.19	0 ± 0	236 ± 93
L6	6/20/14 12:33	1.855	0.945	0.1049	1088	M	3	6/29/14 22:30	150550	362.74	477.39	48 ± 262	1021 ± 231
L9	6/20/14 14:13	0.110	0.110	0.0524	136	J	3	6/20/14 15:59	239105	367.92	477.58	12 ± 201	487 ± 178

The following table contains the results for each individual PONAR sample. A_0 (activity at collection) is in units of Bq, V (volume) is in units of L, DW (dry weight) is in units of kg and area is in units of m^2.

Site	Collection time	^{131}I A_0	^{131}I A_0/V	^{131}I A_0/DW	^{131}I A_0/Area	^{7}Be A_0	^{7}Be A_0/V	^{7}Be A_0/DW	^{7}Be A_0/Area
2H	9/24/14 13:25	0.000 ± 0.060	0.000 ± 0.075	0.00 ± 0.13	0.00 ± 8.06	2.75 ± 0.83	3.44 ± 1.03	5.72 ± 1.72	368 ± 110
3H	6/20/14 14:26	0.152 ± 0.042	0.161 ± 0.044	0.39 ± 0.11	6.62 ± 1.81	42.62 ± 0.48	45.10 ± 0.51	110.29 ± 1.25	1853 ± 21
4H	6/20/14 11:46	0.035 ± 0.071	0.044 ± 0.088	0.06 ± 0.13	3.96 ± 7.98	1.60 ± 0.91	2.00 ± 1.13	2.89 ± 1.64	181 ± 103
4H	9/24/14 13:00	0.042 ± 0.068	0.044 ± 0.072	0.07 ± 0.12	4.99 ± 8.16	0.62 ± 0.42	0.66 ± 0.44	1.09 ± 0.73	75 ± 50
5H	6/20/14 12:05	0.068 ± 0.049	0.086 ± 0.061	0.15 ± 0.11	9.46 ± 6.79	1.27 ± 0.35	1.59 ± 0.44	2.81 ± 0.78	176 ± 49
5H	9/24/14 12:19	0.000 ± 0.178	0.000 ± 0.188	0.00 ± 0.34	0.00 ± 16.69	5.16 ± 0.99	5.46 ± 1.05	9.94 ± 1.91	485 ± 93
6H	9/24/14 14:00	0.112 ± 0.042	0.141 ± 0.053	0.48 ± 0.18	10.72 ± 4.03	6.54 ± 0.72	8.18 ± 0.89	27.87 ± 3.05	624 ± 68
6H 1/3	6/20/14 10:59	0.033 ± 0.133	0.035 ± 0.141	0.05 ± 0.22	3.60 ± 14.68	4.23 ± 0.85	4.48 ± 0.90	7.07 ± 1.42	466 ± 94
6H 2/3	6/20/14 11:15	0.090 ± 0.050	0.095 ± 0.053	0.13 ± 0.07	8.79 ± 4.92	4.39 ± 0.33	4.65 ± 0.35	6.50 ± 0.49	430 ± 33
6H 3/3	6/20/14 11:28	0.113 ± 0.067	0.136 ± 0.081	0.20 ± 0.12	13.87 ± 8.24	2.87 ± 0.35	3.44 ± 0.42	5.12 ± 0.62	352 ± 43
L3-2	6/20/14 13:41	0.000 ± 0.136	0.000 ± 0.000	0.00 ± 0.00	0.00 ± 0.00	61.62 ± 0.42	65.21 ± 0.44	68.15 ± 0.46	1029 ± 7
L4	6/20/14 13:23	0.154 ± 0.116	0.000 ± 0.000	0.00 ± 0.00	0.00 ± 0.00	2.27 ± 0.49	2.40 ± 0.52	2.72 ± 0.59	81 ± 18
L5	6/20/14 13:08	0.000 ± 0.000	0.000 ± 0.000	0.00 ± 0.00	0.00 ± 0.00	0.63 ± 0.25	5.74 ± 2.26	5.16 ± 2.03	34 ± 13
L6	6/20/14 12:33	0.000 ± 0.000	0.054 ± 0.295	0.05 ± 0.26	0.96 ± 5.22	5.24 ± 1.18	5.54 ± 1.25	4.81 ± 1.09	98 ± 22
L9	6/20/14 14:13	0.000 ± 0.000	0.020 ± 0.334	0.02 ± 0.27	0.04 ± 0.70	0.86 ± 0.31	7.80 ± 2.85	6.32 ± 2.31	16 ± 6

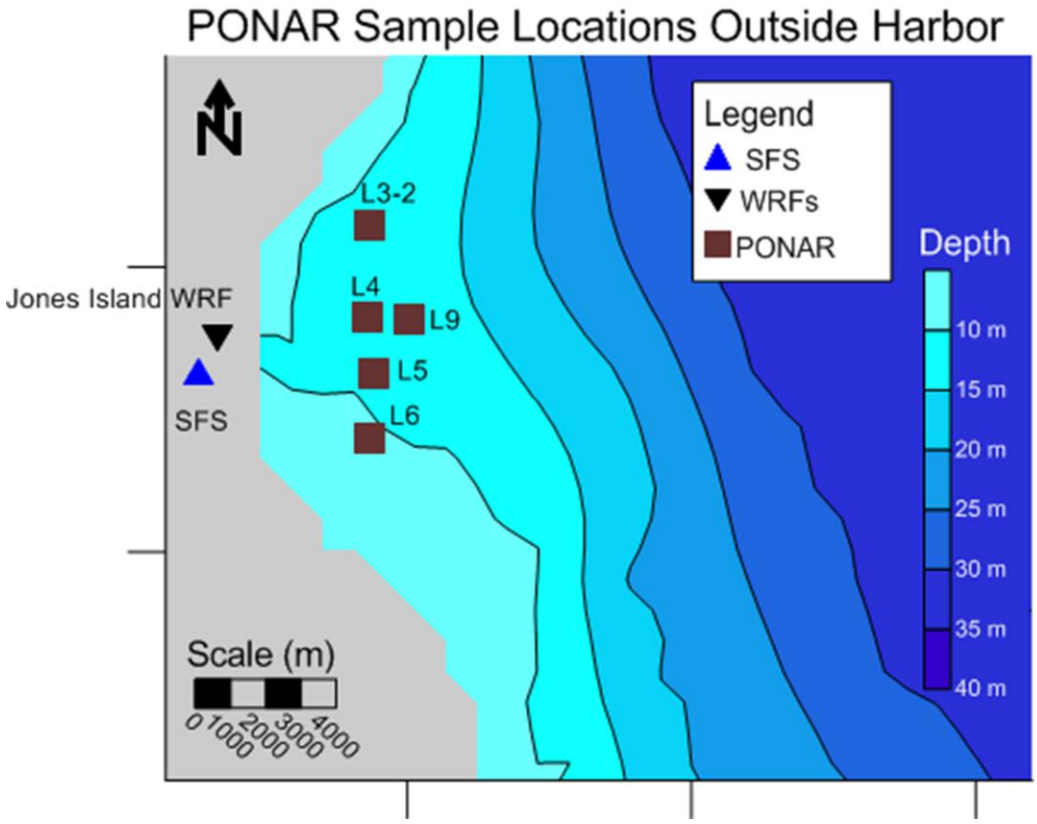
PONAR Sample Locations Outside Harbor
N
Legend
SFS
WRFs
PONAR
Depth
10 m
15 m
20 m
25 m
30 m
35 m
40 m
L3-2
L4
L9
L5
L6
Jones Island WRF
SFS
Scale (m)
0 1000 2000 3000 4000

Appendix D: Gravity core sampling

This appendix contains the raw data for the gravity core sediment samples used to calculate sediment radionuclide activities. Gravity core area for each sample is 36.32cm^2 and all samples were counted in jars. The column descriptions are as follows. Site locations can be seen in **Figure 2**. In addition to the raw data, this appendix also contains the individual sample results and the results of the test samples used to compare PONAR grabs and gravity coring as sediment collection methods.

1. **Site**: name of sampling station. H stands for harbor.
2. **Core**: depth of gravity core (cm).
3. **Collection time**: date and time of sample collection.
4. **V coll**: volume of sediment sample collected (cm^3).
5. **V samp**: volume of counted sediment sample (cm^3).
6. **DW samp**: dry weight of counted sediment sample (g).
7. **Det**: gamma detector used.
8. **Counting start**: start date and time of gamma analysis.
9. **Live time**: live time of gamma analysis (s).
10. **^{131}I Peak**: energy of ^{131}I peak (keV).
11. **^{7}Be Peak**: energy of ^{7}Be peak (keV).
12. **^{131}I Counts**: ^{131}I counts recorded, ± one standard deviation.
13. **^{7}Be Counts**: ^{7}Be counts recorded, ± one standard deviation.

Site	Core	Collection time	V coll	V samp	DW samp	Det	Counting start	Live time	^{131}I Peak	^{7}Be Peak	^{131}I counts	^{7}Be counts
1 H	0-5	7/16/14 12:20	182	166	112.187	2	7/18/14 11:55	184948	364.96	479.09	44 ± 72	595 ± 67
1 H	6-10	7/16/14 12:20	182	168	167.751	1	8/8/14 10:18	172800	364.00	477.50	112 ± 57	168 ± 50
1 H	0-5	7/29/14 11:12	182	181	176.899	1	7/30/14 13:08	103348	364.00	477.50	0 ± 0	150 ± 42
1 H	6-10	7/29/14 11:12	182	181	236.299	2	8/12/14 11:35	173588	363.04	476.58	80 ± 76	14 ± 70
1 H	0-10	8/26/14 12:26	363	273	296.654	3	9/3/14 10:52	174389	366.60	477.98	0 ± 0	175 ± 71
1 H	0-10	10/8/14 9:35	363	256	246.563	2	10/8/14 17:07	176120	365.73	479.30	0 ± 0	106 ± 73
2 H	0-5	7/16/14 12:28	182	170	64.979	3	7/18/14 11:57	184672	367.57	477.70	198 ± 166	574 ± 145
2 H	6-10	7/16/14 12:28	182	166	90.019	1	8/15/14 17:06	172800	364.00	477.50	0 ± 0	0 ± 0
2 H	0-5	7/29/14 11:27	182	181	63.357	2	7/31/14 19:44	159734	365.71	478.49	59 ± 64	347 ± 62
2 H	6-10	7/29/14 11:27	182	181	88.607	3	8/15/14 17:09	245405	366.61	480.82	213 ± 202	0 ± 0
2 H	0-10	8/26/14 13:15	363	264	161.356	2	9/5/14 11:28	246626	363.74	480.05	70 ± 91	65 ± 83
2 H	0-10	10/8/14 10:12	363	221	94.181	1	10/14/14 17:17	159378	364.00	477.50	0 ± 0	161 ± 49
3 H	0-5	7/16/14 12:45	182	161	137.972	3	7/20/14 15:18	165451	364.50	477.71	131 ± 167	548 ± 145
3 H	6-10	7/16/14 12:45	182	167	165.410	3	7/28/14 14:20	97765	365.71	475.57	110 ± 144	113 ± 117
3 H	0-5	7/29/14 12:30	182	181	277.711	3	7/31/14 19:44	160063	364.52	481.35	0 ± 0	189 ± 182
3 H	6-10	7/29/14 12:30	182	181	213.851	2	8/14/14 11:52	105473	364.45	478.51	0 ± 0	0 ± 0
3 H	0-5	8/26/14 14:52	182	166	280.723	2	8/27/14 12:08	189391	366.11	477.91	207 ± 86	0 ± 0
3 H	0-10	10/8/14 11:43	363	242	201.892	2	10/14/14 17:16	171113	366.58	479.15	226 ± 71	249 ± 66
3-4 H	0-5	7/16/14 13:00	182	169	80.142	3	7/23/14 17:11	144019	366.21	478.33	64 ± 154	111 ± 130
3-4 H	6-10	7/16/14 13:00	182	170	111.106	2	7/28/14 18:05	84446	365.36	476.90	0 ± 0	63 ± 44
4 H	0-5	7/16/14 13:18	182	174	86.703	2	7/23/14 17:14	143739	364.71	478.90	11 ± 62	141 ± 62
4 H	6-10	7/16/14 13:18	182	176	86.737	3	7/25/14 17:10	163038	365.42	478.15	0 ± 0	0 ± 0
4 H	0-5	7/29/14 13:55	182	181	61.992	2	8/4/14 16:14	173730	365.92	477.89	0 ± 0	186 ± 68
4 H	6-10	7/29/14 13:55	182	181	82.850	2	8/15/14 17:13	245130	363.65	479.52	87 ± 82	0 ± 0
4 H	0-10	8/26/14 16:00	363	265	178.495	3	9/5/14 11:23	246978	361.36	479.03	0 ± 0	70 ± 202
4 H	0-10	10/8/14 12:25	363	221	82.978	1	10/8/14 17:10	172800	364.00	477.73	310 ± 56	138 ± 67
5 H	0-5	7/16/14 13:40	182	157	65.531	2	7/20/14 12:00	164944	365.98	479.12	88 ± 65	729 ± 110
5 H	6-10	7/16/14 13:40	182	171	132.821	3	7/27/14 14:30	67706	364.28	477.79	0 ± 0	108 ± 99
5 H	0-5	7/29/14 14:15	182	181	174.860	3	7/29/14 17:33	174612	367.17	481.43	124 ± 187	187 ± 159
5 H	6-10	7/29/14 14:15	182	181	83.853	3	8/14/14 11:56	105025	367.20	477.77	0 ± 0	148 ± 116
5 H	0-10	8/26/14 16:19	363	281	178.753	2	9/3/14 10:50	174784	364.43	479.09	57 ± 30	31 ± 25
5 H	0-10	10/8/14 13:05	363	248	136.531	3	10/8/14 17:10	175692	365.46	477.82	0 ± 0	744 ± 153
6 H	0-5	7/29/14 14:40	182	181	112.700	3	8/4/14 16:10	159686	364.47	477.68	161 ± 65	713 ± 147
6 H	6-10	7/29/14 14:40	182	181	121.774	2	8/8/14 17:25	191185	365.32	477.53	137 ± 75	0 ± 0
6 H	0-6	8/26/14 16:42	218	211	378.257	3	8/27/14 12:09	188835	368.83	474.48	310 ± 251	0 ± 0
6 H	0-10	10/8/14 13:35	363	273	197.372	3	10/12/14 20:52	159615	364.22	478.34	172 ± 90	311 ± 61

The following table contains the results for each individual gravity core sample. A_0 (activity at collection) is in units of Bq, V (volume) is in units of L, DW (dry weight) is in units of kg and area is in units of m^2.

Site	Core	Collection time	^{131}I A_0	^{131}I A_0/V	^{131}I A_0/DW	^{131}I A_0/Area	^{7}Be A_0	^{7}Be A_0/V	^{7}Be A_0/DW	^{7}Be A_0/Area
1 H	6-10	7/16/14 12:20	0.210 ± 0.108	1.25 ± 0.64	1.25 ± 0.64	62.3 ± 32.0	0.53 ± 0.16	3.15 ± 0.93	3.17 ± 0.94	158 ± 47
1 H	6-10	7/29/14 11:12	0.101 ± 0.096	0.56 ± 0.53	0.43 ± 0.41	27.9 ± 26.5	0.06 ± 0.30	0.34 ± 1.68	0.26 ± 1.29	17 ± 84
1 H	0-10	8/26/14 12:26	0.000 ± 0.031	0.00 ± 0.11	0.00 ± 0.10	0.0 ± 10.5	0.47 ± 0.19	1.71 ± 0.69	1.57 ± 0.64	160 ± 65
1 H	0-10	10/8/14 9:35	0.000 ± 0.029	0.00 ± 0.11	0.00 ± 0.12	0.0 ± 10.5	0.38 ± 0.26	1.50 ± 1.03	1.55 ± 1.07	140 ± 96
1 H	0-5	7/16/14 12:20	0.019 ± 0.031	0.11 ± 0.18	0.17 ± 0.27	5.6 ± 9.2	2.09 ± 0.24	12.63 ± 1.42	18.65 ± 2.10	632 ± 71
1 H	0-5	7/29/14 11:12	0.000 ± 0.000	0.00 ± 0.00	0.00 ± 0.00	0.0 ± 0.0	0.59 ± 0.17	3.28 ± 0.91	3.36 ± 0.93	164 ± 46
2 H	6-10	7/16/14 12:28	0.000 ± 0.000	0.00 ± 0.00	0.00 ± 0.00	0.0 ± 0.0	0.00 ± 0.00	0.00 ± 0.00	0.00 ± 0.00	0 ± 0
2 H	6-10	7/29/14 11:27	0.167 ± 0.158	0.92 ± 0.87	1.88 ± 1.78	46.0 ± 43.6	0.00 ± 0.40	0.00 ± 2.21	0.00 ± 4.52	0 ± 110
2 H	0-10	8/26/14 13:15	0.045 ± 0.059	0.17 ± 0.22	0.28 ± 0.37	15.9 ± 20.7	0.19 ± 0.24	0.72 ± 0.93	1.19 ± 1.51	67 ± 85
2 H	0-10	10/8/14 10:12	0.000 ± 0.000	0.00 ± 0.00	0.00 ± 0.00	0.0 ± 0.0	0.44 ± 0.13	2.01 ± 0.61	4.72 ± 1.43	184 ± 56
2 H	0-5	7/16/14 12:28	0.054 ± 0.045	0.32 ± 0.26	0.83 ± 0.69	15.8 ± 13.2	1.34 ± 0.34	7.85 ± 1.98	20.59 ± 5.20	392 ± 99
2 H	0-5	7/29/14 11:27	0.030 ± 0.032	0.16 ± 0.18	0.47 ± 0.51	8.2 ± 8.9	1.41 ± 0.25	7.83 ± 1.40	22.33 ± 3.99	392 ± 70
3 H	6-10	7/16/14 12:45	0.128 ± 0.168	0.77 ± 1.01	0.78 ± 1.02	38.4 ± 50.3	0.56 ± 0.58	3.35 ± 3.47	3.39 ± 3.51	168 ± 174
3 H	6-10	7/29/14 12:30	0.000 ± 0.156	0.00 ± 0.86	0.00 ± 0.73	0.0 ± 43.0	0.00 ± 0.46	0.00 ± 2.51	0.00 ± 2.13	0 ± 126
3 H	0-10	10/8/14 11:43	0.149 ± 0.047	0.62 ± 0.19	0.74 ± 0.23	57.4 ± 18.0	1.00 ± 0.26	4.13 ± 1.10	4.95 ± 1.31	384 ± 102
3 H	0-5	7/16/14 12:45	0.047 ± 0.060	0.29 ± 0.37	0.34 ± 0.43	14.5 ± 18.5	1.46 ± 0.39	9.08 ± 2.40	10.61 ± 2.81	454 ± 120
3 H	0-5	7/29/14 12:30	0.000 ± 0.070	0.00 ± 0.39	0.00 ± 0.25	0.0 ± 19.4	0.51 ± 0.50	2.84 ± 2.74	1.85 ± 1.78	142 ± 137
3 H	0-5	8/26/14 14:52	0.078 ± 0.033	0.47 ± 0.20	0.28 ± 0.12	21.4 ± 8.9	0.00 ± 0.29	0.00 ± 1.73	0.00 ± 1.02	0 ± 78
3-4 H	6-10	7/16/14 13:00	0.000 ± 0.109	0.00 ± 0.64	0.00 ± 0.98	0.0 ± 32.2	0.55 ± 0.38	3.23 ± 2.25	4.93 ± 3.44	161 ± 113
3-4 H	0-5	7/16/14 13:00	0.034 ± 0.082	0.20 ± 0.48	0.42 ± 1.02	10.0 ± 24.2	0.35 ± 0.42	2.09 ± 2.45	4.42 ± 5.18	105 ± 122
4 H	6-10	7/16/14 13:18	0.000 ± 0.097	0.00 ± 0.55	0.00 ± 1.11	0.0 ± 27.4	0.00 ± 0.44	0.00 ± 2.50	0.00 ± 5.08	0 ± 125
4 H	6-10	7/29/14 13:55	0.106 ± 0.100	0.58 ± 0.55	1.28 ± 1.20	29.2 ± 27.5	0.00 ± 0.26	0.00 ± 1.43	0.00 ± 3.14	0 ± 72
4 H	0-10	8/26/14 16:00	0.000 ± 0.096	0.00 ± 0.36	0.00 ± 0.54	0.0 ± 33.3	0.14 ± 0.39	0.51 ± 1.48	0.76 ± 2.20	47 ± 137
4 H	0-10	10/8/14 12:25	0.082 ± 0.015	0.37 ± 0.07	0.98 ± 0.18	33.7 ± 6.1	0.33 ± 0.16	1.47 ± 0.72	3.92 ± 1.91	134 ± 65
4 H	0-5	7/16/14 13:18	0.009 ± 0.052	0.05 ± 0.30	0.11 ± 0.60	2.6 ± 14.9	0.68 ± 0.30	3.90 ± 1.72	7.84 ± 3.45	195 ± 86
4 H	0-5	7/29/14 13:55	0.000 ± 0.045	0.00 ± 0.25	0.00 ± 0.73	0.0 ± 12.4	0.73 ± 0.27	4.04 ± 1.48	11.81 ± 4.32	202 ± 74
5 H	6-10	7/16/14 13:40	0.000 ± 0.174	0.00 ± 1.02	0.00 ± 1.31	0.0 ± 50.9	0.77 ± 0.70	4.48 ± 4.11	5.76 ± 5.28	224 ± 206
5 H	6-10	7/29/14 14:15	0.000 ± 0.227	0.00 ± 1.26	0.00 ± 2.71	0.0 ± 62.8	0.72 ± 0.57	3.99 ± 3.13	8.62 ± 6.75	199 ± 156
5 H	0-10	8/26/14 16:19	0.042 ± 0.022	0.15 ± 0.08	0.23 ± 0.12	13.7 ± 7.2	0.12 ± 0.10	0.44 ± 0.36	0.70 ± 0.56	41 ± 33
5 H	0-10	10/8/14 13:05	0.000 ± 0.016	0.00 ± 0.07	0.00 ± 0.12	0.0 ± 6.0	1.78 ± 0.37	7.17 ± 1.48	13.04 ± 2.68	659 ± 135
5 H	0-5	7/16/14 13:40	0.047 ± 0.035	0.30 ± 0.22	0.72 ± 0.53	15.0 ± 11.1	2.92 ± 0.44	18.65 ± 2.81	44.63 ± 6.73	933 ± 141
5 H	0-5	7/29/14 14:15	0.030 ± 0.045	0.17 ± 0.25	0.17 ± 0.26	8.3 ± 12.6	0.45 ± 0.39	2.51 ± 2.13	2.60 ± 2.21	125 ± 107
6 H	6-10	7/29/14 14:40	0.114 ± 0.062	0.63 ± 0.34	0.94 ± 0.51	31.4 ± 17.2	0.00 ± 0.29	0.00 ± 1.58	0.00 ± 2.35	0 ± 79
6 H	0-10	10/8/14 13:35	0.065 ± 0.034	0.24 ± 0.12	0.33 ± 0.17	21.9 ± 11.4	0.86 ± 0.17	3.17 ± 0.62	4.38 ± 0.86	293 ± 57
6 H	0-5	7/29/14 14:40	0.070 ± 0.028	0.39 ± 0.16	0.62 ± 0.25	19.4 ± 7.8	2.02 ± 0.42	11.16 ± 2.30	17.95 ± 3.70	558 ± 115
6 H	0-6	8/26/14 16:42	0.075 ± 0.061	0.35 ± 0.29	0.20 ± 0.16	19.5 ± 15.8	0.00 ± 0.49	0.00 ± 2.30	0.00 ± 1.28	0 ± 127

Comparison of ^{7}Be activity per m^2 (A_0/Area) and precision in test sediment samples taken by gravity coring (GC) and PONAR grab (P) in the slip adjacent to the School of Freshwater Sciences. These data are the basis of our preference for gravity coring for sediment sampling.

#	Gear	Collection time	V coll	V samp	Area	Cont	Det	Counting start	Live time	^{7}Be Peak	^{7}Be counts	^{7}Be A_0/Area (Bq/m^2)	% Error
1	GC	7/1/14 13:30	182	142	36.32	J	1	7/8/14 16:19	151516	477.72	521 ± 65	**538 ± 68**	**13%**
2	GC	7/1/14 13:35	182	129	36.32	J	3	7/11/14 15:40	254322	477.75	802 ± 164	**590 ± 121**	**20%**
3	GC	7/1/14 13:40	182	130	36.32	J	2	7/11/14 15:37	254234	479.07	449 ± 97	**492 ± 106**	**22%**
1	P	7/1/14 13:50	5545	945	524.4	M	2	7/7/14 16:25	172094	479.46	219 ± 136	**104 ± 64**	**62%**
2	P	7/1/14 14:12	5945	945	524.4	M	2	7/2/14 16:48	180025	478.81	245 ± 97	**111 ± 44**	**40%**
3	P	7/1/14 14:25	5845	945	524.4	M	3	7/2/14 16:49	179268	477.35	313 ± 222	**143 ± 101**	**71%**

Appendix E: Water filtration samples

This appendix contains the raw data associated with filtering water collected from the Milwaukee outer harbor and used to calculate harbor water column activities of ^{131}I and ^{7}Be, followed by a table of the results for each individual sample. The column descriptions are as follows.

1. **Site**: location of collected water: outer harbor (OH) or Lake Michigan (L).
2. **Filter**: filtration process: particulate (P), anion resin (AR), iron precipitate (Fe), activated carbon (C), or manganese wool (Mn). First and second filtrations of the same type are numbered 1 and 2, respectively. On 7/16/14, three separate water samples were taken and filtered for particulate matter, denoted 1P, 2P, and 3P.
3. **Collect time**: date and time of sample collection.
4. **DW sed**: dry weight of suspended sediment particles, if applicable (g).
5. **V water**: volume of water filtered, in liters.
6. **Cont**: sample container: jar (J) or vial (V).
7. **Det**: gamma detector used.
8. **Counting start**: start date and time of gamma analysis.
9. **Live time**: live time of gamma analysis (s).
10. **^{131}I Peak**: energy of ^{131}I peak (keV).
11. **^{7}Be Peak**: energy of ^{7}Be peak (keV).
12. **^{131}I Counts**: ^{131}I counts recorded, ± one standard deviation.
13. **^{7}Be Counts**: ^{7}Be counts recorded, ± one standard deviation.

Site	Filter	Collect time	DW sed	V water	Cont	Det	Counting start	Live time	^{131}I Peak	^{7}Be Peak	^{131}I Counts	^{7}Be Counts
OH	AR	7/29/14 12:30		199.1	J	3	8/2/14 16:18	172058	364.43	476.37	371 ± 146	20 ± 119
OH	AR1	8/26/14 13:30		196.4	J	2	8/29/14 16:51	238669	365.61	478.95	482 ± 78	51 ± 36
OH	AR1	10/8/14 11:07		211.6	J	3	10/10/14 18:02	182786	364.75	477.59	2949 ± 78	84 ± 49
OH	AR2	8/26/14 13:30		196.4	J	3	9/1/14 11:09	171200	364.73	477.51	286 ± 148	136 ± 64
OH	AR2	10/8/14 11:07		211.6	J	1	10/10/14 18:06	172800	364.39	477.50	1260 ± 69	21 ± 38
OH	C	7/29/14 12:30		199.1	J	1	8/2/14 10:31	97741	364.00	477.50	37 ± 36	0 ± 0
OH	Fe	7/29/14 12:30		199.1	J	2	8/2/14 16:13	172674	364.62	478.63	79 ± 58	53 ± 57
OH	Fe	8/26/14 13:30		196.4	J	2	9/1/14 11:13	171155	365.61	479.19	37 ± 28	128 ± 41
OH	Fe1	10/8/14 11:07		211.6	J	1	10/12/14 20:25	161450	364.53	477.50	330 ± 64	120 ± 39
OH	Fe2	10/8/14 11:07		211.6	J	3	10/14/14 17:15	171343	364.76	477.11	102 ± 66	31 ± 71
OH	Mn	7/29/14 12:30		199.1	J	1	8/3/14 13:44	170553	364.00	477.50	145 ± 46	0 ± 0
OH	1P	7/16/14 12:20	0.0895	27.6	V	1	7/18/14 11:09	122219	364.00	477.66	0 ± 0	323 ± 47
OH	2P	7/16/14 12:28	0.0658	40.7	V	1	7/19/14 21:08	134369	364.00	477.66	78 ± 40	1010 ± 58
OH	3P	7/16/14 12:45	0.0644	30.1	V	1	7/16/14 20:40	138403	364.00	477.28	0 ± 0	498 ± 50
OH	P	7/29/14 12:30	0.4910	199.5	J	1	7/31/14 19:19	139187	364.00	477.72	108 ± 41	436 ± 53
OH	P	8/26/14 13:30	0.9309	196.4	J	3	8/29/14 16:47	238700	364.54	477.87	18 ± 67	436 ± 152
OH	P	10/8/14 11:07	0.7207	211.6	J	2	10/10/14 18:06	182770	365.58	479.48	312 ± 65	145 ± 44
L	P	8/22/14 15:17	0.0279	65.5	V	1	8/30/14 14:51	172800	364.00	477.50	10 ± 48	400 ± 45

The following table contains the results for each individual water filter. A_0 (activity at collection) is in units of Bq, V (volume) is in units of L, DW (dry weight) is in units of g and TSM is in units of mg/L. The mean of the three particulate samples from 7/16/14 is also shown, as Avg P.

Site	Filter	Collect time	TSM	^{131}I A_0	^{131}I A_0/V	^{131}I A_0/DW	^{7}Be A_0	^{7}Be A_0/V	^{7}Be A_0/DW
OH	AR	7/29/14 12:30		0.128 ± 0.051	6.45E-04 ± 2.54E-04		0.051 ± 0.305	0.00026 ± 0.00153	
OH	AR1	8/26/14 13:30		0.180 ± 0.029	9.17E-04 ± 1.48E-04		0.142 ± 0.100	0.00072 ± 0.00051	
OH	AR1	10/8/14 11:07		0.822 ± 0.022	3.89E-03 ± 1.03E-04		0.199 ± 0.116	0.00094 ± 0.00055	
OH	AR2	8/26/14 13:30		0.116 ± 0.060	5.89E-04 ± 3.05E-04		0.359 ± 0.169	0.00183 ± 0.00086	
OH	AR2	10/8/14 11:07		0.398 ± 0.022	1.88E-03 ± 1.03E-04		0.051 ± 0.093	0.00024 ± 0.00044	
OH	C	7/29/14 12:30		0.023 ± 0.022	1.15E-04 ± 1.12E-04		0.000 ± 0.000	0.00000 ± 0.00000	
OH	Fe	7/29/14 12:30		0.043 ± 0.032	2.16E-04 ± 1.59E-04		0.205 ± 0.220	0.00103 ± 0.00111	
OH	Fe	8/26/14 13:30		0.024 ± 0.018	1.21E-04 ± 9.13E-05		0.511 ± 0.164	0.00260 ± 0.00083	
OH	Fe1	10/8/14 11:07		0.133 ± 0.026	6.28E-04 ± 1.23E-04		0.319 ± 0.103	0.00151 ± 0.00049	
OH	Fe2	10/8/14 11:07		0.042 ± 0.027	2.01E-04 ± 1.30E-04		0.082 ± 0.188	0.00039 ± 0.00089	
OH	Mn	7/29/14 12:30		0.059 ± 0.018	2.95E-04 ± 9.26E-05		0.000 ± 0.000	0.00000 ± 0.00000	
OH	1P	7/16/14 12:20	3.240	0.000 ± 0.000	0 ± 0	0 ± 0	0.135 ± 0.020	0.00490 ± 0.00072	1.51 ± 0.22
OH	2P	7/16/14 12:28	1.615	0.0052 ± 0.0027	1.29E-04 ± 6.63E-05	0.080 ± 0.041	0.393 ± 0.023	0.00964 ± 0.00056	5.97 ± 0.35
OH	3P	7/16/14 12:45	2.138	0.0000 ± 0.0000	0 ± 0	0 ± 0	0.181 ± 0.018	0.00600 ± 0.00061	2.81 ± 0.29
OH	Avg P	7/16/14 12:31	2.331	0.0017 ± 0.0009	4.29E-05 ± 5.25E-05	0.027 ± 0.014	0.236 ± 0.079	0.0068 ± 0.0014	3.4 ± 1.3
OH	P	7/29/14 12:30	2.461	0.042 ± 0.016	2.08E-04 ± 7.94E-05	0.085 ± 0.032	1.306 ± 0.159	0.00655 ± 0.00080	2.66 ± 0.32
OH	P	8/26/14 13:30	4.740	0.004 ± 0.016	2.16E-05 ± 8.05E-05	0.005 ± 0.017	0.802 ± 0.279	0.00408 ± 0.00142	0.86 ± 0.30
OH	P	10/8/14 11:07	3.406	0.138 ± 0.029	6.51E-04 ± 1.36E-04	0.191 ± 0.040	0.518 ± 0.157	0.00245 ± 0.00074	0.72 ± 0.22
L	P	8/22/14 15:17	0.426	0.001 ± 0.004	1.21E-05 ± 5.83E-05	0.028 ± 0.137	0.129 ± 0.014	0.00197 ± 0.00022	4.61 ± 0.51

Appendix F: Sediment trap samples

This appendix contains the raw data from sediment trap sampling to determine particulate radionuclide activities in the rivers of Milwaukee's inner harbor. The site is off the University of Wisconsin-Milwaukee School of Freshwater Sciences dock on the Kinnickinnic River (43.017810°N, 87.903034°W, next to Rain Barrel 2 in **Figure 20**). The sediment trap apparatus consisted of six plastic tubes, each with a coarse grate on the top and a stopper on the bottom, fastened upright to a bar and suspended 2 meters below the surface of the water. Upon collection, overlying water was decanted and all traps were emptied into jar containers and oven dried (60ºC until sediment appears cracked). Jar containers were also used for gamma analysis for all samples. Each trap has a capture area of 19.63cm^2. The column descriptions are as follows.

1. **Deploy time**: date and time of sediment trap deployment.
2. **Collect time**: date and time of sediment trap collection.
3. **Traps**: number of traps in sampling event.
4. **DW total**: total dry weight of collected sediment trap material (g).
5. **DW samp**: dry weight of counted sediment trap sample (g).
6. **Det**: gamma detector used.
7. **Counting start**: start date and time of gamma analysis.
8. **Live time**: live time of gamma analysis (s).
9. **^{131}I Peak**: energy of ^{131}I peak (keV).
10. **^{7}Be Peak**: energy of ^{7}Be peak (keV).
11. **^{131}I Counts**: ^{131}I counts recorded, ± one standard deviation.
12. **^{7}Be Counts**: ^{7}Be counts recorded, ± one standard deviation.

For these samples, in addition to calculating the radionuclide activity at the time of collection (A_0) we also calculate the activity while still in the sediment trap (A_{trap}). Due to the long trap deployment times and short half-lives of the radionuclides, A_{trap} is more representative of the radionuclide activities in the system. A_{trap} is calculated from A_0 using the following equation:

$$A_{trap} = \frac{A_0 t_{trap} \lambda}{1 - e^{-\lambda t_{trap}}}$$

where t_{trap} is the length of trap deployment and λ is the decay constant.

However, sediment trap sampling was not quantitative and should not be interpreted as such. Suspended sediment particles that travel downstream 2m below surface and are collected in a sediment trap are representative of neither the flux of suspended particles downstream nor of settling particles at that point in the river. Sediment trap sampling was performed to simply provide a rough estimate of what radionuclide activities could be found on suspended sediment at one point in the Milwaukee inner harbor.

Deploy time	Collect time	Traps	DW total	DW samp	Detector	Counting start	Live time	^{131}I Peak	^{7}Be Peak	^{131}I Counts	^{7}Be counts
8/21/14 13:25	9/5/14 12:00	6	27.224	26.961	MCB 3	9/10/14 10:01	171174	364.66	477.83	380 ± 68	8544 ± 160
9/5/14 12:00	9/14/14 14:25	5	12.259	12.146	MCB 3	9/16/14 16:34	233797	366.58	477.83	31 ± 179	3369 ± 162
9/14/14 14:30	9/29/14 14:00	6	17.251	18.004	MCB 2	10/2/14 10:17	350374	364.72	479.11	171 ± 95	4407 ± 105
9/29/14 14:00	11/17/14 9:30	3	61.896	61.225	MCB 2	12/1/14 14:47	173222	366.57	482.59	0 ± 0	283 ± 68

The following table contains the results for the sediment trap samples for ^{131}I and ^{7}Be. Sample activity at collection (A_0) and in the trap (A_{trap}) is in units of Bq and activity per unit dry weight (A_{trap}/DW) is in units of Bq/g.

Deploy time	Collect time	^{131}I A_0	^{131}I A_{trap}	^{131}I A_{trap}/DW	^{7}Be A_0	^{7}Be A_{trap}	^{7}Be A_{trap}/DW
8/21/14 13:25	9/5/14 12:00	0.269 ± 0.048	0.479 ± 0.086	0.0178 ± 0.0032	24.57 ± 0.46	27.03 ± 0.51	1.003 ± 0.019
9/5/14 12:00	9/14/14 14:25	0.010 ± 0.059	0.015 ± 0.084	0.0012 ± 0.0070	6.62 ± 0.32	7.01 ± 0.34	0.577 ± 0.028
9/14/14 14:30	9/29/14 14:00	0.085 ± 0.047	0.152 ± 0.084	0.0084 ± 0.0047	9.23 ± 0.22	10.16 ± 0.24	0.564 ± 0.013
9/29/14 14:00	11/17/14 9:30	0 ± 0	0 ± 0	0 ± 0	1.72 ± 0.41	2.32 ± 0.56	0.038 ± 0.009

Appendix G: Dreissenid mussel samples

This appendix contains the raw data associated with dreissenid mussel samples used to calculate their radionuclide activities. The column descriptions are as follows. Site locations are shown in the figure below.

1. **Site**: location of sample collection.
2. **Collect time**: date and time of sample collection.
3. **Part**: part of the mussels used in the sample, i.e. tissue (F), shells (S), or whole (W).
4. **Type**: indicates how the sample was processed prior to counting: freeze dried then ground (F), oven dried then ground (O), or wet (W).
5. **Gear**: method used to collect mussels: by hand (H), by gravity core (GC) or by PONAR grab (PG).
6. **DW samp**: dry weight of the counted sample, or unknown (Unk) (g).
7. **Area**: area of lakebed sampled, or unknown (Unk) (cm^2).
8. **Cont**: sample container: Marinelli beaker (M), jar (J) or vial (V).
9. **Det**: gamma detector used.
10. **Counting start**: start date and time of gamma analysis.
11. **Live time**: live time of gamma analysis (s).
12. **^{131}I Peak**: energy of ^{131}I peak (keV).
13. **^{7}Be Peak**: energy of ^{7}Be peak (keV).
14. **^{131}I Counts**: ^{131}I counts recorded, ± one standard deviation.
15. **^{7}Be Counts**: ^{7}Be counts recorded, ± one standard deviation.

Site	Collect time	Part	Type	Gear	DW samp	Area	Cont	Det	Counting Start	Live time	^{131}I Peak	^{7}Be Peak	^{131}I Counts	^{7}Be Counts
5 H	7/16/14 13:40	W	W	GC	Unk	36.32	J	1	7/21/14 13:58	161468	364.00	477.76	0 ± 0	1600 ± 66
5 H	7/29/14 14:15	W	W	P	Unk	524.41	M	2	7/29/14 15:40	174574	364.82	479.34	109 ± 90	2272 ± 96
5 H	9/24/14 12:35	F	O	P	Unk	524.41	J	3	10/2/14 10:14	1757675	364.04	481.10	0 ± 0	11 ± 128
5 H	9/24/14 12:35	W	W	P	Unk	524.41	M	2	9/24/14 16:49	166201	365.59	479.15	113 ± 76	3644 ± 87
Atwater	9/24/14 10:45	S	O	P	18.22	262.21	J	2	9/30/14 15:28	153975	366.11	479.17	0 ± 0	132 ± 57
Atwater	9/24/14 10:45	F	O	P	0.742	262.21	V	1	9/30/14 15:20	151039	364.00	477.50	0 ± 0	104 ± 36
Bradford	9/4/13 18:10	W	F	H	10.211	Unk	J	1	9/10/13 13:34	172800	364.00	477.50	0 ± 0	0 ± 0
S. Wall	9/24/14 11:35	S	O	P	40.663	349.61	J	2	9/28/14 15:44	171584	365.22	479.17	49 ± 63	407 ± 61
S. Wall	9/24/14 11:35	F	O	P	4.413	349.61	V	1	9/28/14 15:38	171616	364.00	477.83	23 ± 47	318 ± 55
S. Wall	10/14/13 14:00	F	O	H	18.502	Unk	J	1	10/15/13 15:06	172800	364.24	477.50	173 ± 57	0 ± 0
S. Wall	10/14/13 14:00	S	O	H	Unk	Unk	J	1	10/17/13 16:29	81782	364.36	477.56	128 ± 32	185 ± 42
S. Wall	10/14/13 14:00	W	O	H	796.33	Unk	M	1	10/21/13 11:06	168950	364.05	477.19	1080 ± 81	2230 ± 79

The following table contains the results for the sediment trap samples for ^{131}I and ^{7}Be. Sample activity (A_0) is in units of Bq, activity per unit dry weight (A_0/DW) is in units of Bq/g, and activity per unit area (A_0/Area) is in units of Bq/m^2.

Site	Collect time	Part	Type	^{131}I A_0	^{131}I A_0/DW	^{131}I A_0/Area	^{7}Be A_0	^{7}Be A_0/DW	^{7}Be A_0/Area
5 H	7/16/14 13:40	W	W	0 ± 0		0 ± 0	4.29 ± 0.18		1181 ± 49
5 H	7/29/14 14:15	W	W	0.041 ± 0.034		0.79 ± 0.65	8.25 ± 0.35		157.4 ± 6.7
5 H	9/24/14 12:35	F	O	0.045 ± 0.030		0.86 ± 0.58	13.91 ± 0.33		265.3 ± 6.3
5 H	9/24/14 12:35	W	W	0 ± 0		0 ± 0	0.00 ± 0.04		0.06 ± 0.73
Atwater	9/24/14 10:45	S	O	0 ± 0	0 ± 0	0 ± 0	0.59 ± 0.25	0.032 ± 0.014	22.4 ± 9.7
Atwater	9/24/14 10:45	F	O	0 ± 0	0 ± 0	0 ± 0	0.037 ± 0.013	0.050 ± 0.018	1.42 ± 0.50
Bradford	9/4/13 18:10	W	F	0 ± 0	0 ± 0		0 ± 0	0 ± 0	
S. Wall	9/24/14 11:35	S	O	0.027 ± 0.035	0.00066 ± 0.00085	0.77 ± 0.99	1.59 ± 0.24	0.0390 ± 0.0058	45.4 ± 6.8
S. Wall	9/24/14 11:35	F	O	0.0013 ± 0.0027	0.00030 ± 0.00061	0.038 ± 0.076	0.098 ± 0.017	0.0222 ± 0.0038	2.81 ± 0.48
S. wall	10/14/13 14:00	F	O	0.069 ± 0.023	0.0037 ± 0.0012		0 ± 0	0 ± 0	
S. wall	10/14/13 14:00	S	O	0.124 ± 0.031			1.00 ± 0.22		
S. wall	10/14/13 14:00	W	O	0.911 ± 0.068	0.001144 ± 0.000086		7.11 ± 0.25	0.00892 ± 0.00032	

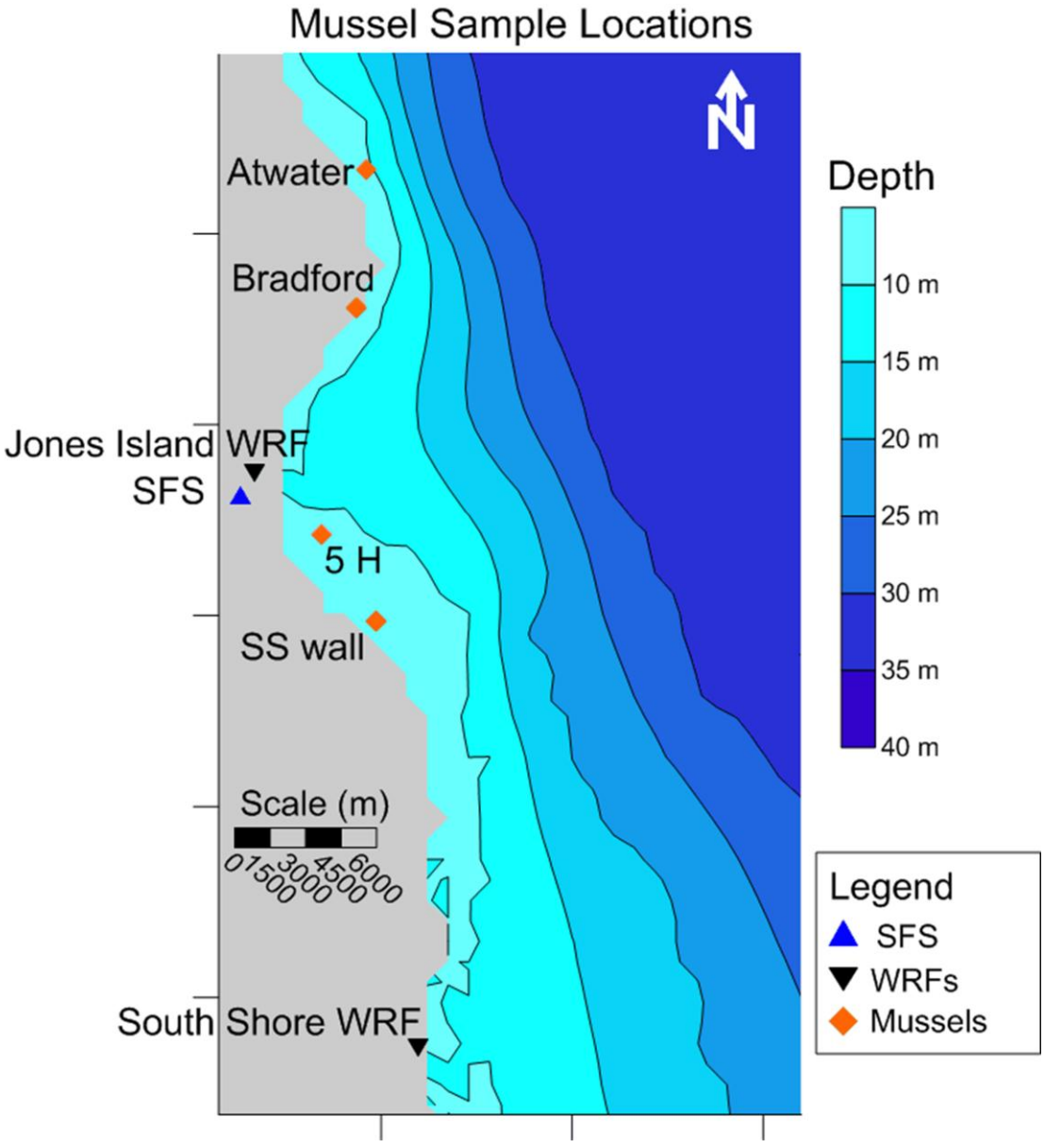
Mussel Sample Locations
Atwater
Bradford
Jones Island WRF
SFS
5 H
SS wall
Scale (m)
0 1500 3000 4500 6000
South Shore WRF
Depth
10 m
15 m
20 m
25 m
30 m
35 m
40 m
Legend
SFS
WRFs
Mussels

Appendix H: *Cladophora* samples

This appendix contains the raw data for *Cladophora* samples, used to calculate their radionuclide activities. The column descriptions are as follows. Site locations are shown in the figure below, except Larson St., which is located 10km south of the Wind Point sites.

1. **Site**: location of sample collection.
2. **Collect time**: date and time of sample collection.
3. **Cond**: collected condition of the algae, i.e. attached to substrate (A) or detached (D).
4. **Type**: indicates how the sample was processed prior to counting: wet and squeezed (W) or dry and ground (D).
5. **DW samp**: dry weight of the counted sample, or unknown (Unk) (g).
6. **Cont**: sample container: Marinelli beaker (M), jar (J), or vial (V).
7. **Det**: gamma detector used.
8. **Counting start**: start date and time of gamma analysis.
9. **Live time**: live time of gamma analysis (s).
10. **^{131}I Peak**: energy of ^{131}I peak (keV).
11. **^{7}Be Peak**: energy of ^{7}Be peak (keV).
12. **^{131}I Counts**: ^{131}I counts recorded, ± one standard deviation.
13. **^{7}Be Counts**: ^{7}Be counts recorded, ± one standard deviation.

Site	Collect time	Cond	Type	DW samp	Cont	Det	Counting start	Live time	^{131}I Peak	^{7}Be Peak	^{131}I Counts	^{7}Be Counts
Atwater	7/8/13 15:00	A	W	Unk	J	1	7/8/13 16:20	75257	364.00	477.28	81 ± 35	5010 ± 80
Atwater	7/8/13 15:00	A	D	31.687	J	1	7/11/13 13:27	7573	364.00	477.57	6 ± 10	492 ± 27
Atwater	8/9/13 13:00	A	D	3.767	V	1	8/19/13 11:05	82478	364.00	477.36	31 ± 34	1870 ± 57
Atwater	7/31/13 11:00	A	D	3.634	V	1	8/2/13 16:42	172800	364.10	477.34	0 ± 0	2390 ± 73
Atwater	9/24/14 10:45	A	D	Unk	V	1	10/2/14 9:18	172800	364.00	477.70	0 ± 0	698 ± 55
Bender	7/10/13 14:30	A	W	Unk	J	1	7/12/13 12:30	172800	364.14	477.26	1160 ± 73	3140 ± 78
Bender	7/10/13 14:30	A	D	27.467	J	1	7/16/13 9:52	172800	363.97	477.35	722 ± 74	2470 ± 74
Bender	8/8/13 15:35	D	D	74.407	J	1	8/14/13 16:56	60734	364.13	477.36	2920 ± 71	1620 ± 55
Bender	9/30/13 14:30	A	D	2.838	V	1	10/5/13 17:56	166754	364.04	477.24	299 ± 61	429 ± 57
Bender	7/3/14 14:30	A	W	117.24	M	2	7/6/14 0:21	144040	365.34	478.96	176 ± 82	2307 ± 77
Bradford	7/16/13 13:38	D	W	Unk	J	1	7/24/13 13:31	172800	364.00	477.33	0 ± 0	1370 ± 63
Bradford	7/16/13 13:50	D	D	58.524	J	1	7/19/13 14:18	172800	364.18	477.32	361 ± 71	5770 ± 95
Bradford	9/5/14 2:00	D	W	Unk	M	2	9/12/14 9:42	192286	365.67	479.18	673 ± 84	12618 ± 134
Bradford	9/4/13 18:10	A	D	51.853	J	1	9/6/13 14:10	172800	364.13	477.28	1110 ± 73	4250 ± 86
Bradford	8/29/13 12:00	A	D	2.606	V	1	9/4/13 19:15	154362	364.28	477.33	390 ± 64	2590 ± 72
Grant	7/10/13 14:50	D	D	43.531	J	1	7/15/13 11:31	80346	364.25	477.52	4910 ± 86	2560 ± 65
Grant	8/8/13 15:00	D	D	62.683	J	1	8/14/13 9:40	26103	364.05	477.32	563 ± 37	639 ± 35
Grant	9/30/13 13:45	A	D	2.332	V	1	10/2/13 13:06	163898	364.27	477.21	430 ± 67	436 ± 54
Larson St.	7/3/14 17:15	A	W	Unk	M	1	7/7/14 16:18	86382	364.47	477.92	565 ± 58	1790 ± 63
Green Can	10/23/13 14:00	A	D	2.555	V	1	10/28/13 10:08	172800	364.00	477.23	219 ± 49	3080 ± 81
Lorier	8/15/13 11:00	A	D	3.460	V	1	8/20/13 10:01	110394	364.49	477.37	748 ± 57	2830 ± 69
Reef 2	8/15/13 15:00	A	D	6.945	V	1	8/21/13 16:43	172800	364.00	477.29	62 ± 49	5700 ± 94
S. wall	9/10/13 11:30	A	D	2.754	V	1	9/14/13 13:46	172800	364.24	477.33	424 ± 67	3020 ± 77
S. wall	9/10/13 11:30	D	D	3.036	V	1	9/12/13 14:04	171603	364.46	477.32	122 ± 69	3680 ± 83
Wind Pt Jetty	7/3/14 16:15	A	W	72.148	J	1	7/5/14 19:05	162668	364.00	477.75	0 ± 0	1240 ± 62
Wind Pt N	7/3/14 16:15	D	W	23.219	J	3	7/7/14 16:22	172079	364.33	477.62	249 ± 152	2109 ± 81
Wind Pt S	7/3/14 16:32	D	W	105.133	M	3	7/6/14 0:18	144103	364.41	477.56	432 ± 155	4728 ± 149

Site	Collect time	^{131}I A_0 (Bq)			^{131}I A_0/DW (Bq/gDW)			^{7}Be A_0 (Bq)			^{7}Be A_0/DW (Bq/gDW)		
Atwater	7/8/13 15:00	0.0461	±	0.0197	-	±	-	26.825	±	0.430	-	±	-
Atwater	7/8/13 15:00	0.0421	±	0.0705	0.001329	±	0.002223	27.051	±	1.460	0.8537	±	0.0461
Atwater	8/9/13 13:00	0.0058	±	0.0063	0.001548	±	0.001677	1.284	±	0.039	0.3410	±	0.0104
Atwater	9/24/14 10:45	0.0000	±	0.0000	-	±	-	0.225	±	0.018	-	±	-
Atwater	7/31/13 11:00	0.0000	±	0.0000	0.000000	±	0.000000	0.714	±	0.022	0.1965	±	0.0060
Bender	7/10/13 14:30	0.3545	±	0.0224	-	±	-	7.556	±	0.188	-	±	-
Bender	7/10/13 14:30	0.3086	±	0.0316	0.011235	±	0.001150	6.252	±	0.187	0.2276	±	0.0068
Bender	8/8/13 15:35	3.4356	±	0.0832	0.046173	±	0.001118	11.607	±	0.393	0.1560	±	0.0053
Bender	9/30/13 14:30	0.0027	±	0.0006	0.000950	±	0.000194	0.138	±	0.018	0.0486	±	0.0064
Bender	7/3/14 14:30	0.0102	±	0.0048	0.000087	±	0.000041	10.440	±	0.348	0.0890	±	0.0030
Bradford	7/16/13 13:38	0.0000	±	0.0000	-	±	-	3.567	±	0.164	-	±	-
Bradford	7/16/13 13:50	0.1213	±	0.0238	0.002073	±	0.000407	14.086	±	0.232	0.2407	±	0.0040
Bradford	9/4/13 18:10	0.1515	±	0.0099	0.002921	±	0.000192	10.216	±	0.207	0.1970	±	0.0040
Bradford	8/29/13 12:00	0.0297	±	0.0049	0.011398	±	0.001867	0.912	±	0.026	0.3499	±	0.0098
Bradford	9/5/14 2:00	0.0259	±	0.0032	-	±	-	45.773	±	0.486	-	±	-
Grant	7/10/13 14:50	3.9782	±	0.0698	0.091388	±	0.001603	13.676	±	0.345	0.3142	±	0.0079
Grant	8/8/13 15:00	1.4787	±	0.0969	0.023590	±	0.001546	10.586	±	0.574	0.1689	±	0.0092
Grant	9/30/13 13:45	0.00362	±	0.0006	0.001552	±	0.000240	0.137	±	0.017	0.0586	±	0.0072
Green Can	10/23/13 14:00	0.0016	±	0.0004	0.000622	±	0.000139	0.952	±	0.025	0.3725	±	0.0099
Larson St.	7/3/14 17:15	0.0341	±	0.0035	-	±	-	10.146	±	0.360	-	±	-
Lorier	8/15/13 11:00	0.0694	±	0.0053	0.020065	±	0.001518	1.365	±	0.033	0.3944	±	0.0096
Reef 2	8/15/13 15:00	0.0042	±	0.0033	0.000601	±	0.000476	1.790	±	0.029	0.2577	±	0.0042
S. wall	9/10/13 11:30	0.0070	±	0.0011	0.002534	±	0.000400	0.924	±	0.024	0.3356	±	0.0086
S. wall	9/10/13 11:30	0.0013	±	0.0007	0.000414	±	0.000234	1.105	±	0.025	0.3640	±	0.0082
Wind Pt Jetty	7/3/14 16:15	0.0000	±	0.0000	0.000000	±	0.000000	3.178	±	0.158	0.0441	±	0.0022
Wind Pt N	7/3/14 16:15	0.0071	±	0.0043	0.000305	±	0.000186	5.409	±	0.208	0.2330	±	0.0089
Wind Pt S	7/3/14 16:32	0.0139	±	0.0050	0.000132	±	0.000048	14.137	±	0.446	0.1345	±	0.0042

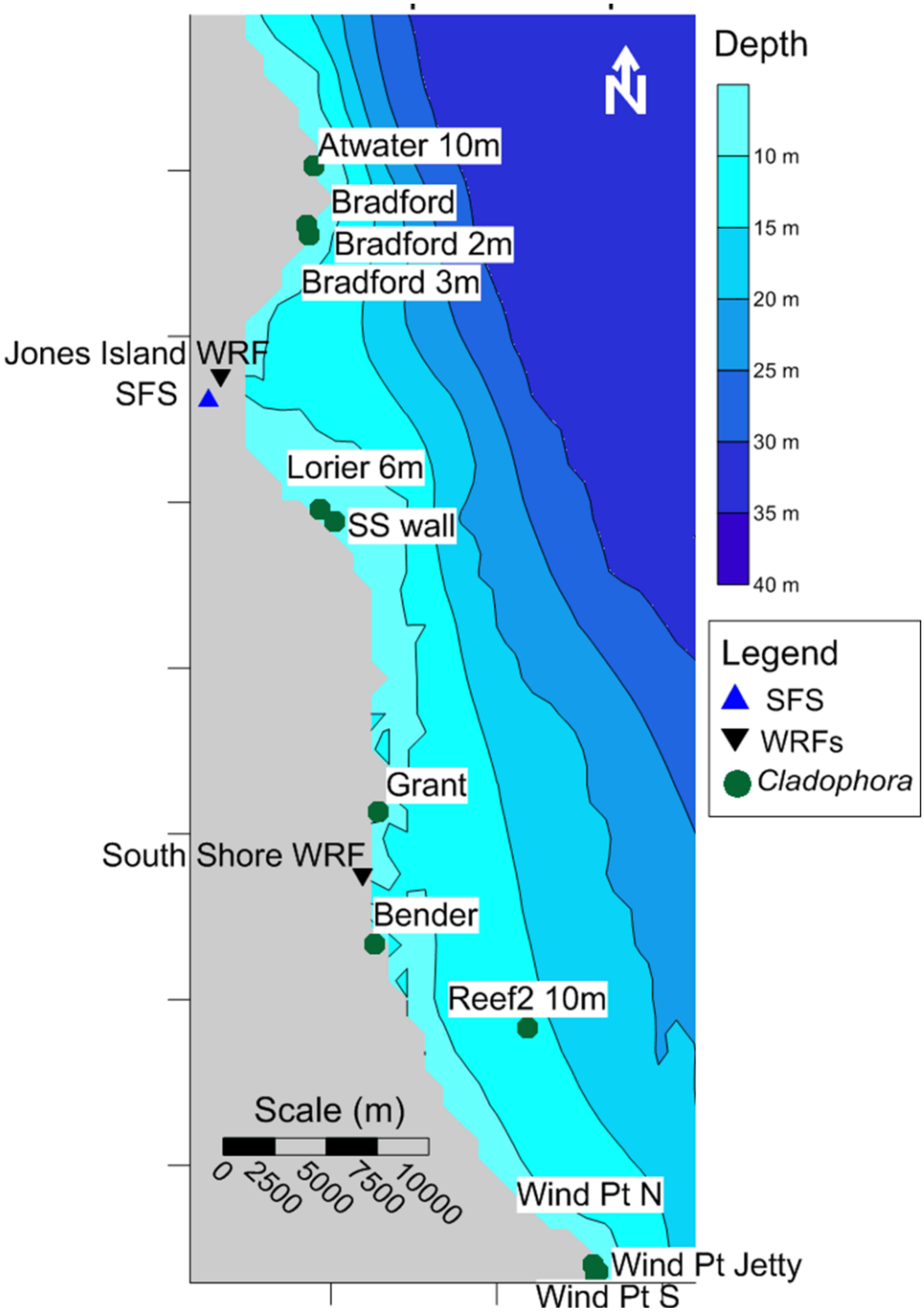
Depth
10 m
15 m
20 m
25 m
30 m
35 m
40 m
Legend
SFS
WRFs
Cladophora
Atwater 10m
Bradford
Bradford 2m
Bradford 3m
Jones Island WRF
SFS
Lorier 6m
SS wall
Grant
South Shore WRF
Bender
Reef2 10m
Scale (m)
0 2500 5000 7500 10000
Wind Pt N
Wind Pt Jetty
Wind Pt S

Appendix I: Benthic Trawls

This appendix contains the raw data for the samples collected by benthic trawling with the epibenthic sled. The column descriptions are as follows.

1. **Site**: location of sample collection. “c2” indicates a second, longer count for the same sample. “1/2” and “2/2” show two halves of a large sample.
2. **Collect time**: date and midpoint time of sample collection.
3. **Part**: part of the sample, i.e. whole sample (W), abiotic material (A), *Cladophora* (C), or dreissenid mussels (M).
4. **Type**: indicates how the sample was processed prior to counting: wet (W) or oven dried (D).
5. **Dist**: Distance of trawling transect (m).
6. **DW samp**: dry weight of the counted sample (g).
7. **Cont**: sample container: Marinelli beaker (M), jar (J), or vial (V).
8. **Det**: gamma detector used.
9. **Counting start**: start date and time of gamma analysis.
10. **Live time**: live time of gamma analysis (s).
11. **^{131}I Peak**: energy of ^{131}I peak (keV).
12. **^{7}Be Peak**: energy of ^{7}Be peak (keV).
13. **^{131}I Counts**: ^{131}I counts recorded, ± one standard deviation.
14. **^{7}Be Counts**: ^{7}Be counts recorded, ± one standard deviation.

Site	Collect time	Part	Type	Dist	DW samp	Cont	Det	Counting start	Live Time	^{131}I Peak	^{7}Be Peak	^{131}I Counts	^{7}Be Counts
County Line 1km	10/20/14 14:26	W	W	380.6	603.41	M	1	10/20/14 18:22	78450	364.37	477.86	327 ± 66.54	1330 ± 66.6
County Line 1km	11/5/14 13:04	W	W	304.3	230.84	M	1	11/7/14 13:10	246177	364.76	477.91	446 ± 109	8876 ± 241
County Line 1km c2	10/20/14 14:26	W	W	380.6	603.41	M	3	10/23/14 17:35	178070	364.81	477.87	461 ± 115	1975 ± 188
County Line 5km	10/20/14 13:43	W	W	877.3	761.243	M	3	10/21/14 17:17	173628	364.53	477.90	827 ± 224	2016 ± 201
County Line 5km	11/5/14 13:54	W	W	735.1	223.156	M	1	11/7/14 13:08	246414	365.51	479.10	46 ± 85	693 ± 80
County Line 8km	11/5/14 14:36	W	W	318.0	501.828	M	1	11/5/14 19:05	164733	364.00	477.65	138 ± 76	2280 ± 104
Main Gap 1km	10/20/14 10:18	W	W	611.4	517.05	M	3	10/20/14 18:29	81925	365.34	477.88	91 ± 154	1502 ± 134
Main Gap 1km c2	10/20/14 10:18	W	W	611.4	517.05	M	1	10/23/14 17:31	172800	364.00	477.81	226 ± 80	5130 ± 115
Main Gap 5km	10/20/14 11:21	W	W	356.5	399.131	M	2	10/21/14 17:14	174033	365.38	479.12	44 ± 43	3762 ± 95
South Shore 1km	10/20/14 15:06	W	W	1086.8	606.737	M	2	10/20/14 18:26	81930	365.60	479.18	913 ± 70	2269 ± 74
South Shore 1km	11/5/14 12:01	W	W	454.7	330.936	M	1	11/7/14 16:52	172800	364.00	477.75	173 ± 58	726 ± 61
South Shore 1km c2	10/20/14 15:06	W	W	1086.8	606.737	M	2	10/23/14 17:38	178114	365.61	479.12	1260 ± 98	4690 ± 110
South Shore 5km	10/20/14 12:49	W	W	345.6	211.244	M	1	10/21/14 16:10	172800	364.78	479.05	219 ± 52	1370 ± 72
South Shore 5km	11/5/14 16:16	W	W	372.3	348.577	M	2	11/5/14 19:15	150552	364.78	479.07	73 ± 75	569 ± 71
South Shore 8km	11/5/14 15:34	W	W	594.9	553.306	M	3	11/5/14 19:13	150873	363.74	477.91	57 ± 101	1167 ± 191
County Line 5km	10/20/14 13:43	M	D		129.509	J	3	10/27/14 10:19	171678	364.64	477.85	105 ± 73	846 ± 131
South Shore 1km	10/20/14 15:06	M	D		121.972	J	3	10/31/14 9:39	188150	364.56	477.97	231 ± 63	1106 ± 136
South Shore 5km	10/20/14 12:49	M	D		179.295	J	3	10/29/14 11:08	167308	364.79	478.00	0 ± 0	961 ± 129
County Line 1km	10/20/14 14:26	C	D		35.095	J	3	10/25/14 19:07	144540	364.66	477.91	423 ± 46	924 ± 116
Main Gap 5km	10/20/14 11:21	C	D		58.91	J	2	11/2/14 13:59	159551	363.48	479.13	42 ± 65	1298 ± 92
South Shore 1km	10/20/14 15:06	C	D		34.96	J	1	10/31/14 9:28	172800	364.84	477.65	516 ± 62	1620 ± 70
South Shore 5km	10/20/14 12:49	C	D		0.376	V	1	11/2/14 12:50	159696	364.00	477.50	62 ± 48	226 ± 40
County Line 1km	10/20/14 14:26	A	D		241.001	J	3	11/10/14 14:27	242824	361.60	477.94	0 ± 0	947 ± 180
County Line 5km 1/2	10/20/14 13:43	A	D		238.806	J	2	11/10/14 14:30	242798	364.47	479.23	0 ± 0	242 ± 80
County Line 5km 2/2	10/20/14 13:43	A	D		368.253	J	2	10/27/14 11:20	171741	364.34	479.51	0 ± 0	294 ± 75
Main Gap 5km	10/20/14 11:21	A	D		156.384	J	2	11/13/14 10:00	343902	363.60	479.19	0 ± 0	696 ± 93
South Shore 1km	10/20/14 15:06	A	D		448.817	J	1	11/4/14 9:12	121855	364.00	477.73	32 ± 56	0 ± 0
South Shore 1km	11/5/14 12:01	A	D		45.712	J	3	11/13/14 9:57	344119	364.04	478.02	137 ± 99	89 ± 100

Site	Collect time	Part	Type	^{131}I A_0	^{131}I A_0/DW	^{131}I A_0/Area	^{7}Be A_0	^{7}Be A_0/DW	^{7}Be A_0/Area
County Line 1km	10/20/14 14:26	W	W	0.2252 ± 0.0458	225 ± 46	3.48E-03 ± 7.08E-04	7.90 ± 0.40	13.09 ± 0.66	0.1220 ± 0.0061
County Line 1km	11/5/14 13:04	W	W	0.1246 ± 0.0304	125 ± 30	2.45E-03 ± 5.98E-04	17.42 ± 0.47	75.46 ± 2.05	0.3419 ± 0.0093
County Line 1km c2	10/20/14 14:26	W	W	0.2457 ± 0.0613	246 ± 61	3.80E-03 ± 9.47E-04	7.92 ± 0.75	13.12 ± 1.25	0.1223 ± 0.0116
County Line 5km	10/20/14 13:43	W	W	0.3797 ± 0.1029	380 ± 103	3.40E-03 ± 9.21E-04	8.08 ± 0.81	10.61 ± 1.06	0.0723 ± 0.0072
County Line 5km	11/5/14 13:54	W	W	0.0128 ± 0.0237	13 ± 24	5.88E-05 ± 1.09E-04	1.36 ± 0.16	6.09 ± 0.70	0.0062 ± 0.0007
County Line 8km	11/5/14 14:36	W	W	0.0473 ± 0.0259	47 ± 26	5.83E-04 ± 3.20E-04	6.49 ± 0.29	12.93 ± 0.58	0.0801 ± 0.0036
Main Gap 1km	10/20/14 10:18	W	W	0.0791 ± 0.1339	79 ± 134	3.21E-03 ± 5.44E-03	12.53 ± 1.12	24.24 ± 2.16	0.5092 ± 0.0454
Main Gap 1km c2	10/20/14 10:18	W	W	0.0970 ± 0.0343	97 ± 34	3.94E-03 ± 1.39E-03	14.50 ± 0.33	28.05 ± 0.63	0.5893 ± 0.0133
Main Gap 5km	10/20/14 11:21	W	W	0.0197 ± 0.0193	20 ± 19	7.97E-04 ± 7.79E-04	14.76 ± 0.37	36.98 ± 0.93	0.5964 ± 0.0151
South Shore 1km	10/20/14 15:06	W	W	0.7557 ± 0.0579	756 ± 58	5.57E-03 ± 4.27E-04	18.51 ± 0.60	30.51 ± 1.00	0.1365 ± 0.0045
South Shore 1km	11/5/14 12:01	W	W	0.0675 ± 0.0228	68 ± 23	4.13E-04 ± 1.39E-04	2.02 ± 0.17	6.11 ± 0.51	0.0124 ± 0.0010
South Shore 1km c2	10/20/14 15:06	W	W	0.6497 ± 0.0505	650 ± 51	4.79E-03 ± 3.72E-04	18.42 ± 0.43	30.36 ± 0.71	0.1358 ± 0.0032
South Shore 5km	10/20/14 12:49	W	W	0.0781 ± 0.0186	78 ± 19	2.34E-03 ± 5.57E-04	3.77 ± 0.20	17.86 ± 0.93	0.1130 ± 0.0059
South Shore 5km	11/5/14 16:16	W	W	0.0339 ± 0.0348	34 ± 35	4.71E-04 ± 4.83E-04	2.54 ± 0.32	7.28 ± 0.91	0.0352 ± 0.0044
South Shore 8km	11/5/14 15:34	W	W	0.0273 ± 0.0483	27 ± 48	2.67E-04 ± 4.74E-04	5.30 ± 0.87	9.58 ± 1.57	0.0520 ± 0.0085
County Line 5km	10/20/14 13:43	M	D	0.0000 ± 0.0000	0 ± 0		0.00 ± 0.00	0 ± 0	
South Shore 1km	10/20/14 15:06	M	D	0.0410 ± 0.0721	41 ± 72		0.00 ± 0.00	0 ± 0	
South Shore 5km	10/20/14 12:49	M	D	0.0082 ± 0.0063	8 ± 6		0.08 ± 0.01	223.19 ± 39.08	
County Line 1km	10/20/14 14:26	C	D	0.0000 ± 0.0000	0 ± 0		2.16 ± 0.41	8.96 ± 1.70	
Main Gap 5km	10/20/14 11:21	C	D	0.0531 ± 0.0823	53 ± 82		6.10 ± 0.43	103.57 ± 7.34	
South Shore 1km	10/20/14 15:06	C	D	0.3391 ± 0.0408	339 ± 41		4.38 ± 0.19	125.15 ± 5.37	
South Shore 5km	10/20/14 12:49	C	D	0.0000 ± 0.0000	0 ± 0		2.70 ± 0.36	15.08 ± 2.02	
County Line 1km	10/20/14 14:26	A	D	0.0000 ± 0.0000	0 ± 0		0.00 ± 0.00	0 ± 0	
County Line 5km 1/2	10/20/14 13:43	A	D	0.0000 ± 0.0000	0 ± 0		0.83 ± 0.28	3.49 ± 1.15	
County Line 5km 2/2	10/20/14 13:43	A	D	0.0000 ± 0.0000	0 ± 0		1.19 ± 0.30	3.22 ± 0.82	
Main Gap 5km	10/20/14 11:21	A	D	0.0006 ± 0.0046	1 ± 5		0.04 ± 0.01	28.39 ± 9.92	
South Shore 1km	10/20/14 15:06	A	D	0.1305 ± 0.0356	130 ± 36		2.84 ± 0.35	23.27 ± 2.86	
South Shore 1km	11/5/14 12:01	A	D	0.0355 ± 0.0257	36 ± 26		0.12 ± 0.14	2.66 ± 2.99	

Appendix J: Site locations

This appendix contains the locations of the sampling sites for benthic trawl, PONAR, gravity core, mussel and *Cladophora* sampling. The column descriptions are as follows. Site locations are shown in the figure below. For benthic trawls, the coordinates refer to the midpoint of the transect.

1. **Category**: the type of sample collected at the site.
2. **Site**: name of the site, corresponding to the sample in its appropriate appendix
3. **Collection time**: date and time of sample collection.
4. **Latitude**: site latitude (DD).
5. **Longitude**: site longitude (DD).

Category	Site	Collection time	Latitude	Longitude
Benthic Trawl	County Line 1km	10/20/14 14:26	42.843950	-87.811003
Benthic Trawl	County Line 1km	11/5/14 13:04	42.844732	-87.813017
Benthic Trawl	County Line 5km	10/20/14 13:43	42.845533	-87.767767
Benthic Trawl	County Line 5km	11/5/14 13:54	42.838317	-87.766565
Benthic Trawl	County Line 8km	11/5/14 14:36	42.838883	-87.728647
Benthic Trawl	Main Gap 1km	10/20/14 10:18	43.027195	-87.866457
Benthic Trawl	Main Gap 5km	10/20/14 11:21	43.027307	-87.824333
Benthic Trawl	South Shore 1km	10/20/14 15:06	42.892250	-87.826989
Benthic Trawl	South Shore 1km	11/5/14 12:01	42.891733	-87.825040
Benthic Trawl	South Shore 5km	10/20/14 12:49	42.891754	-87.780340
Benthic Trawl	South Shore 5km	11/5/14 16:16	42.890119	-87.773250
Benthic Trawl	South Shore 8km	11/5/14 15:34	42.889183	-87.743120
Cladophora	Atwater 10m	7/8/13 15:00	43.080660	-87.866061
Cladophora	Atwater 10m	7/8/13 15:00	43.080660	-87.866061
Cladophora	Atwater 10m	8/9/13 13:00	43.080660	-87.866061
Cladophora	Atwater 10m	9/24/14 10:45	43.080660	-87.866061
Cladophora	Bender	7/10/13 14:30	42.869670	-87.840953
Cladophora	Bender	7/10/13 14:30	42.869670	-87.840953
Cladophora	Bender	8/8/13 15:35	42.869670	-87.840953
Cladophora	Bender	9/30/13 14:30	42.869670	-87.840953
Cladophora	Bender	7/3/14 14:30	42.869670	-87.840953
Cladophora	Bradford	7/16/13 13:38	43.064450	-87.868664
Cladophora	Bradford	7/16/13 13:50	43.064450	-87.868664
Cladophora	Bradford	9/5/14 2:00	43.064450	-87.868664
Cladophora	Bradford 2m	9/4/13 18:10	43.061982	-87.867579
Cladophora	Bradford 3m	8/29/13 12:00	43.061982	-87.867579
Cladophora	Grant	7/10/13 14:50	42.905643	-87.840161
Cladophora	Grant	8/8/13 15:00	42.905643	-87.840161
Cladophora	Grant	9/30/13 13:45	42.905643	-87.840161
Cladophora	Larson St.	7/3/14 17:15	42.693188	-87.791564
Cladophora	Lorier 6m	8/15/13 11:00	42.987333	-87.862500
Cladophora	Reef2 10m	8/15/13 15:00	42.847291	-87.784028
Cladophora	SS wall	9/10/13 11:30	42.984120	-87.857395
Cladophora	SS wall	9/10/13 11:30	42.984120	-87.857395
Cladophora	Wind Pt Jetty	7/3/14 16:15	42.781089	-87.757248
Cladophora	Wind Pt N	7/3/14 16:15	42.783210	-87.759182
Cladophora	Wind Pt S	7/3/14 16:32	42.779746	-87.758416
Gravity Core	1 H	7/16/14 12:20	43.043523	-87.883385
Gravity Core	1 H	7/29/14 11:12	43.042867	-87.881917
Gravity Core	1 H	8/26/14 12:26	43.041050	-87.888300
Gravity Core	1 H	10/8/14 9:35	43.042125	-87.884876
Gravity Core	2 H	7/16/14 12:28	43.035095	-87.887820
Gravity Core	2 H	7/29/14 11:27	43.036600	-87.886100
Gravity Core	2 H	8/26/14 13:15	43.035670	-87.888080
Gravity Core	2 H	10/8/14 10:12	43.037138	-87.886954
Gravity Core	3 H	7/16/14 12:45	43.027099	-87.886980
Gravity Core	3 H	7/29/14 12:30	43.025900	-87.887233
Gravity Core	3 H	8/26/14 14:52	43.023200	-87.886070

Category	Site	Collection time	Latitude	Longitude
Gravity Core	3 H	10/8/14 11:43	43.023177	-87.886535
Gravity Core	3-4 H	7/16/14 13:00	43.024534	-87.886728
Gravity Core	4 H	7/16/14 13:18	43.016788	-87.887162
Gravity Core	4 H	7/29/14 13:55	43.016700	-87.887983
Gravity Core	4 H	8/26/14 16:00	43.018050	-87.887730
Gravity Core	4 H	10/8/14 12:25	43.014542	-87.889710
Gravity Core	5 H	7/16/14 13:40	43.008460	-87.880406
Gravity Core	5 H	7/29/14 14:15	43.009550	-87.880817
Gravity Core	5 H	8/26/14 16:19	43.010350	-87.879730
Gravity Core	5 H	10/8/14 13:05	43.007923	-87.885712
Gravity Core	6 H	7/29/14 14:40	43.023600	-87.893467
Gravity Core	6 H	8/26/14 16:42	43.023430	-87.893630
Gravity Core	6 H	10/8/14 13:35	43.022962	-87.893353
Mussels	5 H	7/16/14 13:40	43.008460	-87.880406
Mussels	5 H	7/29/14 14:15	43.009550	-87.880817
Mussels	5 H	9/24/14 12:35	43.008333	-87.878033
Mussels	5 H	9/24/14 12:35	43.008333	-87.878033
Mussels	Atwater	9/24/14 10:45	43.094700	-87.864883
Mussels	Atwater	9/24/14 10:45	43.094700	-87.864883
Mussels	Bradford	9/4/13 18:10	43.061982	-87.867579
Mussels	S. Wall	9/24/14 11:35	42.988033	-87.860317
Mussels	S. Wall	9/24/14 11:35	42.988033	-87.860317
Mussels	SS wall	10/14/13 14:00	42.988033	-87.860317
Mussels	SS wall	10/14/13 14:00	42.988033	-87.860317
Mussels	SS wall	10/14/13 14:00	42.988033	-87.860317
PONAR	2 H	9/24/14 13:25	43.010183	-87.878383
PONAR	3 H	6/20/14 14:26	43.026665	-87.882750
PONAR	4 H	6/20/14 11:46	43.014842	-87.887507
PONAR	4 H	9/24/14 13:00	43.023430	-87.893630
PONAR	5 H	6/20/14 12:05	43.008335	-87.879510
PONAR	5 H	9/24/14 12:19	43.010183	-87.860317
PONAR	6 H	9/24/14 14:00	43.043523	-87.883385
PONAR	6 H 1/3	6/20/14 10:59	43.021233	-87.891527
PONAR	6 H 2/3	6/20/14 11:15	43.021825	-87.891548
PONAR	6 H 3/3	6/20/14 11:28	43.021173	-87.892498
PONAR	L3-2	6/20/14 13:41	43.040842	-87.867717
PONAR	L4	6/20/14 13:23	43.026360	-87.867813
PONAR	L5	6/20/14 13:08	43.017688	-87.866388
PONAR	L6	6/20/14 12:33	43.007250	-87.867063
PONAR	L9	6/20/14 14:13	43.026105	-87.858680

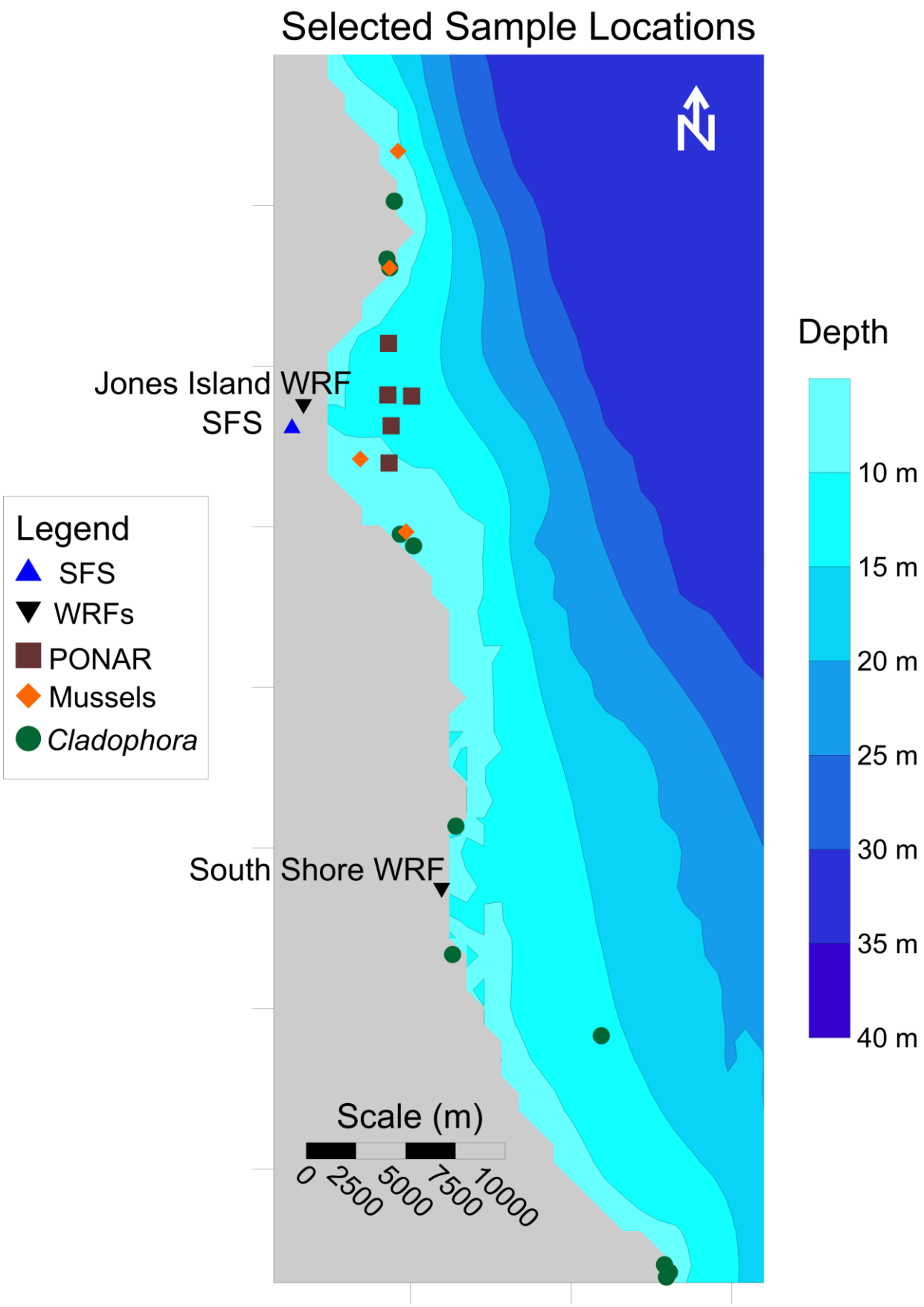
Selected Sample Locations
Jones Island WRF
SFS
South Shore WRF
Legend
SFS
WRFs
PONAR
Mussels
Cladophora
Depth
10 m
15 m
20 m
25 m
30 m
35 m
40 m
Scale (m)
0
2500
5000
7500
10000

Appendix K: US Army Corps of Engineers Sediment Deposition Calculations

This appendix demonstrates the calculations used to derive sediment deposition estimates from an US Army Corps of Engineers dredging report (US ACE 2008) and shows the associated data.

The report estimated future dredging needs for the Milwaukee harbor at 70,000 cubic yards every four years. In terms of liters and days, this is

$$70000\ cu\ yd\ \times \frac{764.55\ L}{1\ cu\ yd} = 5.35 \times 10^7 L$$

$$4\ y\ \times \frac{365.25\ d}{1y} = 1461\ d$$

Next, we used the mean dry weight to volume ratio of bed sediment in the Milwaukee harbor to convert liters of sediment to grams (dry weight) of sediment. This was estimated using the outer harbor sediment data collected during our gravity core sampling, 763.4 g DW/L (raw data available in Appendix D).

$$5.35 \times 10^7 L \times \frac{763.4\ gDW}{1\ L} = 4.09 \times 10^{10} g\ DW$$

This makes sediment burial in the harbor:

$$\frac{4.09 \times 10^{10} g\ DW}{1461\ d} = 2.80 \times 10^7\ g\ DW/d$$

or

$$2.80 \times 10^7\ g \frac{DW}{d} \times \frac{1\ MT}{1 \times 10^6 g} = 28.0\ MT/d$$

*This figure, however, is for the area dredged by the US ACE, which does not include all of the outer harbor and includes some of the inner harbor. Using a figure from US ACE (2008) as a guide, the inner and outer harbor dredging areas were reproduced in the mapping program Surfer (**Figure 33**), which calculated the areas of each. This produced the following results:*

Location	Area (m^2)	% of dredging	% of total outer harbor area
Dredged inner harbor	1.98E+05	10.1%	4%
Dredged outer harbor	1.75E+06	89.9%	40%
Total dredged area	1.95E+06	100%	44%
Total outer harbor area	4.43E+06		100%

Therefore, 10.1% of the dredged area is in the inner harbor, and should not be included in an estimate of outer harbor sediment deposition.

To estimate sediment deposition in the outer harbor, the burial estimate above is scaled to the dredged area of the outer harbor:

$$28.0\ MT/d\ \times\ 89.9\% = \mathbf{25.1\ MT/d}$$

Appendix L: ^{152}Eu standards

This appendix contains the raw data and activities associated with the gamma detector efficiency calibration using ^{152}Eu, used to derive the detector efficiency equations ($t_{1/2}$ = 4.941×10^3 d; Nichols et al. 2008). The ^{152}Eu standard in Marinelli beakers is in an aqueous medium, and for the other containers it is in a solid, dry sediment medium. The column descriptions are as follows.

1. **Cont**: sample container: Marinelli beaker (M), jar (J) or vial (V).
2. **Det**: gamma detector used.
3. **Mass**: mass of standard medium (g).
4. **Peak**: energy of the ^{152}Eu peak (keV).
5. **Branching**: percentage of ^{152}Eu emissions at the peak energy.
6. **Counts**: counts recorded ± one standard deviation.
7. **Counting start**: start date and time of gamma analysis.
8. **Live time**: live time of gamma analysis (s).
9. **Std activity**: official activity of the ^{152}Eu standard on October 9, 2009 (Bq/g).
10. **Det A'**: "Activity" of the standard on the detector at counting start without accounting for efficiency (Bq).
11. **Std A'**: Activity of the standard at counting start according to decay of the official activity.

Cont	Det	Mass	Peak	Branching	Counts	Counting start	Live time	Std activity	Det A'	Std A'
J	1	60.13	121.46	28.41%	1.29E+06 ± 1277	7/25/14 9:16	9876	182.58	459.78	8588.20
J	1	60.13	344.34	26.58%	6.93E+05 ± 726	7/25/14 9:16	9876	182.58	264.01	8588.20
J	1	60.13	779.31	12.96%	1.79E+05 ± 525	7/25/14 9:16	9876	182.58	139.86	8588.20
J	1	60.13	964.75	14.62%	1.71E+05 ± 483	7/25/14 9:16	9876	182.58	118.44	8588.20
J	2	60.13	122.15	28.41%	1.73E+06 ± 1510	7/25/14 12:08	16422	182.58	370.27	8588.06
J	2	60.13	345.43	26.58%	7.91E+05 ± 1008	7/25/14 12:08	16422	182.58	181.31	8588.06
J	2	60.13	781.69	12.96%	1.82E+05 ± 572	7/25/14 12:08	16422	182.58	85.73	8588.06
J	2	60.13	967.49	14.62%	1.64E+05 ± 523	7/25/14 12:08	16422	182.58	68.22	8588.06
J	3	60.13	121.97	28.41%	3.06E+06 ± 3472	7/28/14 9:20	16610	182.58	648.33	8584.58
J	3	60.13	344.42	26.58%	1.30E+06 ± 1641	7/28/14 9:20	16610	182.58	293.93	8584.58
J	3	60.13	779.12	12.96%	2.59E+05 ± 953	7/28/14 9:20	16610	182.58	120.14	8584.58
J	3	60.13	964.31	14.62%	2.16E+05 ± 839	7/28/14 9:20	16610	182.58	89.02	8584.58
M	1	847.57	121.36	28.41%	2.23E+04 ± 185	7/11/13 11:57	3758	0.931	20.89	650.98
M	1	847.57	343.88	26.58%	1.59E+04 ± 143	7/12/13 11:57	3758	0.931	15.92	651.66
M	1	847.57	778.74	12.96%	4.32E+03 ± 82	7/13/13 11:57	3758	0.931	8.87	652.33
M	1	847.57	963.40	14.62%	3.97E+03 ± 80	7/14/13 11:57	3758	0.931	7.23	653.01
M	2	847.57	122.23	28.41%	8.71E+04 ± 331	7/28/14 14:27	12583	0.931	24.36	617.00
M	2	847.57	345.53	26.58%	4.08E+04 ± 219	7/28/14 14:27	12583	0.931	12.19	617.00
M	2	847.57	781.89	12.96%	9.28E+03 ± 122	7/28/14 14:27	12583	0.931	5.69	617.00
M	2	847.57	967.75	14.62%	8.27E+03 ± 112	7/28/14 14:27	12583	0.931	4.49	617.00
M	3	847.57	121.97	28.41%	8.67E+04 ± 535	8/6/14 12:40	13997	0.931	21.81	616.23
M	3	847.57	344.47	26.58%	4.44E+04 ± 319	8/6/14 12:40	13997	0.931	11.93	616.23
M	3	847.57	779.28	12.96%	9.49E+03 ± 198	8/6/14 12:40	13997	0.931	5.23	616.23
M	3	847.57	964.52	14.62%	8.08E+03 ± 164	8/6/14 12:40	13997	0.931	3.95	616.23
V	1	2.283	121.43	28.41%	6.41E+03 ± 88	8/8/14 10:09	361	182.58	62.48	325.43
V	1	2.283	344.29	26.58%	6.09E+03 ± 83	8/8/14 10:09	361	182.58	63.45	325.43
V	1	2.283	779.42	12.96%	9.15E+02 ± 43	8/8/14 10:09	361	182.58	19.55	325.43
V	1	2.283	964.59	14.62%	4.31E+02 ± 33	8/8/14 10:09	361	182.58	8.16	325.43

Appendix M: ^{152}Eu efficiency curves and equations

This appendix contains the calculated efficiency curves and the corresponding equations used to calculate detector efficiencies for all samples. It is based on the raw data in Appendix J. Equations and curves were calculated using SigmaPlot (v.11.0, Systat Software Inc.). There is one equation for every combination of sample container and detector. All equations are in the form of 3-parameter exponential decay, except for the vial, which is 4-parameter sigmoidal. Adjusted R^2 values are used where applicable to account for the artificial increase in R^2 due to multiple parameters. In the equations, y is detector efficiency and x is peak energy in (keV).

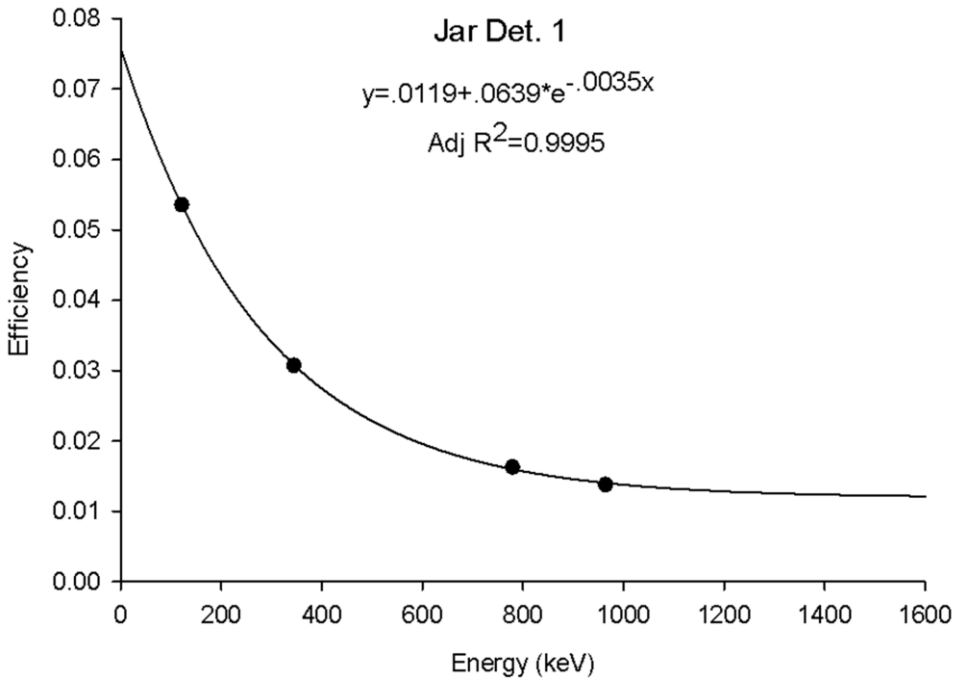

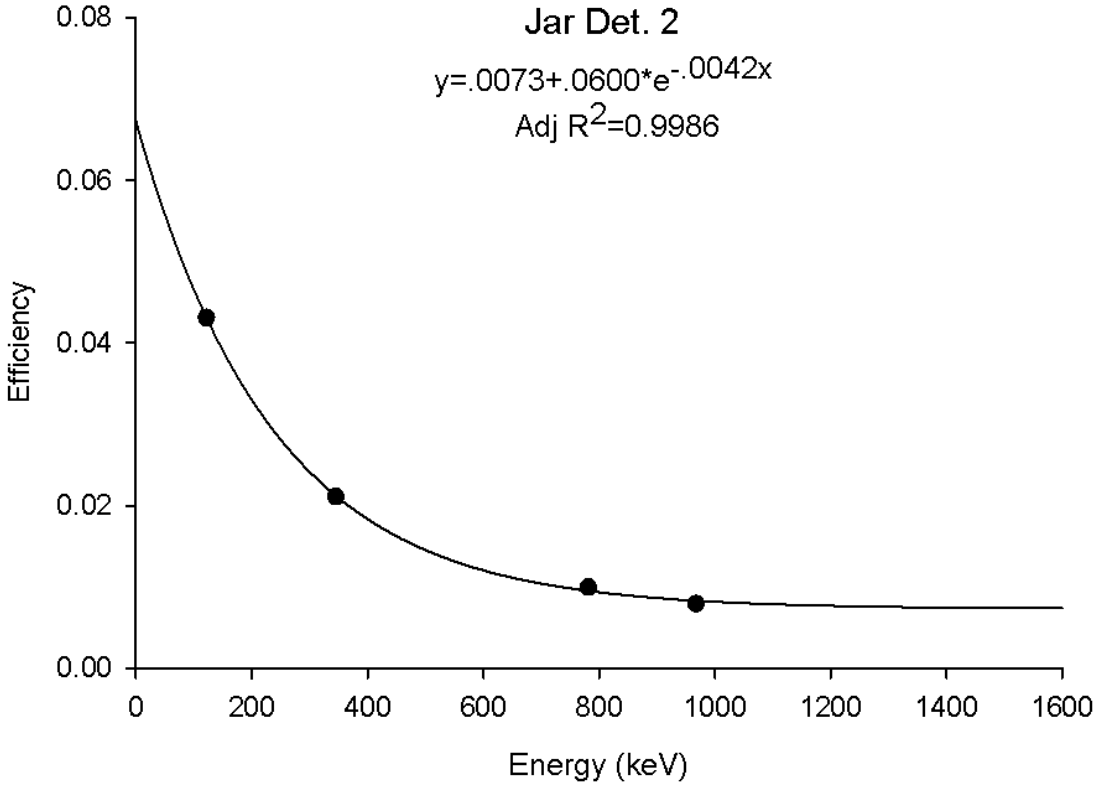
Jar Det. 2
y=.0073+.0600*e^-.0042x
Adj R^2=0.9986
Efficiency
0.08
0.06
0.04
0.02
0.00
0
200
400
600
800
1000
1200
1400
1600
Energy (keV)

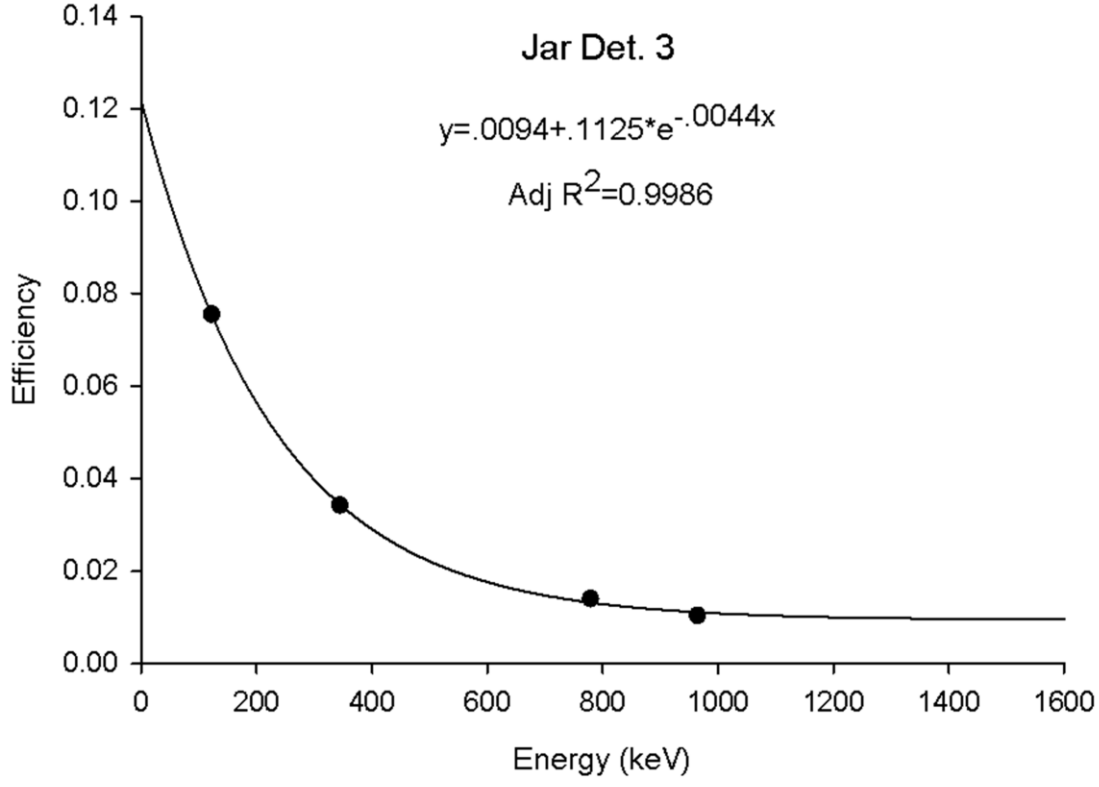
Jar Det. 3
y=.0094+.1125*e^-.0044x
Adj R^2=0.9986
Efficiency
0.14
0.12
0.10
0.08
0.06
0.04
0.02
0.00
0
200
400
600
800
1000
1200
1400
1600
Energy (keV)

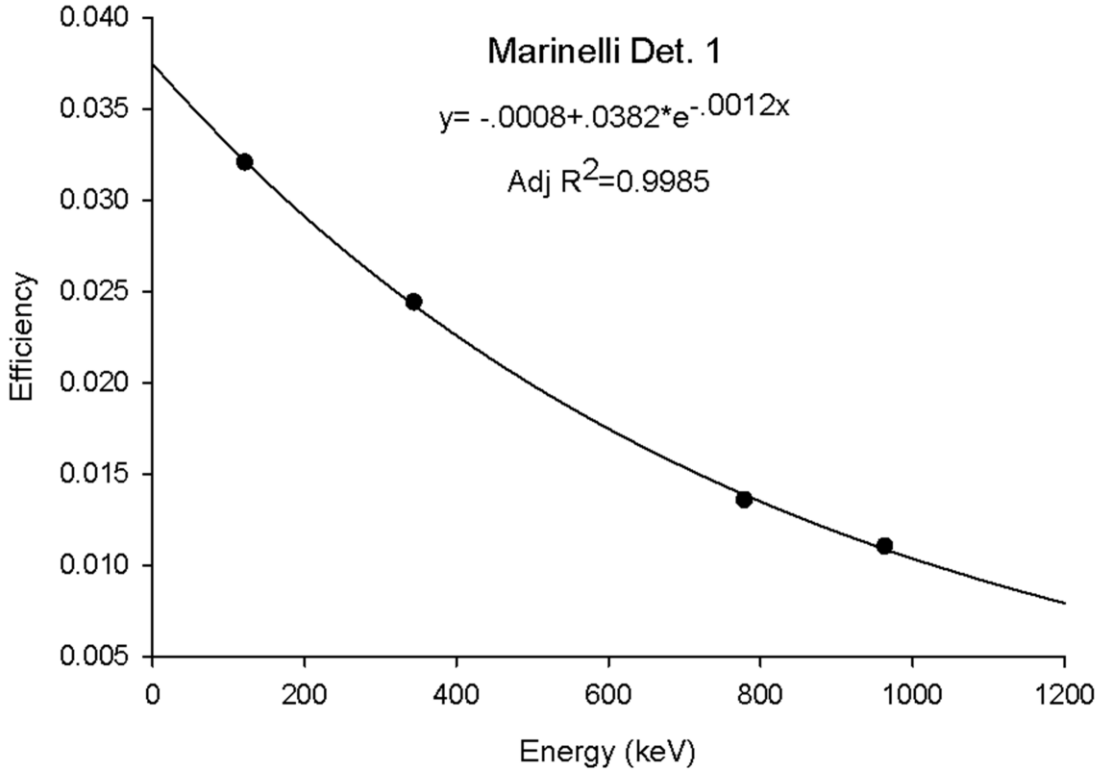
Marinelli Det. 1
y= -.0008+.0382*e^-.0012x
Adj R^2=0.9985
Efficiency
0.040
0.035
0.030
0.025
0.020
0.015
0.010
0.005
0
200
400
600
800
1000
1200
Energy (keV)

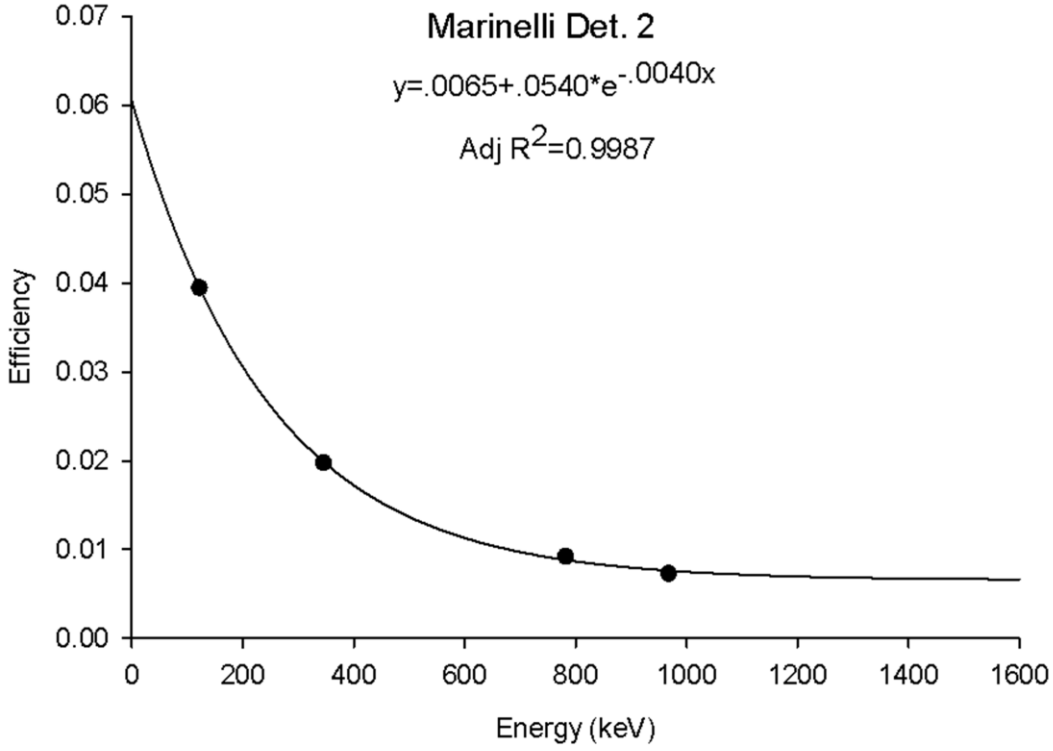
Marinelli Det. 2
y=.0065+.0540*e^-.0040x
Adj R^2=0.9987
Efficiency
0.07
0.06
0.05
0.04
0.03
0.02
0.01
0.00
0
200
400
600
800
1000
1200
1400
1600
Energy (keV)

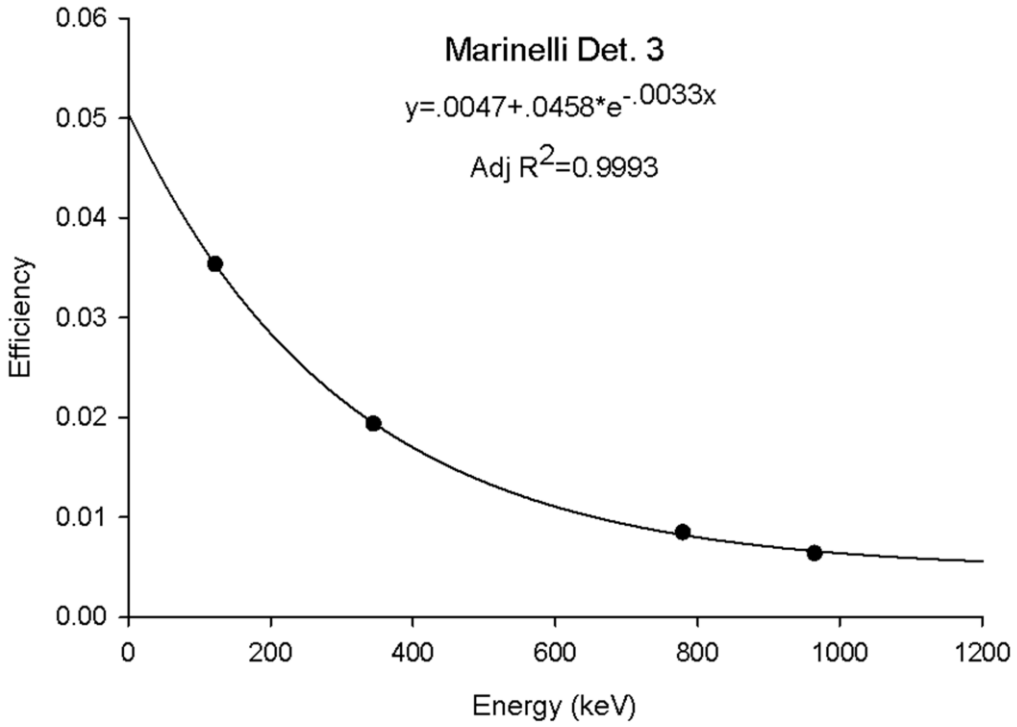
Marinelli Det. 3
y=.0047+.0458*e^-.0033x
Adj R^2=0.9993
Efficiency
0.06
0.05
0.04
0.03
0.02
0.01
0.00
0
200
400
600
800
1000
1200
Energy (keV)

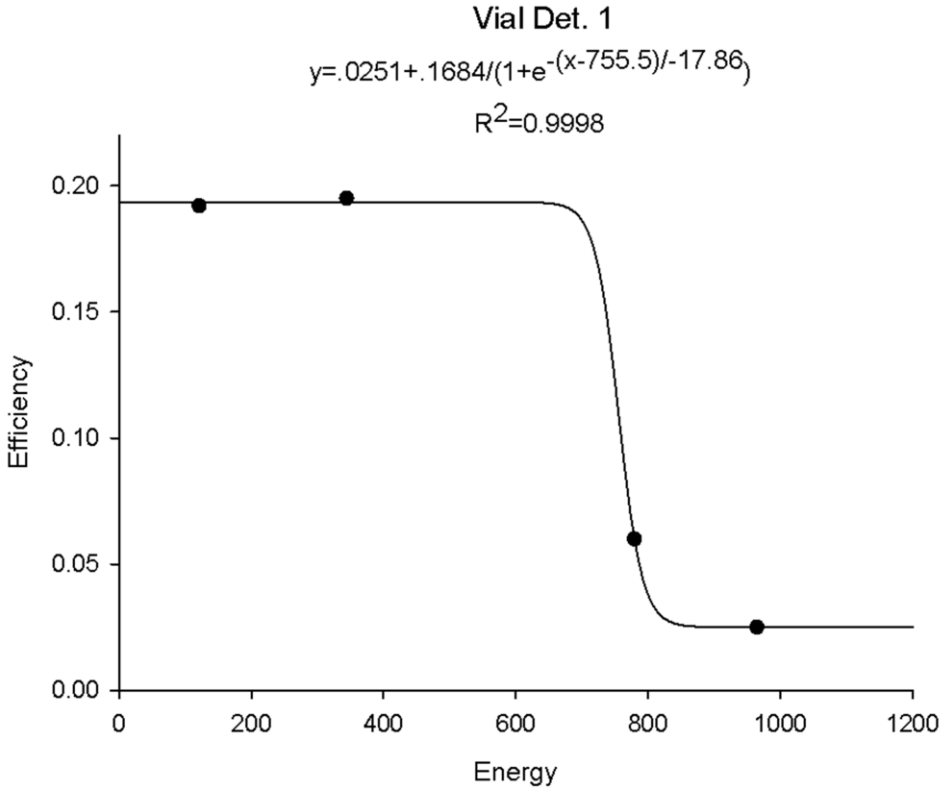
Vial Det. 1
y=.0251+.1684/(1+e^-(x-755.5)/-17.86)
R^2=0.9998
Efficiency
0.20
0.15
0.10
0.05
0.00
0
200
400
600
800
1000
1200
Energy